İSTANBUL TECHNICAL UNIVERSITY ★ INSTITUTE OF SCIENCE AND TECHNOLOGY

INTEGRATED RADIO-INS ALTIMETER DEVELOPMENT VIA KALMAN FILTERING

M.Sc. Thesis by
Remzi SALTOĞLU, B.Sc.
(511971009)

Date of submission : 8 June 2001

Date of defence examination : 29 June 2001

Supervisor (Chairman) : Prof. Dr. Çingiz HACIYEV

Members of the Examining Committee : Prof. Dr. Elbrus CAFEROV

Assoc. Prof. Dr. Aydın MISIRLIOĞLU

JUNE 2001

FOREWORD

Coming to the aviation industry of today, safety has always been the main issue. Everyday, new regulations are proposed, or the exiting ones are constricted particularly about the navigation of the aircraft. The accurate and cost effective solution to encounter these requirements is the development of the integrated navigation systems.

Precision altitude determination is an objective in instrumental landing systems of the civil airliners. In this study, the integrated Radio-INS altimeter is suggested and discussed for this task. In Section 1, some of the past studies related with the subject are presented, and the improvement that is granted with this study is stated. The following two sections are included to give brief information about INS and Radio systems. These sections focus on the error models of the two navigators, instead of their mechanization and operating principles, which will be the base of the integration. Kalman filter basics and the *Robust Kalman Filter* algorithms are described in Section 4. In the last three sections, integration mechanization, computer simulation results, and the conclusion are presented respectively.

It should be underlined that, this is a preliminary study about the Radio-INS integration via *Robust Kalman Filter* in aircraft navigation.

I am especially grateful to my supervisor, Prof. Dr. Çingiz M. Hacıyev, for sharing his knowledge and experience about navigation with me. I also would like to acknowledge the *never ending* encouragement I received from my family towards my academic improvement. I thank Gözde and Alper Ünal for supplying missing papers from thousands miles away, aeronautical engineer Elvin Coşkun for her creative effort on the illustrations, and the rest of the Turkish Airlines engineering family for any kind of support.

June, 2001 Remzi SALTOĞLU

TABLE OF CONTENTS

ABBREVIATIONS

ADF	:	Automatic Direction Finder
AHRS	:	Attitude and Heading Reference System
ATC	:	Air Traffic Controller
CW	:	Continuous Wave
DME	:	Distance Measuring Equipment
EKF	:	Extended Kalman Filter
FAA	:	Federal Aviation Administration
FM-CW	:	Frequency Modulated Continuous Wave
GPS	:	Global Positioning System
ILS	:	Instrumental Landing System
IMU	:	Inertial Measurement Unit
INS	:	Inertial Navigation System
IRS	:	Inertial Reference System
IRU	:	Inertial Reference Unit
JTIDS	:	Joint Tactical Information Distribution System
LORAN	:	Long Range Navigation
MLS	:	Microwave Landing System
NASA	:	National Aeronautics and Space Administration
NAVAIDS	:	Navigations aids
OKF	:	Optimal Kalman Filter
OMEGA	:	Low Frequency Automatic Radio Navigation
PVAT	:	Position, velocity, attitude and time
RA1	:	Robust Algorithm 1
RA2	:	Robust Algorithm 2
RLG	:	Ring Laser Gyroscope
VOR	:	VHF Omni Range

LIST OF TABLES

Page

LIST OF FIGURES

Page

NOMENCLATURE

A	: System dynamics matrix
a_z	: Vertical acceleration
B	: System control matrix
e_k^-	: *A priori* estimate error
e_k	: *A posteriori* estimate error
f_d	: Signal frequency
F_M	: Modulation frequency
g	: Gravitational acceleration
$G(k,k-1)$	: Noise transition matrix
$H_a(t)$	: Altitude (radio)
H_g	: Real altitude
$H_g(t)$	: Real value of altitude (radio)
H_I	: Vertical position (altitude)
H_R	: Altitude (radio)
$\hat{H}_{Int}$	: Estimated integrated system measurement
K	: Gain, blending factor
p	: Probability
P_k	: Error covariance
$P(k/k),\ P_k$	: Value error's correlation vector
$P(k/k-1),\ P_k^-$	: Extrapolation error's correlation vector
Q	: Process noise covariance
R	: Measurement noise covariance
$R_1, R_2, \ldots R_i,\ \hat{R}_i$	: Angled distance from ground
$U_{\Delta a_z}, U_{\Delta g}, U_{\Delta H_R}$	: White noise with zero mean
$V(k)$	: Noise of the system
W_z	: Vertical speed
$X(k), x_k$	: State vector
$\hat{X}(k/k), \hat{x}_k$	: $X(k)$'s estimation vector, *a posteriori* state estimate
$\hat{X}(k/k-1), \hat{x}_k^-$	: Extrapolation value vactor, *a priori* state estimate
$Z(k),\ z_k$	: Measurement vector
Δ	: Innovation sequence
$\widetilde{\Delta}$	: Normalized innovation sequence
Δa_z	: Measurement error of the vertical acceleration

Δf_d	: Signal frequency difference
ΔF_M	: Modulation frequency difference
Δg	: Measurement error of the gravitational acceleration
$\Delta \hat{H}_I$	: Estimated value of error (INS)
$\Delta H_{dyn}(t)$	: Dynamical error (radio altimeter)
$\Delta H_F(t)$	: Fluctuation error (radio altimeter)
ΔH_I	: Measurement error of the altitude
$\Delta H_{ins}(t)$	: Hardware error (radio altimeter)
ΔH_R	: Error of finding altitude (radio altimeter)
$\Delta H_S(t)$	: Shift of the mean value (radio altimeter error)
ΔQ_a	: Spot area diameter (radio altimeter)
Δt	: Discrete time
$\Delta t_{\hat{R}_I}$	: Time delay of the backscattering signals
ΔW_z	: Measurement error of the vertical speed
ϕ	: System transfer matrix
σ_H^2	: Error variance (radio)
v	: Pitch angle
γ	: Roll angle
$\gamma(k)$	: Independent variable
Ω	: Confidence interval

INTEGRATED RADIO-INS ALTIMETER DEVELOPMENT VIA KALMAN FILTERING

SUMMARY

In this study, the integrated navigation system, consisting of radio and INS altimeters, is presented. INS and the radio altimeter have different benefits and drawbacks. While having outstanding high frequency characteristics, the INS is a dead-reckoning system, at which the errors accumulate time by time. The radio altimeter, as a stand-alone system, gets timely updated measurements, but as it has an indolent principle of operation, it generates dynamical errors. The reason for integrating these two navigators is mainly to combine the best features, and eliminate the shortcomings, briefly described above.

The integration is achieved by using an indirect Kalman filter. Hereby, the error models of the navigators are used by the Kalman filter to estimate vertical channel parameters of the navigation system. In the open loop system, INS is the main source of information, and radio altimeter provides discrete aiding data to support the estimations. In this manner, the protection for computation failures of the Kalman filter is attained at the design level.

The simulation results demonstrate successful operation of the Kalman filter, thus the integrated altimeter. The filter is able to generate very close estimates to the model parameters through the entire simulation.

At the next step of the study, in case of abnormal measurements, the performance of the integrated system is examined. The optimal Kalman filter reacts with *abnormal* estimates to this situation as expected. To recover such a possible malfunctioning, the *Robust Kalman Filter* algorithms are suggested. In the fist algorithm, when the abnormal measurement is detected, it is disregarded, and instead of estimated value, extrapolation value is used. In the second algorithm, rather than the abnormal measurement, the limit value determined with the confidence probability is used.

These two algorithms are analyzed side by side. The results point out the better response of the first robust algorithm in case of abnormal measurements.

Regarding the given facts, the integrated navigation system described and developed in this study has acceptable benefits to be used in aviation applications.

BİRLEŞTİRİLMİŞ RADYO-INS ALTİMETRESİNİN KALMAN FİLTRESİ KULLANILARAK GELİŞTİRİLMESİ

ÖZET

Bu çalışmada, radyo ve atalet altimetrelerinden oluşan birleştirilmiş bir navigasyon sistemi tanıtılmıştır. INS ve radyo altimetrelerinin birbirlerinden farklı avantaj ve dezavantajları bulunmaktadır. Çok olumlu yüksek frekans karakteristiğinin yanında, INS, hataların zamanla üst üste eklendiği 'dead-reckoning' şeklinde tanımlanan bir sistemdir. Tek başına çalıştığında radyo altimetre zamanla yenilenen ölçümler alır, fakat ataletli bir çalışma prensibi olduğu için dinamik hatalar oluşturur. Bu iki navigasyon aletini birleştirmenin de ana sebebi yukarıda kısaca belirtilen olumlu özellikleri bir araya getirip, olumsuzları ortadan kaldırmaktır.

Birleştirme indirekt Kalman filtresi kullanılarak gerçekleştirilmiştir. Navigasyon aletlerinin hata modelleri Kalman filtresi tarafından düşey kanal parametrelerinin tahmin edilmesi için kullanılmaktadır. Açık çevrim sistemde INS ana bilgi kaynağı olurken, radyo altimetere tahminlere yardımcı olacak ayrık zamanlı bilgiyi sağlar. Böylelikle dizayn aşamasında, Kalman filtresinde meydana gelebilecek hesaplama hatalarına karşı sistemin korunması sağlanmıştır.

Simulasyon sonuçları Kalman filtresinin, dolayısıyla birleştirilmiş sisteminin başarıyla çalıştığını göstermektedir. Simulasyon boyunca filtre, model parametrelerine çok yakın tahminler üretebilmektedir.

Çalışmanın ikinci basamağında anormal ölçümler olması durumu incelenmiştir. Önceki Kalman filtesi beklendiği üzere bu duruma anormal tahminlerle karşılık vermektedir. Böyle muhtemel bir bozukluğu gidermek için *Robust Kalman Filtresi* algoritmaları önerilmektedir. Birinci robust filtrede anormal ölçüm tesbit edildiginde ihmal edilir ve tahmin edilen değer yerine ekstrapolasyon değeri kullanılır. İkinci algoritmada ise tesbit edilen anormal ölçüm yerine, bu ölçümün yüksek güvenilir olasılık ile saptanmış sınır değeri kullanılır.

Bu iki algoritmanın karşılaştırmalı analizi yapılmıştır. Sonuçlar anormal ölçüm durumunda ilk algoritmanın daha iyi sonuçlar verdiğini ortaya çıkarmaktadır.

Belirtilen koşullara göre, çalışmada açıklanan ve geliştirilen birleştirilmiş navigasyon sistemi, havacılık uygulamalarında kullanılması durumunda kabul edilebilir yararlar sağlayacaktır.

1. INTRODUCTION

Navigation is the process of determining significant position, velocity, attitude, and time (PVAT) information relative to specified references. Guidance is the process of using navigation information to steer or maneuver in an intelligent way.

Three types of navigation came to these days: celestial navigation, deduced reconnaissance, (commonly called dead reckoning), and pilotage. Today, modern airborne navigation systems are classified as either autonomous or position fixing, passive or active, stand-alone or aided, analog or digital. An autonomous passive system, such as an inertial guidance system, provides reasonably accurate instantaneous PVAT output with no dependence on any external man-made device or signal; that is, it is neither jammable nor capable of being sensed from outside the vehicle. Stand-alone navigation systems, on the other hand, usually require externally provided electro magnetic signals from ground-based radio navigation aids (NAVAIDS) or from space-based satellites [1].

1.1 Navigation Systems Overview

Regarding the issue of this study, navigation systems can be categorized as positioning and dead-reckoning. In the further sections, examples for both categories will be discussed in stand-alone and integrated type.

Positioning systems measure the state vector without regard to the path traveled by the vehicle in the past. There are three kinds of positioning systems:

1. Radio systems. They consist of a network of transmitters (sometimes also receivers) on the ground, in satellites or on other vehicles. The airborne navigation set detects the transmissions and computes its position relative to the known positions of the stations in the navigation coordinate frame. The aircraft's velocity is measured from the Doppler shift of the transmissions or from a sequence of position measurements.

2. Celestial systems. They compute position by measuring the elevation and azimuth of celestial bodies relative to the navigation coordinate frame at precisely known times. Celestial navigation is used in special-purpose high-altitude aircraft in conjunction with an inertial navigator.

3. Mapping navigation systems. They observe images of the ground, profiles of altitude, or other external features.

Dead-reckoning navigation systems derive their state vector from a continuous series of measurements relative to an initial position. There are two kinds of dead-reckoning measurements:

1. Aircraft heading and either speed or acceleration. For example, heading can be measured with gyroscopes or magnetic compasses, while speed can be measured with air-data sensors or Doppler radars. Vector acceleration is measured with inertial sensors.

2. Emissions from continuous-wave radio stations. They create ambiguous lanes that must be counted to keep track of coarse position. Their phase is measured for fine positioning. They must be reinitialized after any gap in the radio coverage.

Dead-reckoning systems must be re-initialized as errors accumulate and if electric power is lost.

The navigation-system designer conducts trade-offs for each aircraft and mission to determine which navigation systems to use. Trade-offs consider the following attributes:

1. Cost. Included are the construction and maintenance of transmitter stations and the purchase of on-board hardware and software. Users are concerned only with the cost of on-board hardware and software.

2. Accuracy of position and velocity. This is specified in terms of the statistical distribution of errors as observed on a large number of flights. The accuracy of military systems is often characterized by circular error probable, in meters or nautical miles. For civil aircraft carriers, the allowable en-route navigation error is based on the calculated risk of collision. This error depends on runway width, aircraft handling characteristics and flying weather.

3. Autonomy. This is the extend, to which the vehicle determines its own position and velocity without external aids. Autonomy is important to certain military vehicles and to civil vehicles operating in areas of inadequate radio-navigation coverage. Autonomy can be subdivided into five classes:

   a. Passive self-contained systems that neither receive nor transmit electromagnetic signals. They emit no radiation that would betray their presence and require no external stations. Failures are detected and corrected on-board. They include dead-reckoning systems such as inertial navigators.

   b. Active self-contained systems that radiate but do not receive externally generated signals. Examples are radars and sonars. They do not depend on the existence of navigation stations.

   c. Receivers of natural radiation. These systems measure naturally emitted electromagnetic radiation. Examples are magnetic compasses, star trackers, and passive map correlators. Some unmanned military weapons guide themselves toward acoustic emissions. These systems do not announce their presence by emitting, nor do they need navigation stations.

   d. Receivers of artificial radiation. These systems measure electromagnetic radiation from Earth based or space based navaids, but do not themselves transmit. Examples are LORAN, Omega, VOR, and GPS.

   e. Active radio navaids that exchange signals with navigation stations. These include DME, JTIDS, and collision-avoidance systems. The vehicle betrays its presence by emitting and requires cooperative external stations. These are the least autonomous of navigation systems.

4. Time delay in calculating position and velocity, caused by computational and sensor delays. Time delay can be caused by computer-processing delays, scanning by a radar beam, or gaps in satellite coverage as an example [2].

1.2 Integrated Systems

Integrated navigation systems combine the best features of both autonomous and stand-alone systems and are not only capable of good short-term performance in the autonomous or stand-alone mode of operation, but also provide exceptional performance over extended periods of time when in the aided mode. Integration thus brings increased performance, improved reliability and system integrity, and of course increased complexity and cost. Moreover, outputs of an integrated navigation system are digital, thus they are capable of being used by other resources of being transmitted without loss or distortion.

1.3 Past Studies

The new century's improvements in computer technology, and increased data processing rates brought the ability to improve the navigation systems of air vehicles in precision, correctness and reliability.

The integrated navigation systems concept with the application of the Kalman filter was a milestone, and we were witnesses to these improvements in the near past. A great amount of study has already been made about this issue. Many more seem to be observed in the future. As many of these studies were examined, and some useful information was reached.

In the paper of Robert A. Gray and Peter S. Maybeck dated 1995, named as 'An Integrated GPS/INS/Baro and Radar Altimeter System for Aircraft Precision Approach Landings', integrated navigation system issue has been discussed. In the abstract of the paper it is stated that, with the demand from the aviation industry, Instrumental Landing Systems (ILS) tend to be improved. This could not only be through replacement with the Microwave Landing System (MLS), but also by integrating Global Positioning System to the ILS that is practically in service.

Due to the paper, the majority of current precision landing research has exploited stand-alone GPS receiver techniques. This paper, as an improvement, exploits the possibilities of using and Extended Kalman Filter (EKF) that integrates an Inertial Navigation System (INS), GPS, Barometric Altimeter, and Radar Altimeter for precision aircraft approaches. As a result, it is seen that Federal Aviation Authority (FAA) requirements for Category I and II approaches could be met through this new approach.

The work in the paper is conducted through a computer simulation. The simulation program is basically developed on Kalman filter algorithms. The plotted outputs are generated by the commercial software package MATLAB. In this manner, regarding the subject and the tools, this paper is very close to the issue discussed in this study [3].

In the paper of K. Deergha Rao dated 1997, named as 'Integration of GPS and Baro-Inertial Loop Aided Strapdown and Radar Altimeter', development of a Kalman filter for optimal combination of GPS, INS and Radar Altimeter data is presented.

Due to the paper, being two independent navigation systems, GPS and INS have their own shortcomings when used in a stand-alone mode. The ever-growing drift in position accuracy of the INS, and the possible unavailability of the GPS signals are discussed. The author suggests that, these shortcomings would be eliminated, and each system's best performances combined through the Kalman filter.

The benefits of integrating GPS with a strapdown INS are significant. However, altitude accuracy can further be improved by integrating the GPS, baro-inertial loop aided strapdown INS, and radar altimeter data. An error model of the strapdown INS plays an important role in the development of a Kalman filter for optimal combination of navigation data provided by GPS, strapdown INS and radar altimeter.

Integrating the error models of each system with the use of the Kalman filter simulates this. The simulation results show an undeniable improvement in the demanded properties. The approach, tools and the data are identical to the ones in this study and the results are somehow in the same manner [4].

Another work on the integration of INS and GPS was done by a group of scientists at the Technical University of Darmstadt. The group named 'High Precision Navigation' showed some experimental effort to prove the improvement of navigation parameters in an integrated navigation system. The main tool was the Kalman filter as usual, but this time the attitude of the vehicle was monitored as shown in their paper dated 1994 [5].

NASA was also interested in the application of Kalman filter in the navigation systems. The need for the precision altitude determination at low altitude flight phases was the main issue. On a multi-sensor navigation suite, again using Kalman filter as the main tool for integrating navigation data from different origins, radar altimeter and INS data was used for selecting the most similar digital map profile in obtaining horizontal position.

A close subject was discussed by a working group of NASA and U.S. Army in 1993. The improvement of a terrain-referenced guidance system with the implementation of radar altimeter into the traditional navigation system by the help of the Kalman filter was exploited. Starting from mathematical models, this group was able to accomplish some flight tests and experiments on a Blackhawk Helicopter, as a navigation test bed [6,7].

Starting from the famous paper of Kalman dated 1960, many efforts could be found in the navigation improvements history, about Kalman filter and integrated navigation systems. This is a very rapid development, and the future trend seems to climb and accelerate about the integrated navigation systems.

1.4 Advances In This Study

The integrated systems designed in the past studies do not have robust character towards abnormal measurements. Generally, more than 10% of the radio measurements, and 5% of the whole navigation measurements are expected to be abnormal in the navigation systems. In some measurement periods, the abnormal rate of the radio measurements might exceed %10. This fact certainly decreases the efficiency of most of the standard statistical processing methods [8].

Thus, these abnormal measurements resulting from some possible failures at the measurement channels significantly decrease the effectiveness of the integrated navigation systems. In this study, to overcome such a problem, design of an integrated system, which is robust to the abnormal measurements, is intended as an improvement.

2. INERTIAL NAVIGATION SYSTEM

2.1 Introduction

Inertial navigation is a technique for determining a vehicle's position and velocity by measuring its acceleration and processing the acceleration information in a computer. Starting at a non-moving position, by adding the position change in all directions, vehicle position and attitude is determined. Instantaneous acceleration is measured, and then converted to velocity and position information.

In the general application of inertial navigation systems, an alternative navigation source is used to carry out navigation and control purposes collectively, where these accompanying sources are air data systems. This integration is in such a way that, in the navigation systems of the modern airliners, these two systems are tightly bonded to each other, forming the aircraft's main navigation system for attitude and direction determination.

The techniques of inertial navigation evolved from the marine gyrocompass, and conventional aircraft instrumentation. The earliest practical applications were ballistic-missile-guidance systems and ship's inertial navigation systems. The increased procurement of military aircraft led the development of aircraft inertial navigators. Many disadvantages of inertial systems could be eliminated through aiding with other sensors such as GPS, radars and star-trackers. Coming to our days, inertial navigation systems are widely used in military vehicles. Many ships, submarines, guided missiles, space vehicles, and virtually all modern military aircraft are equipped with inertial navigation systems due to the fact that, they cannot be jammed or spoofed. Large commercial airliners routinely make use of inertial systems for navigation and steering [2].

2.2 Inertial Navigation System Definitions

'Inertial Navigation System' (INS) is a system that provides navigation information without the help of any external navigation source. Although in most of the references, the term 'INS' is used for such systems, in practical applications some other terms are used instead of, or together with this definition.

As mentioned before, in the general application, INS is accompanied by other navigation systems for providing navigation information. The general term for these *combined* systems is *Attitude and Direction Systems*. The system, where position, velocity and acceleration are sensed inertially is called *Inertial Reference System* (IRS). The component, in which the inertial navigation technique is applied, is called *Inertial Reference Unit* (IRU) [9]. In Figure 2.1, one of the three IRU's of an A310 aircraft is shown.

Through the coverage of this study, any of these terms could be used, but the 'INS' is chosen. It should be noted that, the integrated navigation system that will be introduced in the following sections is in demand of altitude, vertical speed, and vertical acceleration information from any kind of an inertial system's vertical channel. The rest of the navigation parameters that are available at the inertial system are somehow useless in this study.

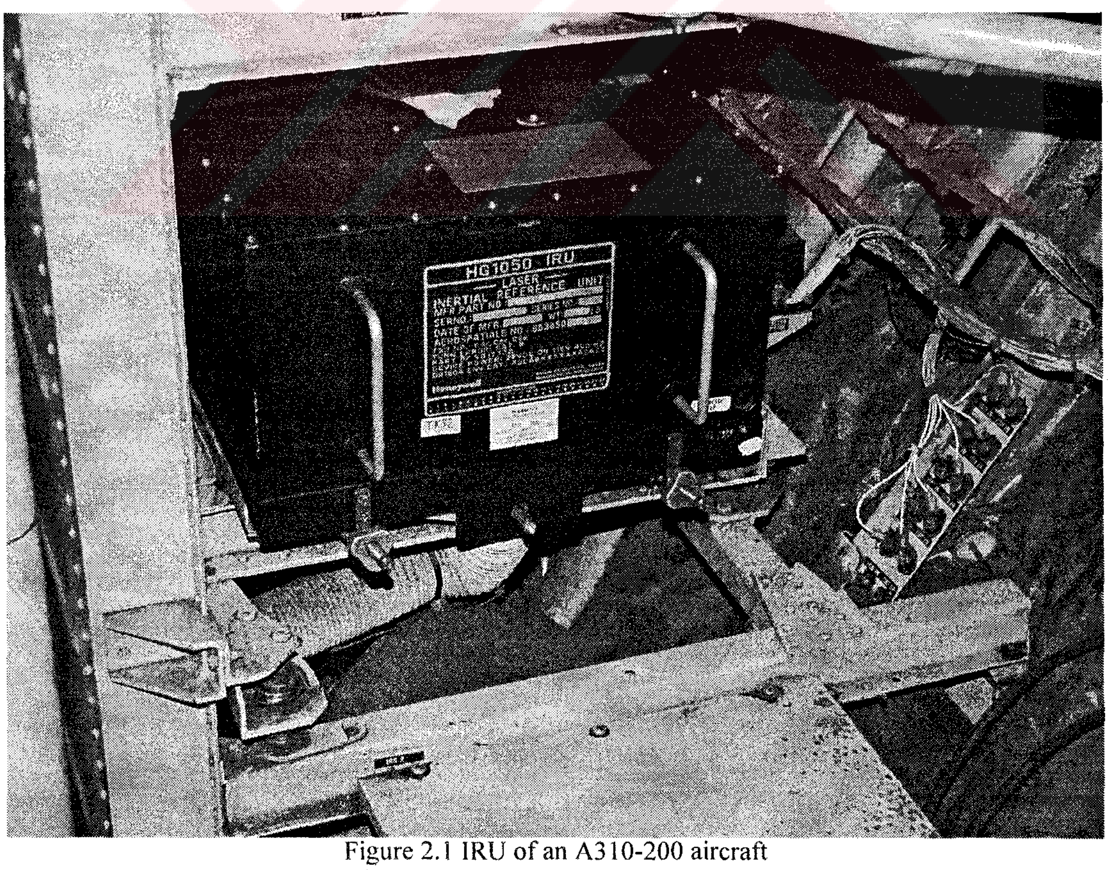

Figure 2.1 IRU of an A310-200 aircraft

2.3 INS Development

In the earliest inertial navigation systems, gimballed platforms isolated the instruments from the angular motions of the vehicle. The gyroscopes acted as null-sensors, driving gimbal servos that held the gyroscopes and accelerometers at a fixed orientation relative to Earth. This permitted the accelerometer outputs to be integrated into velocity and position. In the late 1970s and early 1980s, the invention of large-dynamic-range gyroscopes and of more powerful airborne computers permitted the development of *strapdown* inertial systems in which the gyroscopes and accelerometers were mounted directly on the vehicle. The gyroscopes track the rotation of the vehicle, and algorithms in the computer transform accelerometer measurements from vehicle coordinates to the navigation coordinates, where they can be integrated. In strapdown systems, the transformation generated by the computer performs the angular-stabilization function of a gimbal set in a platform system [1].

2.4 INS Mechanization

A platform (either gimballed or analytic) measures acceleration in a coordinate frame that has a prescribed orientation relative to Earth. Usually, the stabilized coordinate frame is locally level (two horizontal axes, one vertical). The computer, which may be the aircraft's central computer or navigation computer, calculates the aircraft's position and velocity from the outputs of the two horizontal accelerometers. The computer also calculates gyroscope-torquing signals that maintain the platform in the desired orientation relative to Earth. In a strapdown system, the analytic platform is torqued computationally. A vertical accelerometer is usually added in order to smooth the indication of altitude, as measured by a barometric altimeter or air-data computer.

In a platform system, the gimbal-isolated structure, on which the gyroscopes and accelerometers are mounted, is called the *stable element*. The gimbals allow the aircraft to rotate without disturbing the attitude of the stable element. The gimbal angles are measured by transducers, usually resolvers whose outputs indicate the aircraft's roll, pitch and heading to the displays, autopilot, and sometimes to the computer. In strapdown systems, attitude angles are mathematically extracted from the analytic platform transformation matrix.

When the inertial system is turned on, it must be aligned so that the computer knows the initial position and groundspeed of the vehicle, and so that the platform (gimballed or analytic) has the correct initial orientation relative to the Earth. The platform is typically aligned in such a way that, its accelerometer input axes are horizontal, often with one of them pointed north. As the vehicle accelerates, maneuvers, and cruises, the accelerometers measure changes in velocity, and the computer faithfully records the position and velocity. The general block diagram of an inertial navigator is given in Figure 2.2 [2].

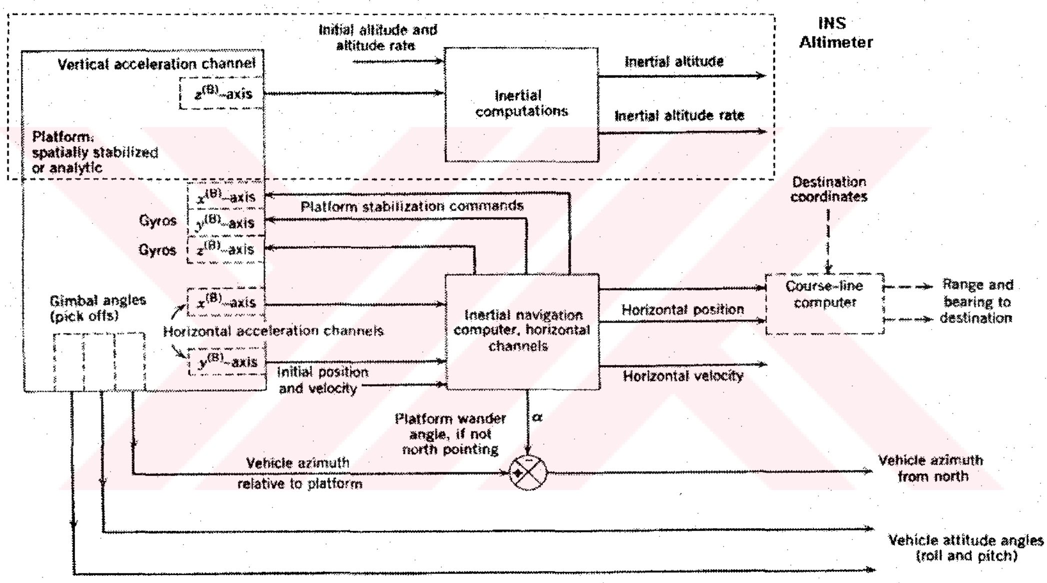

Figure 2.2 General block diagram of an inertial navigator [2]

2.5 Advantages and Shortcomings of the INS

Compared with other sources of navigation, an inertial navigator has the following advantages.

1. Its indications of position and velocity are instantaneous and continuous. High data rates and bandwidths are easily achieved.
2. It is completely self-contained, since it is based on measurements of acceleration and angular rate made within the vehicle itself. It is nonradiating and nonjammable.

3. Navigation information (including azimuth) is obtainable at all latitudes (including polar regions), in all weather, without the need for ground stations.

4. The inertial system provides outputs of position, ground speed, azimuth, and vertical. It is the most accurate means of measuring azimuth and vertical on a moving vehicle.

The disadvantages of the inertial navigators are the following.

1. The position and velocity information degrades with time. This is true, whether the vehicle is moving or stationary.

2. The equipment is expensive compared to other avionics devices.

3. Initial alignment is necessary. Alignment is simple on a stationary vehicle at moderate latitudes, but it degrades at high latitudes and on moving vehicles.

The accuracy of navigation information is somewhat dependent on vehicle maneuvers [2].

2.6 Inertial Navigation System Errors

Fundamentally, a navigation system regardless of type will output estimates of position (latitude, longitude, and height), velocity (North, East, and Down), and attitude (heading, pitch angle, roll angle). These estimates will have two types of errors associated with them; initial errors that result from the inherent accuracies of the devices and the medium through which they operate, and propagation errors that increase in time between system update measurements. Inertial navigation systems are the very first examples to produce these propagation errors.

2.6.1 Error Analysis

After mechanizing an inertial navigation system, the designer must investigate the propagation of errors in the proposed system, based on mathematical analysis and on the results of the past tests. The error analysis establishes the maximum permissible component tolerances; to simplify the mechanization equations (and thus the computer complexity) when advantageous; and to predict compliance with the position, velocity, attitude, and azimuth specifications established by the user.

The error that should be considered in performing analysis depends on the system design, the components used, and the required accuracy of the navigation system. Some types errors are given below.

1. Gyro drift errors caused by temperature variation, acceleration, magnetic fields and vibration.
2. Gyro scale factor errors including nonlinearity and asymmetry.
3. Accelerometer bias errors caused by variations in temperature or by rectification of vibration inputs. Accelerometer resonance and dynamic response are important considerations.
4. Accelerometer scale factor errors including nonlinearity and asymmetry.
5. Sensor assembly errors such as nonorthogonality of the gyro and accelerometer input axes, transmission of vibration inputs through the shock mounts, and thermal gradients that affect instrument performance and alignment.
6. Computational errors due to round off, truncation, readout accuracy, as well as approximations in the algorithms. Detailed evaluation of computational error propagation often requires a bit-by-bit simulation.
7. Initial condition errors (position, velocity, tilt, and azimuth) must be considered as they propagate with time.

Error analysis is performed by assuming a flight path and processing the resulting acceleration and angular-rate profile in a mathematical model of the inertial system and computer. The indicated positions and velocities are compared to the assumed flight path, and the error histories are recorded. Azimuth and tilt errors can similarly be derived. Analyses are done either with fixed instrument errors or with statistically distributed errors in a large number of runs [2].

2.6.2 INS Error Sources

Two fundamental error sources affect the error behavior of an inertial system. These are,

1. The errors in the measurements of force made by the accelerometers.

2. The errors in the measurement of angular change of orientation with respect to inertial space made by the gyroscopes.

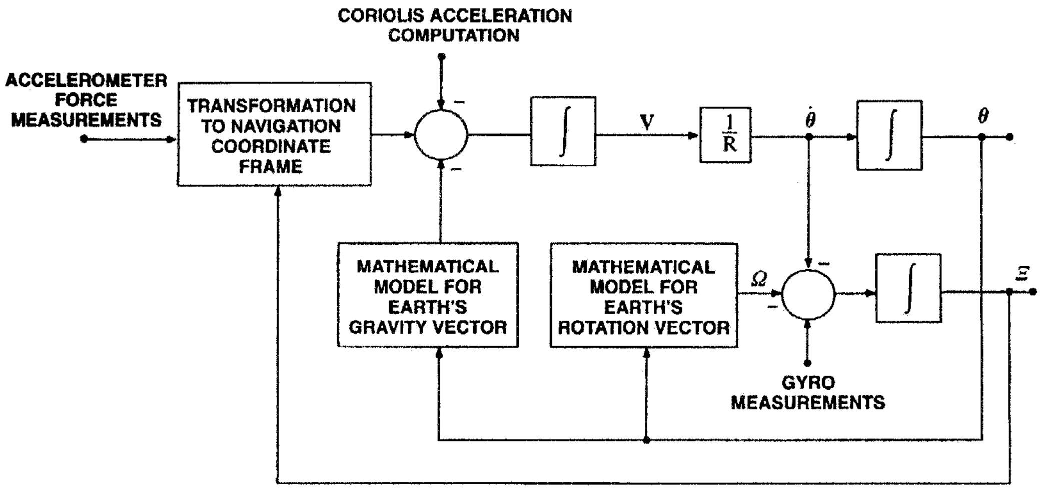

R– LOCAL RADIUS OF EARTH'S CURVATURE
V – SYSTEM COMPUTED VELOCITY
$\dot{\theta}$ – SYSTEM COMPUTED ANGULAR RATE OF CHANGE OF POSITION (θ) OVER THE EARTH'S SURFACE
Ω – SYSTEM COMPUTED EARTH RATE VECTOR
Ξ – SYSTEM COMPUTED ACCELEROMETER SENSING AXES ORIENTATION WITH RESPECT TO THE NAVIGATION COORDINATE SYSTEM

Figure 2.3 Basic mechanization of an inertial system [2]

In the basic mechanization of an inertial system, that is given in Figure 2.3, it is seen that the force measurements made by accelerometers are first transformed to a selected navigation coordinate frame that is typically the local geodetic coordinates of east, north and local vertical. These measurements are then compensated for the force of gravity with a mathematical model, such that vehicle acceleration with respect to inertial space is obtained. The resulting variable, after correction for Coriolis acceleration, is then integrated once into velocity and a second time into position change with respect to the Earth. Additionally, the gyroscopic measurements of angular change with respect to inertial space are modified using the system computed velocity and the Earth's rotation rate vector to reflect the rotation of the local vertical due to earth rotation and the vehicle change in position as it travels over the surface of the Earth. In this manner, the orientation of the accelerometer axes relative to Earth at the present position of the vehicle is continuously computed. The result is that, there are three sources of change in orientation error of the accelerometers with respect to Earth-fixed reference coordinate frame.

1. Integrated gyro drift rate.
2. Integrated error in system computed velocity which results from error in the measurement of acceleration – due to accelerometer measurement errors, imperfect knowledge of the local force of gravity and the current error in the knowledge of orientation of the accelerometer sensing axes which causes a misresolution of any accelerometer force measurement including that of the gravity vector.
3. Error in the orientation of the navigation coordinate axes which changes as they rotate with respect to inertial space.

Clearly inertial systems tend to 'drift off' in terms of the accuracy in the system computed navigation variables of position, velocity and orientation over an extended time of operation. Consequently other sensors are used with inertial systems to arrest this divergent error behavior for those applications that require upper bounds with system error with time. It is the usual case that an inertial system remains as the core element of an integrated aircraft navigation system because it offers the unique properties of being self contained on the vehicle and stealthy in that produces no emissions, cannot be jammed, or deceived because it has no reliance on signals generated by external sources; the inertial system is normally required to provide a continuous high-bandwidth reference coordinate system relative to Earth whose use is required by other avionics sensors [1].

2.7 INS Error Model, The Altimeter

Having numerous output parameters out of different channels, the INS has a complex error model. This model is nevertheless useless in this study, because the issue covers the INS altimeter. For this reason, only the vertical channel of the INS is considered.

Although the subject is about the INS altimeter, not only the vertical position (altitude), but also the other vertical channel parameters will be discussed, and included in the calculations. The INS vertical channel parameters are,

1. Vertical position (altitude). H_I
2. Vertical speed. W_z

3. Vertical acceleration. a_z

4. Gravitational acceleration. g

The system design in the following sections will be in discrete form, so the Kalman filter. The linear and discrete error model of the INS altimeter is given as follows [9].

$$\Delta H_I(k) = \Delta H_I(k-1) + \Delta t \Delta W_z(k-1) \tag{2.1}$$

$$\Delta W_z(k) = \Delta W_z(k-1) + \frac{2g\Delta t}{R}\Delta H_I(k-1) + \Delta t \Delta a_z(k-1) + \Delta t \Delta g(k-1) \tag{2.2}$$

$$\Delta a_z(k) = \Delta a_z(k-1) - \Delta t \alpha \Delta a_z(k-1) + \Delta t U_{\Delta a_z}(k-1) \tag{2.3}$$

$$\Delta g(k) = \Delta g(k-1) - \Delta t \beta_g \Delta g(k-1) + \Delta t U_{\Delta g}(k-1) \tag{2.4}$$

In the error model expressions, the following are the explanations for the terms.

$\Delta W_z(k-1)$	:	Measurement error of the vertical speed
$\Delta H_I(k)$	:	Measurement error of the altitude
$\Delta a_z(k-1)$	:	Measurement error of the vertical acceleration
$\Delta g(k-1)$	:	Measurement error of the gravitational acceleration
$U_{\Delta a_z}(k-1)$	:	White Gauss noise with zero mean
$U_{\Delta g}(k-1)$	:	White Gauss noise with zero mean
β_g	:	The term for the correlation period
Δt	:	Discrete time

3. RADIO ALTIMETER

3.1 Introduction

The radio altimeter, which is named as radar altimeter in some references, is basically a device that provides data on the vertical position (altitude) of the aircraft. The radio altimeter system enables the aircraft height above the ground to be precisely and continuously determined, independently of the atmospheric pressure.

In the text, the terms *radio* and *radar* are used in combination. The meanings of radio and radar are in close interaction with each other in the coverage of this study. While some of the academic resources chose the word *radar*, most of the aircraft documents present this system as *radio altimeter system*, which is basically accepted in this study.

3.2 Radio Navigation Systems

There might be confusion, when the subject is the radio altimeter. There are different types of radio navigation systems, of which one is the radio altimeter. A basic classification of radio navigation systems would clarify the issue. These systems are basically divided into two, by means of their operating principles [10].

1. Radio navigation data dependent position determining.
2. Radio navigation data independent position determining.

3.2.1 Radio Navigation Data Dependent Position Determining

Within the operating principle of such systems, in addition to airborne systems on the aircraft, ground stations and installations are required for position finding.

The examples of these ‘ground station dependent’ systems are, Distance Measuring Equipment (DME), Air Traffic Control (ATC), Automatic Direction Finder (ADF), and VHF Omni-Range (VOR) systems.

3.2.2 Radio Navigation Data Independent Position Determining

This is the part of radio navigation, which is basically independent from ground installations, and provides data on the position of the aircraft.

This group of radio navigation instruments consists of these systems: Weather radar system, radio altimeter system, and the ground warning proximity system.

3.3 Radio Altimeter Functions

The basic function of the radio altimeter is to provide terrain clearance or altitude with respect to ground level directly beneath the aircraft. The altimeter may also provide vertical rate of climb or descent, and selectable low altitude warnings. Performance characteristics are designed to match particular applications. High-performance low-flying military aircraft and cruise missile systems require accurate altitude tracking at vertical rates of 2000 ft/sec while maintaining a high degree of covertness and jam immunity. Altimeters designed for terrain correlation for navigational purposes must process an extremely small ground illumination spot size at high altitudes to provide the required altitude resolution. Altitude marking radars are generally low altitude altimeters designed specifically to provide mark signals at specific altitudes for initiation of an automatic operation, such as fuze triggering on submunitions, or chute opening on lunar-landing systems. Radio altimeters for civil aviation are designed to support automatic landing, flare and touchdown computations. Figure 3.1 is the picture of one of the two radio altimeters of an A310 aircraft.

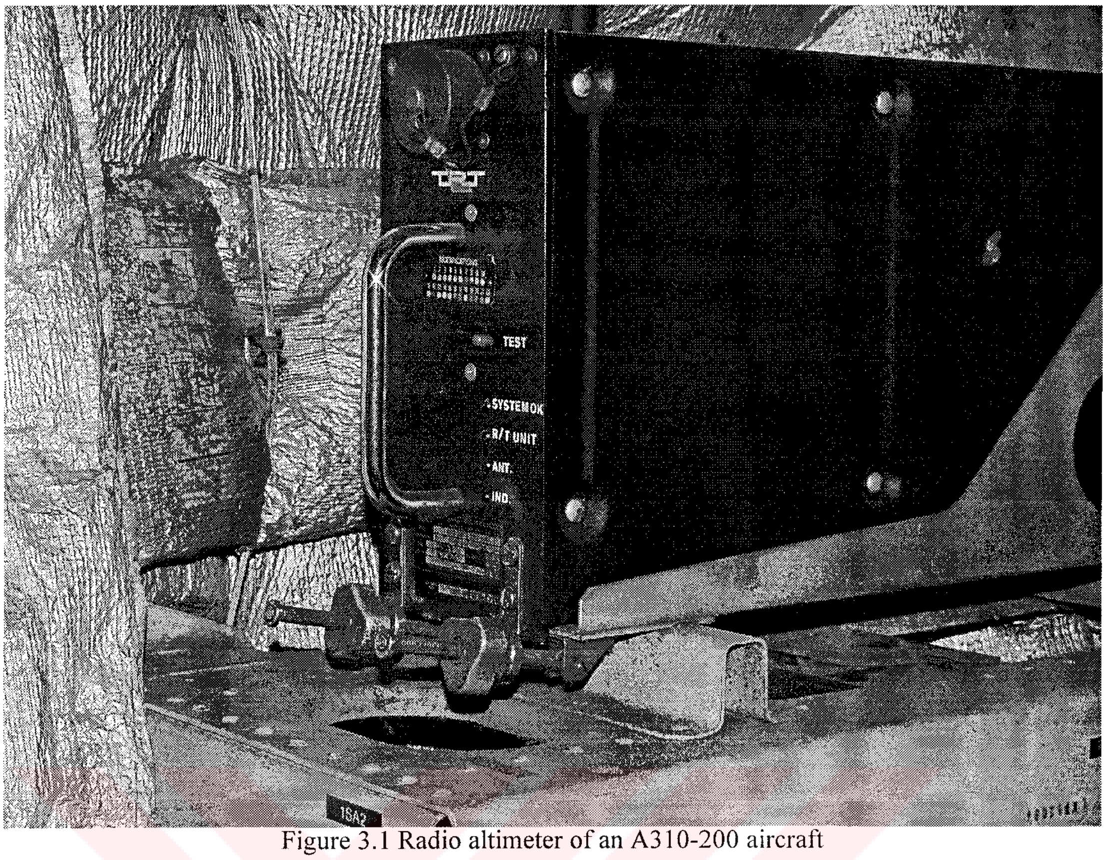

Figure 3.1 Radio altimeter of an A310-200 aircraft

Altimeters perform the basic function of a range measuring radar. A modulated signal is transmitted towards the ground. The modulation provides a time reference to which the reflected return signal can be referenced, thereby providing radar-range on time delay and therefore altitude. The ground represents an extended target, as opposed to a point target, resulting in the delay path extending from a point directly beneath the aircraft out to the edge of the antenna beam. Furthermore, the beam width of a dedicated radio altimeter antenna must be wide enough to accommodate normal roll-and-pitch angles of the aircraft, resulting in a significant variation in return delay [2].

A picture of the radio altimeter antennas of an A310-200 aircraft is given in Figure 3.2. These antennas are located at the backside of, and underneath the fuselage, so that any part of the aircraft does not obstacle the transmitted and received signals.

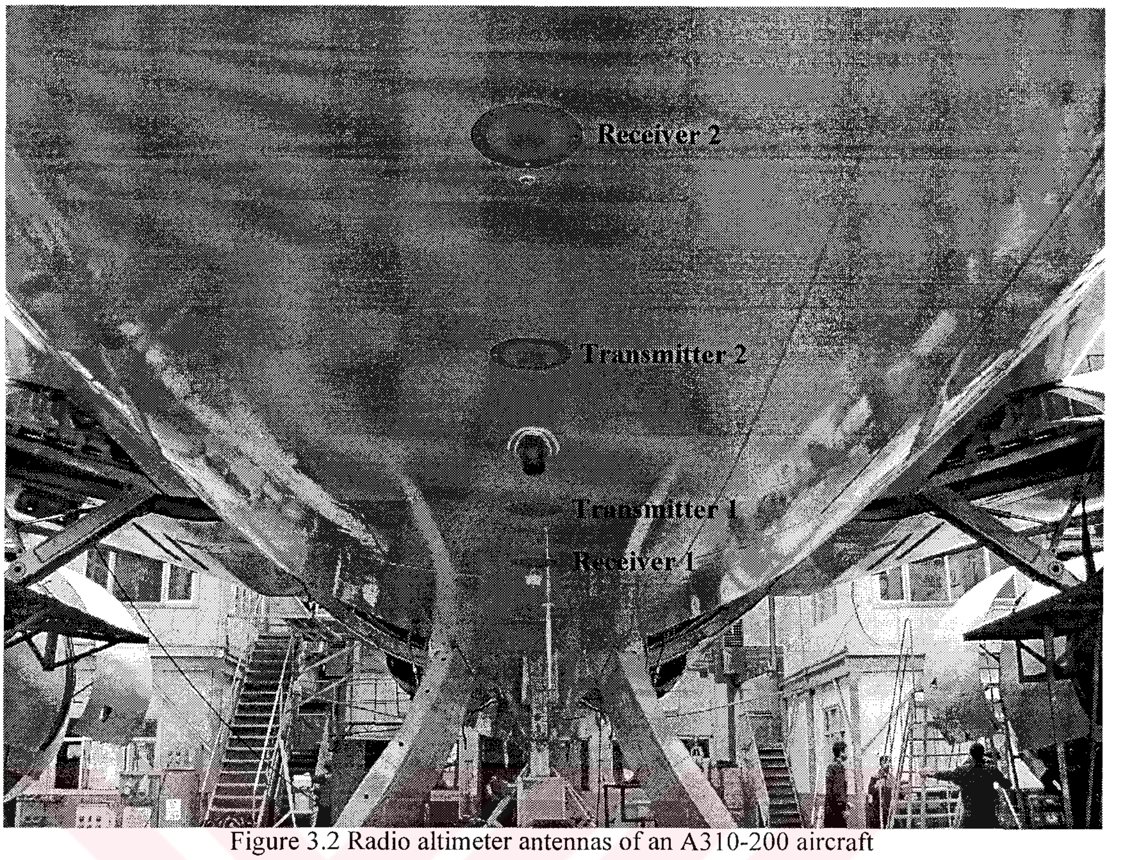

Figure 3.2 Radio altimeter antennas of an A310-200 aircraft

3.4 Radio Altimeter Errors

The following are the main groups of the errors that the radio altimeter generates [9].

Group 1, methodical errors. These errors are related with the following factors.

a. The random behavior of received signals.

b. Varying ground surface reflecting character through the entire flight.

c. The effect of aircraft's pitch and roll angles.

d. Signals fluctuations (vibrations) arising from electromagnetic wave propagation period.

e. Internal and external noise.

All of these types of errors could be distributed into two.

1. The error arising from the shift of the mean value of altitude measurement. ($\Delta H_S(t)$)

2. Fluctuation errors. ($\Delta H_F(t)$)

Group 2, dynamic errors. The dynamic errors at the radio altimeter arise because of the following reasons.

a. The effects of the maneuvers of the aircraft.

b. When the altitude is measured over areas where profiles are discontinuously varying, such as agricultural areas, forests, urban areas or high mountain peaks, the mathematical model of these surfaces cannot be differentiated.

c. As the radio altimeter is integrated in the flight control systems, its measurement has a certain order dynamical characteristic. This leads to a delay in the altitude measurement, so to an error. ($\Delta H_{dyn}(t)$)

Group 3, instrument errors. These errors arise when the $\Delta H_{ins}(t)$ signals pass through the antenna, measurement and transmission channels. These are related with the radio altimeter hardware, the models at the certain blocks of the whole system.

As a result, the output signal of the radio altimeter could the expressed as the following.

$$H(t) = H_g(t) + \Delta H_S(t) + \Delta H_F(t) + \Delta H_{dyn}(t) + \Delta H_{ins}(t) \tag{3.1}$$

Here in the expression (3.1), $H_g(t)$ is the real value of the altitude, the distance from the aircraft to the ground level.

The following is a more detailed classification for the error components that might occur in the radio altimeter.

3.5 Error Classification

3.5.1 Shifting of the Value

There are two main reasons for this type of error to occur.

First. Backscattering of the radio signals from a large surface area. At this condition, the signals will provide information not only about the flight altitude H_g, but also the angled distances from the surface ($R_1, R_2, ...R_i$). This is sketched at the Figure 3.3.

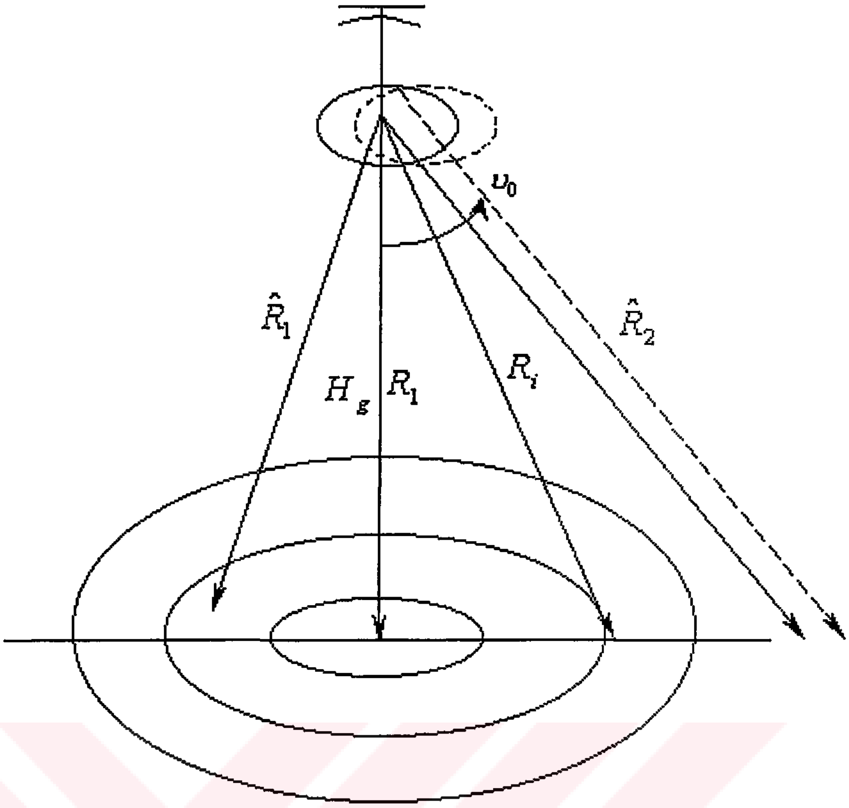

Figure 3.3 Backscattering of the radar signals [9]

When the altitude is calculated due to the time delay of the backscattering signals $\Delta t_{\hat{R}_1}$, the result will not be the altitude value H_g, but an angled distance from the surface $\hat{R}_1$. The value of the time delay depends on the statistical characteristic of the reflecting surface, spotting size of the radio antenna, parameters of the transmitted signals, and the processing method of the received signal.

There are two different methods for processing these signals, local and integrated.

In the local method, only the signals, which are close to the H_g normal, are chosen to be processed, and used in the calculations.

In the integrated method, to calculate the altitude value, all received signals are used.

Second. The effects of pitch and roll movements of the aircraft. Generally, the antenna of the radio altimeter is rigidly installed under the fuselage of the aircraft. In case of maneuvers, the angle change of the spot beam of the radio altimeter antenna v_0 causes a time delay at the received signal. In general applications, the information of the angle change resulting from pitch and roll movements is not fed back to the altimeter for correction. So, when the signal processing is carried out by the integrated method, the altitude value becomes $\hat{R}_2 > \hat{R}_1 > \hat{H}_g$. To minimize the shifting of the value, diameter of the radio altimeter's spot area is selected with trade-off between operational pitch and roll angles (ν, γ) of the aircraft.

$$\Delta Q_a \approx \gamma_{\max} \approx \nu_{\max} \tag{3.2}$$

Here, ΔQ_a is the diameter of the spot area of the radio altimeter antenna. $\hat{R}_1$ is the measured distance when the aircraft is in level flight. $\hat{R}_2$ is the measured distance at an angle change of ν_0.

The advantage of the local method is that, at this method ΔH_S errors are inversely proportional to the diameter of the transmitted signals spectrum (spot area) and independent from the altitude. At the integrated method, shifting of the value is linearly proportional to the flight altitude.

The varying landscape conditions beneath the flight route of the aircraft, when integrated method is applied, results to a slight shifting of the value in both directions around a mean (Figure 3.4). This shift will be practically constant, if the terrain conditions beneath the aircraft is continuous.

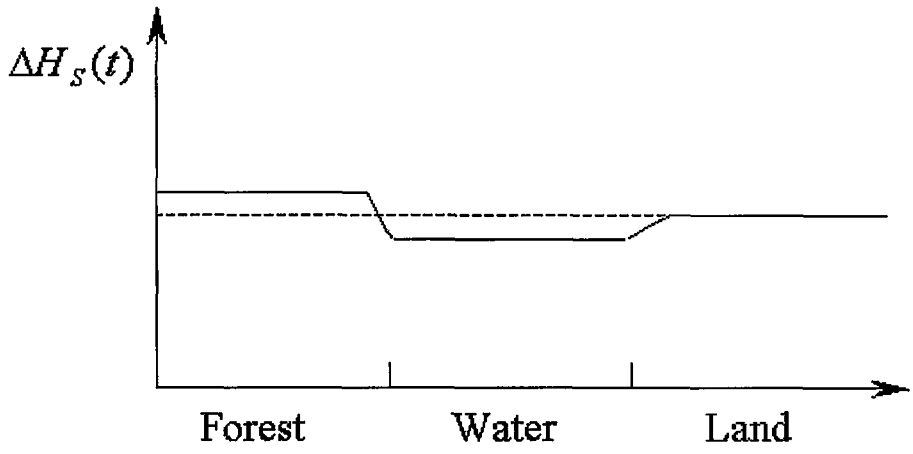

Figure 3.4 Shifting of the value above different terrain conditions [9]

3.5.2 Fluctuation Errors

This type of error arises from the transmitted signal fluctuations and the noise at the radio altimeter input. Generally, this error can be characterized by the variance σ_H^2, as it shows a normal dispersion. In the analysis's, it is seen that, at high signal/noise rates, the fluctuation error because of the signal components' vibrations is commonly observed at σ_H^2.

3.5.3 Dynamic Errors

The dynamic error for the radio altimeter is analogous to any measurement instrument's dynamic error. This type of error is observed, because in many applications, the response time and the inertia of such instruments might be slower than the rate of change in the measured parameters.

3.5.4 Instrument Errors

There are several reasons for the instrument errors. Heating, electrical supply deficiencies and instabilities, instant problems at certain blocks of the radio altimeter would be examples. A list of the most important errors of this type is given as follows.

a. The installation of transmitter and receiver antennas of the radar at non-optimal locations of the aircraft.

b. Instability of the signal and modulation frequencies, f_d, F_M. These are directly proportional with the altitude measurement error.

$$\Delta f_d / f_d = \Delta H / H \quad , \quad \Delta F_M / F_M = \Delta H / H$$

c. Ineffective receiver hardware. Irregular and unstable gain/frequency characteristic would lead to an error of this type.

d. Time delay measurement error (Impulse modulated radio altimeters) and modulation frequency measurement error (Frequency modulated radio altimeters). These errors are directly related with the deficiencies at the radar hardware such as gain, filter and period sensing instruments.

e. Altitude calculation error arising from time delay measurement.

f. Calibration errors of the radio altimeter. The values and the acceptable limits of these errors should be and generally given at the component documents.

3.6 Error Model, The Radio Altimeter

The error model of the radio altimeter, which will be used in our calculations, is as follows [9].

$$\Delta H_R(k) = \Delta H_R(k-1) - \Delta t \beta \Delta H_R(k-1) + \Delta t U_{\Delta H_R}(k-1) \tag{3.3}$$

In the error model expressions, the following are the explanations for the terms.

$\Delta H_R(k)$	:	Measurement error of the radio altitude
$U_{\Delta H_R}(k-1)$	:	White Gauss noise with zero mean
β	:	The term for the correlation period
Δt	:	Discrete time

4. KALMAN FILTER

4.1 Introduction

In 1960, R.E. Kalman published his famous paper [11] describing a recursive solution to the discrete-data linear filtering problem. Since that time, with the help of the advances in digital computing, the Kalman filter has been the subject of extensive research and application, particularly in the area of autonomous or assisted navigation [12].

Kalman filtering is an optimal state estimation process applied to a dynamic system that involves random perturbations. More precisely, the Kalman filter gives a linear, unbiased, and minimum error variance recursive algorithm to optimally estimate the unknown state of a dynamic system from noisy data taken at discrete real-time intervals. With the recent development of high-speed computers, the Kalman filter has become more useful even for very complicated real-time applications [13].

General applications of Kalman filter in navigation measurement processing could be practiced. The filter is used for the following tasks [14].

1. Minimizing the measurement errors and finding a better value of a measured parameter.
2. Integrating more than one sources of information.
3. Calculating the unknown parameters of the state vector of the aircraft.
4. Diagnosis of the errors that occur in an aircraft system.

4.2 Kalman Filter Basics

4.2.1 The Estimation Process

The Kalman filter addresses the general problem of trying to estimate the state $x \in \Re^n$ of a discrete-time controlled process that is governed by the linear stochastic difference equation [12].

$$x_k = Ax_{k-1} + Bu_k + w_{k-1} \tag{4.1}$$

with a measurement $z \in \Re^m$ that is

$$z_k = Hx_k + v_k \tag{4.2}$$

The random variables w_k and v_k represent the process and measurement noise respectively. They are assumed to be independent of each other, white, and with normal probability distributions.

$$p(w) \approx N(0, Q) \tag{4.3}$$

$$p(v) \approx N(0, R) \tag{4.4}$$

In practice, the process noise covariance Q and measurement noise covariance R matrices might change at each time step or the measurement, however it is assumed that, they are constant.

The n x n matrix A in the difference equation (4.1) relates the state at the previous time step k-1 to the state at the current state k, in the absence of either a driving function or process noise. Note that in practice A might change with each time step, but here we assume it is constant. The n x l matrix B relates the optional control input $u \in \Re^l$ to the state x. The m x n matrix H in the measurement equation (4.2) relates the state to the measurement z_k. In practice H might change with each time step or measurement, but here we assume it is constant.

4.2.2 The Filter Computations

We define $\hat{x}_k^- \in \Re^n$ (the super minus) to be our *a priori* state estimate at step k given knowledge of the process prior to step k, and $\hat{x}_k \in \Re^n$ to be the *a posteriori* state estimate at step k given measurement z_k. We can define *a priori* and *a posteriori* estimate errors as

$e_k^- \equiv x_k - \hat{x}_k^-$ and,

$e_k \equiv x_k - \hat{x}_k$

The *a priori* estimate error covariance is then,

$$P_k^- = E\left[e_k^- e_k^{-T}\right] \tag{4.5}$$

and the *a posteriori* estimate error covariance is,

$$P_k = E\left[e_k e_k^T\right] \tag{4.6}$$

In deriving the equations for the Kalman filter, we begin with the goal of finding an equation that computes an *a posteriori* state estimate $\hat{x}_k$ as a linear combination of an *a priori* estimate $\hat{x}_k^-$ and a weighted difference between an actual measurement z_k and a measurement prediction $H\hat{x}_k^-$ as shown below in (4.7).

$$\hat{x}_k = \hat{x}_k^- + K\left(z_k - H\hat{x}_k^-\right) \tag{4.7}$$

The difference $\left(z_k - H\hat{x}_k^-\right)$ in (4.7) is called the measurement *innovation*, or the *residual*. The residual reflects the discrepancy between the predicted measurement $H\hat{x}_k^-$ and the actual measurement z_k. A residual of zero means that the two are in complete agreement.

The n x m matrix K in (4.7) is chosen to be the *gain* or *blending factor* that minimizes the *a posteriori* error covariance (4.6). The minimization can be accomplished by first substituting (4.7) into the above definition for e_k, substituting that into (4.6), performing the indicated expectations, taking the derivative of the trace of the result with respect to *K*, setting that result equal to zero, and then solving for *K*. One form of the resulting *K* that minimizes (4.6) is given by,

$$K_k = P_k^- H^T \left(HP_k^- H^T + R\right)^{-1}$$

$$= \frac{P_k^- H^T}{HP_k^- H^T + R} \tag{4.8}$$

Looking at (4.8), we see that, as the measurement error covariance R approaches zero, the gain *K* weights the residual more heavily. Specifically,

$$\lim_{R_k \to 0} K_k = H^{-1}$$

On the other hand, as the *a priori* estimate error covariance P_k^- approaches zero, the gain K weights the residual less heavily. Specifically,

$$\lim_{P_k^- \to 0} K_k = 0$$

Another way of thinking about the weighting by K is that as the measurement error covariance R approaches zero, the actual measurement z_k is 'trusted' more and more, while the predicted measurement $H\hat{x}_k^-$ is trusted less and less. On the other hand, as the *a priori* estimate error covariance P_k^- approaches zero the actual measurement z_k is trusted less and less, while the predicted measurement $H\hat{x}_k^-$ is trusted more and more.

4.2.3 The Probabilistic Origins of the Filter

The justification for (4.7) is rooted in the probability of the *a priori* estimate $\hat{x}_k^-$ conditioned on all prior measurements z_k (Bayes' rule). We can point out that the Kalman filter maintains the first two moments of the state distribution.

$$E[x_k] = \hat{x}_k$$

$$E\left[(x_k - \hat{x}_k)(x_k - \hat{x}_k)^T\right] = P_k$$

The *a posteriori* state estimate (4.7) reflects the mean (the first moment) of the state distribution – it is normally distributed if the conditions of (4.3) and (4.4) are met. The *a posteriori* estimate error covariance (4.6) reflects the variance of the state distribution (the second non-central moment). In other words,

$$p(x_k | z_k) \approx N\left(E[x_k], E\left[(x_k - \hat{x}_k)(x_k - \hat{x}_k)^T\right]\right)$$

$$= N(\hat{x}_k, P_k)$$

4.2.4 The Discrete Kalman Filter Algorithm

The Kalman filter estimates a process by using a form of feedback control; the filter estimates the process state at some time and then obtains feedback in the form of (noisy) measurements. As such, the equations of the Kalman filter fall into two groups: *time update* equations and *measurement update* equations. The time update equations are responsible for projecting forward (in time) the current state and error covariance estimates to obtain the *a priori* estimates for the next time step. The measurement update equations are responsible for feedback – as an example for incorporating a new measurement into the *a priori* estimate to obtain an improved *a posteriori* estimate.

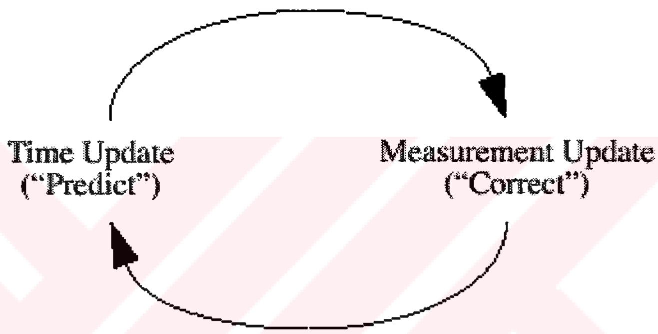

Figure 4.1 Prediction-correction cycle [12].

The time update equations can also be thought of as *predictor* equations, while the measurement update equations can be thought of as *corrector* equations. Indeed the final estimation algorithm resembles that of a *predictor-corrector* algorithm for solving numerical problems.

The specific equations for the time updates are,

$$\hat{x}_k^- = A\hat{x}_{k-1} + Bu_k \tag{4.9}$$

$$P_k^- = AP_{k-1}A^T + Q \tag{4.10}$$

and the measurement update equations,

$$K_k = P_k^- H^T \left(HP_k^- H^T + R\right)^{-1} \tag{4.11}$$

$$\hat{x}_k = \hat{x}_k^- + K_k\left(z_k - H\hat{x}_k^-\right) \tag{4.12}$$

$$P_k = \left(I - K_k H\right)P_k^- \tag{4.13}$$

It could be seen from the time update equations that they project the state and covariance estimates forward from time step k-1 to step k. A and B are from (4.1), while Q is from (4.3).

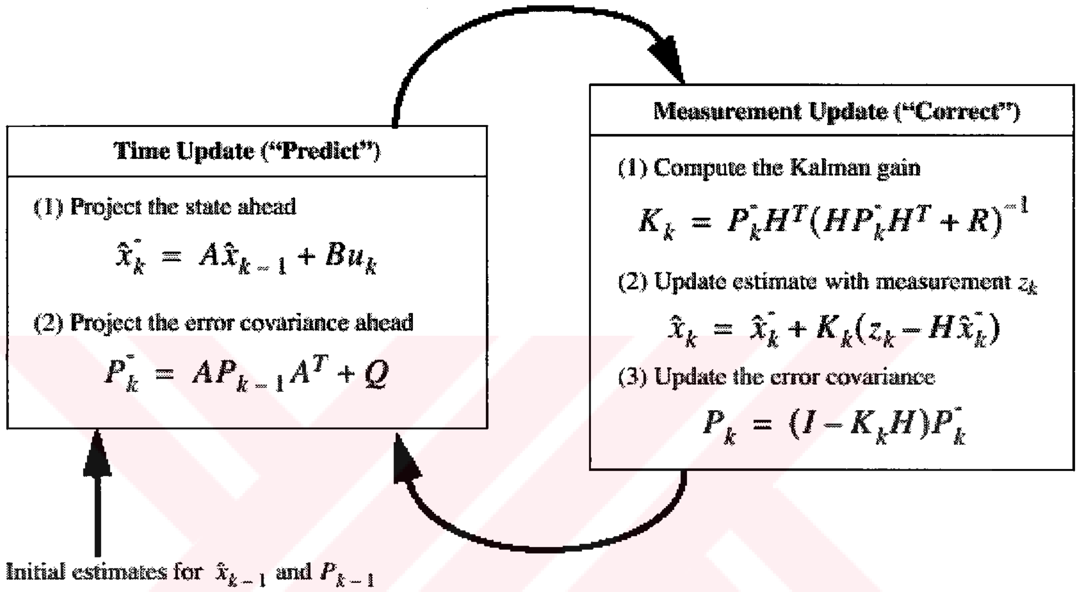

Figure 4.2 Measurement and estimation equations [12].

The first task during the measurement update is to compute the Kalman gain, K_k. Note that the equation given here as (4.11), is the same as (4.8). The next step is to actually measure the process to obtain z_k, and then to generate an *a posteriori* state estimate by incorporating the measurement as in (4.12). Again (4.12) is simply (4.7) repeated here for completeness. The final step is to obtain an *a posteriori* error covariance estimate via (4.13). The order of these calculations is shown in Figure 4.1 and 4.2.

After each time and measurement update pair, the process is repeated with the previous *a posteriori* estimates used to project or predict the new *a priori* estimates. This recursive nature is one of the very appealing features of the Kalman filter – it makes practical applications much more feasible than previous methods. Basically, the Kalman filter recursively conditions the current estimate on all of the past measurements.

4.3 Kalman Filter for The Integrated System

The Kalman filter designed for the integrated navigation system of this study is in one dimension. It is linear and discrete. The following are the final expressions of the Kalman equations to be used in the calculations [11].

$$\hat{X}(k/k) = \hat{X}(k/k-1) + K(k)\Delta(k) \tag{4.14}$$

$$\Delta(k) = Z(k) - H(k)\hat{X}(k/k-1) \tag{4.15}$$

$$K(k) = P(k/k-1)H^T(k)\left[H(k)P(k/k-1)H^T(k) + R(k)\right]^{-1} \tag{4.16}$$

$$\hat{X}(k/k-1) = \phi(k,k-1)\hat{X}(k-1/k-1) \tag{4.17}$$

$$P(k/k) = \left[I - K(k)H(k)\right]P(k/k-1) \tag{4.18}$$

$$P(k/k-1) = \phi(k,k-1)P(k-1/k-1)\phi^T(k,k-1) + G(k,k-1)Q(k-1)G^T(k,k-1) \tag{4.19}$$

The definitions of the terms at the Kalman equations are presented below.

$\hat{X}(k/k)$	:	$X(k)$'s estimation vector
$\hat{X}(k/k-1)$	:	Extrapolation value vactor
$K(k)$	:	Filter gain coefficient
$\Delta(k)$	:	Innovation sequence
$P(k/k-1)$	:	Extrapolation error's correlation vector
$P(k/k)$	:	Value error's correlation vector

4.4 Robust Kalman Filter

In case of a failure at the measurement channel of a system, a robust Kalman filter is developed to consider, and take action against these measurement errors.

In the linear dynamic system, with the equations (4.14)-(4.19), let's assume the observation (measurement) model to be like the following [15].

$$z(k) = H(k)X(k) + \gamma(k)v(k)$$

Here, the parametric variable $\gamma(k)$ is an independent and random variable at each step. Also the following is the assumed rule.

$$\gamma(k) = \begin{cases} 1....p(k) & \text{probability of normal operation} \\ \sigma \rightarrow 1 - p(k) & \text{probability of failure} \end{cases}$$

The variance of the measurement error is highly effective on the error formation, rather than the normal operation. Thus, when $\gamma(k) = \sigma > 1$, the following suboptimal filter algorithm is valid:

$$\hat{X}(k/k) = \hat{X}(k/k-1) + p(1/k)K(k)\Delta(k) \qquad (4.20)$$

The other filter parameters are the same as the expressions (4.14)-(4.19).

Here, $p(1/k)$ is the *a posteriori* probability of $\gamma(k)$ variable to be equal to 1, so the normal operation of the measurement channel at the k time step. It could be seen that, only the matrix with the $p(k)$ parameter in front of the filter gain coefficient is missing. When $p(1/k) = 1$, this filter will be exactly same with the optimal Kalman filter, but when $p(1/k) = 0$, it disregards the new measurements, acting as an extrapolator.

Note that the calculation of $p(1/k)$ probability brings excessive mathematical operations.

Due to the probability theory's limit theorem, uncountable random factors act on the output of the system. Through this assumption, at normal operation of the measurement channel, $\Delta(k)$ innovation sequence will provide normal distribution. The distribution function will be as follows:

$$f[\Delta(k)] = \frac{1}{\sigma_{\Delta}(k)\sqrt{2\pi}} e^{-\frac{\Delta^2(k)}{2\sigma_{\Delta}(k)}}$$

Here in this expression,

$$\sigma_{\Delta}^2(k) = H(k)P(k/k-1)H^T + R(k)$$

It will be useful to use the normalized innovation sequence instead, because at this time, $\sigma_{\tilde{\Delta}}^2(k) = 1$. The expression will be:

$$\tilde{\Delta}(k) = \Delta(k)\left[H(k)P(k/k-1)H^T(k) + R(k)\right]^{-\frac{1}{2}} \tag{4.21}$$

For the measurements $z(k)$, the robust Kalman filter is designed which basically depends on the $\tilde{\Delta}(k)$ vector (4.21) to fit in the tolerance region (confidence interval) Ω, where the following relations for $p(1/k)$ is accepted [15].

when $\quad \tilde{\Delta}(k) \in \Omega, \quad$ then $p(1/k) = 1$

and when $\quad \tilde{\Delta}(k) \notin \Omega, \quad$ then $p(1/k) = 0 \quad$ (4.22)

4.4.1 Robust Algorithm 1

Considering $\tilde{\Delta}(k)$ innovation sequence with normal distribution of zero mean and identity variances, the condition that it settles in the confidence interval and the resulting $p(1/k)$ would be stated as follows:

when $\quad -m\sigma_{\tilde{\Delta}}(k) < \tilde{\Delta}(k) < m\sigma_{\tilde{\Delta}}(k), \quad$ then $p(1/k) = 1$

and when $\quad \tilde{\Delta}(k) < -m\sigma_{\tilde{\Delta}}(k)$,

or when $\quad \tilde{\Delta}(k) > m\sigma_{\tilde{\Delta}}(k), \quad$ then $p(1/k) = 0 \quad$ (4.23)

By selecting the *m* value, the appropriate limits of the confidence interval can be found.

In the expression (4.23), it is seen that, when the normalized innovation sequence $\widetilde{\Delta}(k)$ is settled in the confidence interval, $p(1/k)$ will be equal to 1. At this case, the filter will be exactly the same as the optimal Kalman filter (4.14)-(4.19), designed for the normal operation, when $\gamma(k)=1$.

At the abnormal measurement conditions, when there becomes a failure at the measurement channel, $p(1/k)$ will be equal to 0, as seen from (4.23). This time, the Kalman filter will disregard the new measurements and consider extrapolation values for the output vector. The resulting term of the filter is as follows.

$$\hat{X}(k/k)=\hat{X}(k/k-1)$$

Then, the correlation matrix of the error is calculated by the help of the following equality.

$$P(k/k)=\begin{cases}[1-K(k)H(k)]P(k/k-1) & \widetilde{\Delta}(k)\in\Omega \\ P(k/k-1) & \widetilde{\Delta}(k)\notin\Omega\end{cases} \tag{4.24}$$

The algorithm of the robust Kalman filter, until this point, will be referred as *Robust Algorithm 1*.

4.4.2 Robust Algorithm 2

Another robust Kalman filter could be designed, which again considers the possible failures at the measurement channel of the system. The new design, which is a variant of the previous design, will be referred as *Robust Algorithm 2*.

The new algorithm will include the following rule for the normalized innovation sequence:

if $-m\sigma_{\widetilde{\Delta}}(k)<\widetilde{\Delta}(k)<m\sigma_{\widetilde{\Delta}}(k)$

then the algorithm will be exactly the same as the optimal Kalman filter, (4.14)-(4.19),

if $\widetilde{\Delta}(k)<-m\sigma_{\widetilde{\Delta}}(k)$, then $\widetilde{\Delta}(k)=-m\sigma_{\widetilde{\Delta}}(k)$,

or if $\widetilde{\Delta}(k)>m\sigma_{\widetilde{\Delta}}(k)$, then $\widetilde{\Delta}(k)=m\sigma_{\widetilde{\Delta}}(k)$ (4.25)

Briefly, if the normalized innovation sequence value exceeds the confidence limit, it will be equalized to the corresponding limit value.

4.5 Advances of the Robust Filter

Advantages of the presented Robust Kalman filters are [14],

1. Excessive mathematical operations are not necessary to calculate $p(1/k)$ probability at each step.
2. The algorithm could easily be executed in real time applications. (As depicted in the simulation section of this study).

Disadvantages of the presented Robust Kalman filters are,

1. This filter considers only the instantaneous failures (abnormal measurements) at the measurement channel.
2. The possible failures at the entire system will not be captured with this algorithm.

5. INTEGRATED RADIO-INS ALTIMETER

5.1 Introduction

In a maneuvering aircraft, to increase the correctness, reliability, and the immunity for noise and disturbances, integrating radio altimeter and the INS with the use of an optimal Kalman filter is a good and practical solution.

In general, when the topic is navigation, instead of using only one source of a measurement, using more than one source and combining these measurements to benefit from their leading advantages has always been a popular approach. Such systems using more than one source of measurement to achieve the best navigation parameter value are named as multisensor navigation systems.

5.2 Multisensor Navigation Systems

Multi-sensor navigation is the process of estimating the navigation variables of position, velocity, and attitude from a sequence of measurements from more than one navigation sensor. There are essentially two broad categories for sensors used in avionics suites for navigation and related functions: dead-reckoning sensors and positioning sensors.

Dead reckoning sensors provide a measure of acceleration or velocity with respect to Earth-referenced coordinate system, consequently requiring integration with respect to time to provide vehicle position with respect to Earth. Examples of these types of sensors are inertial systems, Doppler radars (not radar altimeter), and air-data sensors. The latter two require an attitude and heading reference (AHRS) or an inertial navigation system (INS) to provide the required angular orientation with respect to Earth.

Positioning sensors provide a position measurement that can be related to Earth-referenced coordinates. Examples of these sensors are radio systems such as the terrestrial based LORAN and the satellite based Global Positioning System (GPS), which provide the position of the antenna in geodetic coordinates. A star-tracker can also be used for fixing position when its orientation with respect to Earth is determinable through some means such as an Attitude and Heading Reference System (AHRS) or INS.

Maybe the most important subject here is the filtering algorithm, whereby measurements from combinations of these sensors can be employed to satisfy the functional output variable requirements of an avionics suite. In general, avionics system users require a variety of information on the state of the air vehicle depending on the complexity of the application and accordingly will include a variety of complementary sensors in their equipment suite.

The deficiencies that exist in the individual sensors employed in a multi-sensor avionics suite include at least one of the following characteristics:

1. Increase in error of the navigation variables as a function of time or distance traveled. This is a characteristic of all dead-reckoning sensors that eventually accumulate unbounded errors. Examples are inertial and Doppler radar navigation sensors.

2. High noise level or low bandwidth in any derivative variable. This is a characteristic of radio sensors that require differentiation with respect to time of the basic measured variable to obtain rate or acceleration. For example, with Loran, position must be differentiated to obtain velocity. For Doppler radar, differentiation of speed can yield acceleration, once the result is transformed to an Earth-referenced coordinate system using attitude from an AHRS or inertial system.

3. Reliance on sensors requiring off-board components to accomplish the required functions. This includes radio sensors using terrestrial or satellite-based assets whose access can be denied, due to intentional (jamming) or non-intentional interference (transmission blockage or interfering transmissions) of the propagated signal from the off-board assets, or failure of the transmitters due to other causes.

To overcome individual sensor deficiencies, system designers have sought combinations of avionic sensors. These multi-sensor systems are designed to provide reliable, dynamically accurate measurements of the air vehicle's state for all specification-required flight conditions.

The most typical solution has been to use an inertial system in conjunction with an appropriate set of complementary sensors that arrest the random, time increasing error in velocity, position, and orientation resulting from integration of the fundamental high-bandwidth inertial measurements of acceleration (force corrected for the a priori known effect of gravity) from accelerometers and angular change from gyroscopes [2].

5.3 Radio-INS Integration

The core task of this study is to combine two different navigation sources with the use of Kalman filter. In fact, the main task for any kind of navigation study is to fight with the disadvantages of a navigation equipment, thus to increase correctness and reliability. By integrating Radio and INS altimeters, the objective is to benefit from the advantages of both of the systems, while eliminating the shortcomings.

There are two possible Kalman filter designs for integrating such systems.

1. Total state space Kalman filter (direct method).
2. Error state space Kalman filter (indirect method).

In the direct method, all of the states of the system are used by the Kalman filter, where the INS accelerometer and the aiding navigator signals are the sources [16-20]. But in the indirect method, which is basically chosen in this study, Kalman parameters are the errors. While the INS is the main source for determining vertical navigation information, with the discrete aiding signals from the Radio altimeter, Kalman filter estimates the instantaneous errors.

Through the design, the outcoming dynamical characteristic of the INS is proposed to be carried to the complete system, and the possibility of a total system breakdown in case of a Kalman filter failure is eliminated.

By integrating INS and Radio altimeter through an indirect feed forward Kalman filter,

1. The good characteristics of the INS with high bandwidth and frequencies are maintained.
2. In certain operation periods, acceptable accuracy is attained.
3. A dynamic system, which is easily adapted to the computer environment, is developed.

The two navigators of the integrated Radio-INS altimeter provide different types of altitude data. The radio altimeter measures the real altitude from the ground level, but the INS measures the relative altitude from an initial alignment location. In a system where these two navigators are combined, this difference could easily be eliminated. This elimination is done in the data processing unit of the integrator.

The block diagram of an integrated Radio-INS altimeter is shown in the Figure 5.1.

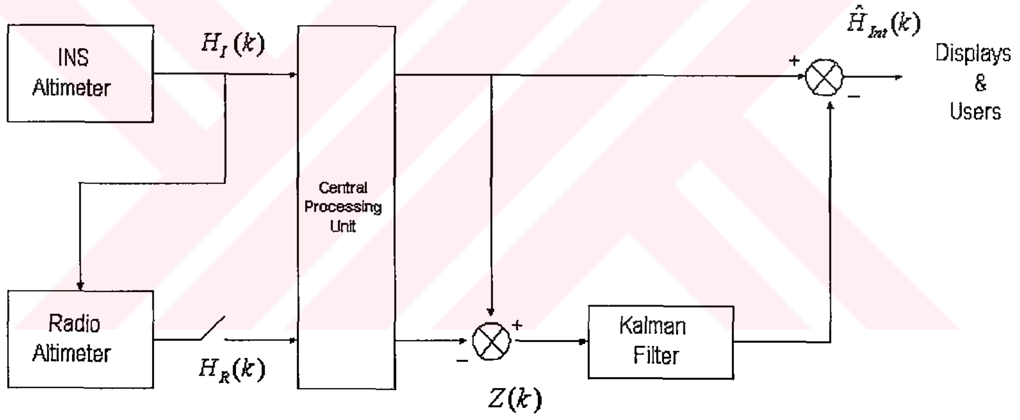

Figure 5.1 Integrated Radio-INS altimeter block diagram.

The integrated Radio-INS altimeter contains the following components:

1. INS altimeter
2. Radio altimeter
3. Data (central) processing unit
4. Control block (Kalman filter)
5. Display (avionics users)

Here, the INS altimeter is not a dedicated stand-alone instrument, but the altitude or the vertical position channel of the Inertial Reference Unit (IRU) of a certain aircraft.

The switch sign on the block diagram refers to the discrete character of the data provided by the radio altimeter for the integrated navigation system. However, Kalman filter could be applied in both continuous and discrete systems.

The main source of altitude data is INS, and the radio altimeter acts as a correcting element supporting the Kalman filter for estimations. By the use of the data processing unit, radio altimeter output is transformed to the main coordinate system of the aircraft navigation and control.

The radio-INS integration is feasible for the cases when the aircraft route is over landscapes such as seas, oceans, lakes and deserts where the altitude above ground level does not have fluctuating character. (Not over mountains, valleys, etc.)

When this condition is set, the real altitude value at the Kalman filter input will be compensated, and the input signal will be designated as the difference between the altitude measurements of the two sources.

$$r(t) = H_I(t) - H_R(t) \tag{5.1}$$

$$= (H_g(t) + \Delta H_I(t)) - (H_g(t) + \Delta H_R(t)) \tag{5.2}$$

$$= \Delta H_I(t) - \Delta H_R(t) \tag{5.3}$$

In the expressions (5.1), (5.2), and (5.2), $H_I(t)$ and $H_R(t)$ are the altitude measurements of INS and radio altimeter, $\Delta H_I(t)$ and $\Delta H_R(t)$ are the measurement errors of the two sources respectively. $H_g(t)$ is the real altitude value.

In this block diagram of the integrated system, INS is the main error source. In the previous sections, dead-reckoning character of the INS was mentioned. This causes a severe error of measurement, increasing by time.

The mathematical models of the INS (2.1)-(2.4) and the radio altimeter (3.3) given in this study are first or second order stochastic Markov processes [9]. The model parameters are estimated by the use of the Kalman filter. The filter will give the optimum (estimated) value of the INS error $\Delta\hat{H}_I(t)$, in the condition where the standard error is minimized.

Finally, the estimated value of error $\Delta\hat{H}_I(t)$ is subtracted from the altitude measurement of the INS.

$$\hat{H}_{Int} = H_I(t) - \Delta\hat{H}_I(t) \tag{5.4}$$

The calculated altitude value is the output of the integrated system, and it would be used for navigation and control purposes.

As the INS error increases with time in a cumulative manner, the integration diagram is valid and effective for short periods of operation. (For example, 1 hour period).

In such periods when the linear operation regime of INS is provided, the output signal will be as follows.

$$H_I(t) = H_{\mathrm{Re}l}(t) + \Delta H_I(t) \tag{5.5}$$

where, $H_{\mathrm{Re}l}(t)$ is the relative altitude.

One of the most important improvements of the integrated radio altimeter is that, a dynamic error of measured altitude is not generated. As this is an open loop system for the measured altitude, the filter will not limit the operation rate of the navigators. For this reason, the radio-INS altimeter will have outstanding dynamic character like a stand-alone INS.

Another important feature is that, an in-flight failure at the Kalman filter will not result in a whole system breakdown. In such a case, when the Kalman block at the integrated system fails, the INS measurements could be used without corrections for a certain period of operation.

The results at the simulation section of this study show that, the altitude information provided by the integrated radio-INS altimeter will be approximately 3 times correct than the stand-alone radio altimeter measurement, with the regarded error models.

5.4. The Error of The Error

It should be underlined that, the integration algorithm here in this study is based upon error models and error values. The use of the system designed in this study is to find out instantaneous errors at the integrated altimeter. So the discrimination between navigation error and filter error is somehow very important. The error definition in the results is standing for *the error of finding the error*. As the system design is mainly based on Kalman filter, it will be more convenient to express this definition as *the error of estimating the error*.

5.5. Integrated System Parameters

The state space model of the integrated radio-INS altimeter system is expressed with the following equations.

$$X(k) = \phi(k,k-1)X(k-1) + G(k,k-1)U(k-1) \tag{5.6}$$

$$Z(k) = H(k)X(k) + V(k) \tag{5.7}$$

Equation 5.6 is the combination of error models of INS and the radio altimeter, (2.1)-(2.4) and (3.3), which were given in the previous sections. This expression contains all of the error parameters that act on the integrated system. The definitions of the terms at the state space model of the system are,

$\phi(k,k-1)$	:	System transfer matrix [5x5]
$X(k)$	:	State vector
$G(k,k-1)$	:	Noise transition matrix
$V(k)$	:	Noise of the system

The elements of the vector $X(k)$, (5.6) are the measurement error components, where the open form of the vector is depicted in the following expression.

$$X^T(k) = [\Delta H_I(k) \quad \Delta W_z(k) \quad \Delta a_z(k) \quad \Delta g(k) \quad \Delta H_R(k)] \tag{5.8}$$

These terms in (5.8) are the main four error parameters of the INS altimeter, which are the error of finding the altitude $\Delta H_I(k)$, vertical speed $\Delta W_z(k)$, acceleration $\Delta a_z(k)$, and gravitational acceleration $\Delta g(k)$; and the altitude finding error of the radio altimeter $\Delta H_R(k)$.

The following is the transfer matrix of the system, which combines equations (2.1)-(2.4) and (3.3) in the state space form.

$$\phi(k,k-1)=\begin{vmatrix} 1 & \Delta t & 0 & 0 & 0 \\ \frac{2g\Delta t}{R} & 1 & \Delta t & \Delta t & 0 \\ 0 & 0 & 1-\alpha\Delta t & 0 & 0 \\ 0 & 0 & 0 & 1-\beta_g\Delta t & 0 \\ 0 & 0 & 0 & 0 & 1-\beta\Delta t \end{vmatrix} \tag{5.9}$$

The noise transition matrix of the system is given as,

$$G(k,k-1)=\begin{vmatrix} 0 & 0 & 0 \\ 0 & 0 & 0 \\ \Delta t & 0 & 0 \\ 0 & \Delta t & 0 \\ 0 & 0 & \Delta t \end{vmatrix} \tag{5.10}$$

where, the zero mean white (Gauss) noise vector is,

$$U^T(k-1)=\left[U_{\Delta a_z}(k-1) \quad U_{\Delta g}(k-1) \quad U_{\Delta H_R}(k-1)\right] \tag{5.11}$$

Equation 5.7 is the measurement equation of the system. The measurement matrix $H(k)$ in this expression is highly important, as it gives a general idea of the whole design of the integrated system. In this design, the measurement matrix is,

$$H(k)=|\ 1 \quad 0 \quad 0 \quad 0 \quad -1\ |$$

As easily seen by combining this matrix with equation (5.8), the system integrates two independent navigation sources in means of subtracting the radio altimeter error from the INS altimeter error. However, this operation is carried out through the Kalman filter, and the divergent error character of the INS is compensated. This is one of the ideas that should be underlined in this study.

The remaining parameters of the state space model of the system are the system noise correlation matrix $Q(k)$, and the measurement error correlation matrix $R(k)$. The following are the open forms of these matrices.

$$Q(k) = \begin{vmatrix} \frac{\sigma^2_{\Delta a_z}}{\Delta t} & 0 & 0 \\ 0 & \frac{\sigma^2_{\Delta g}}{\Delta t} & 0 \\ 0 & 0 & \frac{2\beta\sigma^2_s}{\Delta t} \end{vmatrix} \tag{5.12}$$

$$R(k) = \frac{N_{fl}}{2\Delta t} \tag{5.13}$$

6. SIMULATION

6.1 Introduction

The simulation section of this study is mainly based on the error models of each of the separate navigation sources of the integrated radio-INS altimeter.

Error models of the INS and the radio altimeter are combined using Kalman filter, so the estimated values of error is calculated. In the algorithm of the filter design at this study, INS is a primary; radio altimeter is a secondary source of navigation.

6.2 Simulation Tools

The main tool for the simulation is the MATLAB[1] software, which is a popular computation program that enables extensive matrix operations and visualization [22,23].

The software package of this study includes a number of 'M Files', which can be run on MATLAB. These m-files are attached to the study inside a floppy disk (Appendix F).

The four main files of the software package are,

1. *Kalman.m* is the m-file, where the integrated navigation system is simulated in optimal conditions.
2. *Kaler.m* is the file, in which the failure condition at the measurement channel is implemented into the simulation. The filter is still optimal, and has no robust character towards abnormal measurements.
3. *Robust1.m* is the tool for simulating *Robust Algorithm 1* given in section 4.4.1, with the definitions (4.24).

---

[1] MATLAB™ is a registered trademark of The MathWorks Inc.

4. *Robust2.m* is the tool of simulation for section 4.4.2, *Robust Algorithm 2*, with the expressions (4.25).

The supporting files are *kaldata.m*, where the model parameters and initial conditions are entered; *kalgraph1.m*, *kalgraph2.m*, and *kalprint.m*, by the help of which simulation is visualized and results recorded.

Note that, no additional toolboxes are necessary for running these programs, however all of the m-files should be located in the same disk folder.

6.3 Algorithm of the Simulation

In the simulation codes of this study, instead of using *for* loops for calculating values at each time step, the loops are set to produce matrices with the size [parameter count x iteration count]. This method shortens the process time, and enables to access and evaluate the output values of each time step after the simulation. Simulations at the study have 500 iterations. As an example, the size of the estimated error values matrix $\hat{X}(k/k)$ is [5 x 500] at the end of a normal simulation run.

The sections of the programs, which are unique to this study, will be described below.

6.3.1 Optimal Kalman Filter

The simulation program for the integrated system in optimal conditions is *Kalman.m*. In the beginning of the algorithm, the error values regarding the error model of the system $X(k)$, (5.6) are calculated.

Afterwards, the measurement equation (5.7) is implemented, and the error of the model, which is the difference between INS and radio errors are found, as stated in Section 5.5. Here, it should be noted that, this step of the algorithm contains a term for the system noise, which is expected to be a white noise with random character at each iteration. In this manner, the outputs of the simulation might be slightly different at each run.

The next step is the Kalman filter (4.14)-(4.19), which is followed by the calculation of normalized innovation sequence, *DeltaN* (4.21). Many other matrix manipulations take place at the algorithm for visualization, and those could be reviewed over the attached m-files.

6.3.2 Kalman Filter at Failure Conditions

The program *Kaler.m* simulates the case, when failures occur at the measurement channel of the integrated system. The whole algorithm is exactly the same with the one for the optimal conditions, but errors are implemented into 100^{th}, 200^{th}, 300^{th}, and 400^{th} iterations. These abrupt errors, which represent the failure condition at the measurement channel, are formed by increasing the standard deviation of the normal error by 100 times. Note that, these impulsive errors have random character. This results in the output variation at each simulation run, however the system responses are in the same manner.

6.3.3 Robust Algorithm 1

The first algorithm of the robust Kalman filter design includes the rule (4.23), which is given in Section 4.4.1. The rest of the program is alike the system designs involving optimal Kalman filter in failure conditions.

6.3.4 Robust Algorithm 2

This is the simulation program, at which the second type of robust Kalman filter (4.25) is used in the integrated system design.

In both of these applications, abrupt error was implemented into the algorithm. Otherwise, in the abrupt error free operation of measurement channel, the results will be exactly the same as the ones in the optimal case.

6.4 Simulation Data

In this study, integrated navigation system for altitude determination of an aircraft is simulated. The actual flight altitude of the aircraft is taken as 1000 *m*. The following are the data, and the initial conditions for the system.

$\sigma^2_{\Delta a_z}\left[m^2/s^4\right]=10^{-6}$

$\sigma^2_{\Delta g}\left[m^2/s^4\right]=10^{-8}$

$\tau_s\left[s\right]=10$

$\sigma^2_s\left[m^2\right]=1000$

$N_{fl}\left[m^2/Hz\right]=100$

$$R(k)=\frac{100}{2.0,1}=500m^2$$

$$\beta\left[s^{-1}\right]=\frac{1}{\tau_s}=0.1$$

$\tau_{a_z}\left[s\right]=1000$

$$\alpha\left[s^{-1}\right]=\frac{1}{\tau_{a_z}}=0.001$$

$\tau_g\left[s\right]=200$

$$\beta_g\left[s^{-1}\right]=\frac{1}{\tau_g}=0.005$$

$H=1km$

$R=R_0+H=6371+1=6372km$

$\Delta t\left[s\right]=0.1$

$g\left[m/s^2\right]=9.89$

The initial conditions for the measurement system include the following errors.

$\Delta H_I(0)=23m$

$\Delta W_z(0)=0.002m/s$

$\Delta a_z(0)=0.001m/s^2$

$\Delta g(0)=0.0001m/s^2$

$\Delta H_R(0)=2m$

In the Kalman filter, the following initial estimations are used.

$\Delta\hat{H}_I(0/0)=1m$

$\Delta\hat{W}_z(0/0)=0.05m/s$

$\Delta\hat{a}_z(0/0)=0.002m/s^2$

$\Delta\hat{g}(0/0) = 0.0002 m/s^2$

$\Delta\hat{H}_R(0/0) = 5m$

These estimations are inserted into the expression (4.17) with the following vector form.

$\hat{X}^T(0/0) = | 1 \quad 0.05 \quad 0.002 \quad 0.0002 \quad 5 |$

And the following are the matrices that will be used in the first step of the simulation algorithm.

$$P(k-1/k-1) = \begin{vmatrix} 10 & 0 & 0 & 0 & 0 \\ 0 & 10 & 0 & 0 & 0 \\ 0 & 0 & 10 & 0 & 0 \\ 0 & 0 & 0 & 10 & 0 \\ 0 & 0 & 0 & 0 & 10 \end{vmatrix}$$

$$G(k/k-1) = \begin{vmatrix} 0 & 0 & 0 \\ 0 & 0 & 0 \\ 0.1 & 0 & 0 \\ 0 & 0.1 & 0 \\ 0 & 0 & 0.1 \end{vmatrix}$$

$$Q(k-1) = \begin{vmatrix} 10^{-5} & 0 & 0 \\ 0 & 10^{-7} & 0 \\ 0 & 0 & 2000 \end{vmatrix}$$

$$\phi(k/k-1) = \begin{vmatrix} 1 & 0,1 & 0 & 0 & 0 \\ 3.1.10^{-4} & 1 & 0,1 & 0,1 & 0 \\ 0 & 0 & 0.9999 & 0 & 0 \\ 0 & 0 & 0 & 0.9995 & 0 \\ 0 & 0 & 0 & 0 & 0.99 \end{vmatrix}$$

$H(k) = | 1 \quad 0 \quad 0 \quad 0 \quad -1 |$

$R(k) = | 500 |$

6.5 Simulation Results

6.5.1 Optimal Kalman Filter Simulation

In the simulation of the integrated system equipped with the optimal Kalman filter, the results were quite satisfactory. In all altimeter parameters, Kalman estimations were able to catch the model values, and this tendency was kept until the last iteration.

As the estimations are correct, the integrated system error is kept around zero through the simulation. That is one of the goals of this study, as the system error has been stabilized, thus the drifting character of the INS error has been eliminated.

The resulting data are given in Table 6.1 and Figure 6.1-6.3.

Table 6.1 INS error versus integrated system error (Altitude)

Iterations	INS Error (*m*)	Integrated Altimeter Error (*m*)
50	23.8841	11.1194
100	26.7612	-1.6229
150	31.9571	4.3391
200	39.9773	7.3407
250	51.5466	-5.0445
300	67.6660	1.5723
350	89.6901	-10.7381
400	119.4324	9.7124
450	159.3070	0.1315
500	212.5156	-2.1919

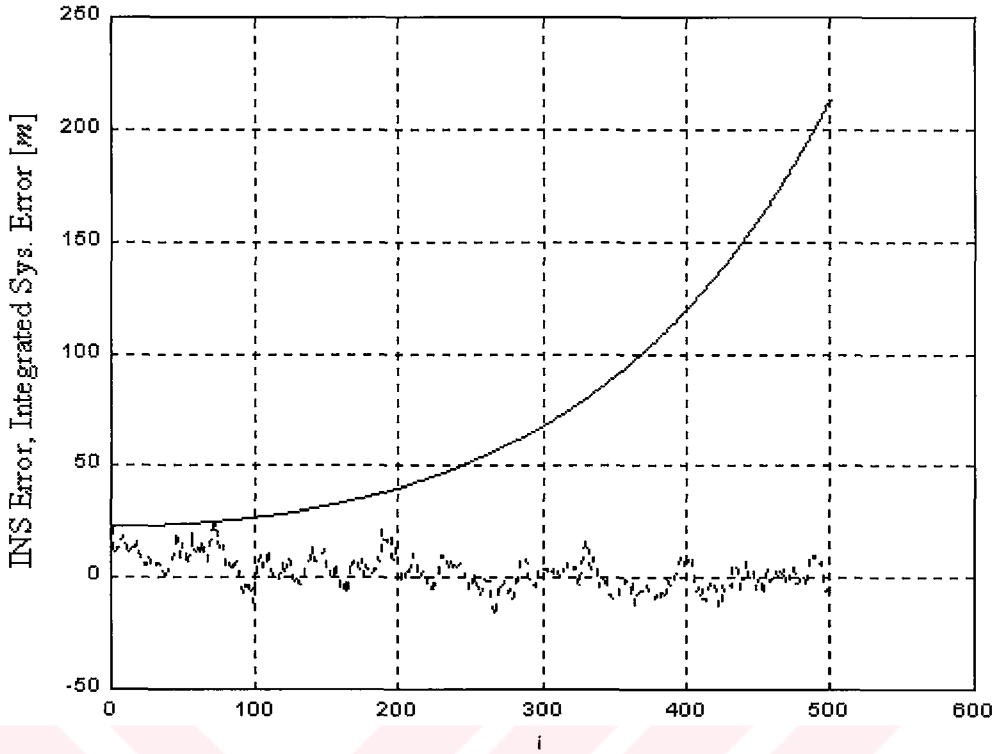

Figure 6.1 INS error versus integrated system error (Optimal Kalman filter)

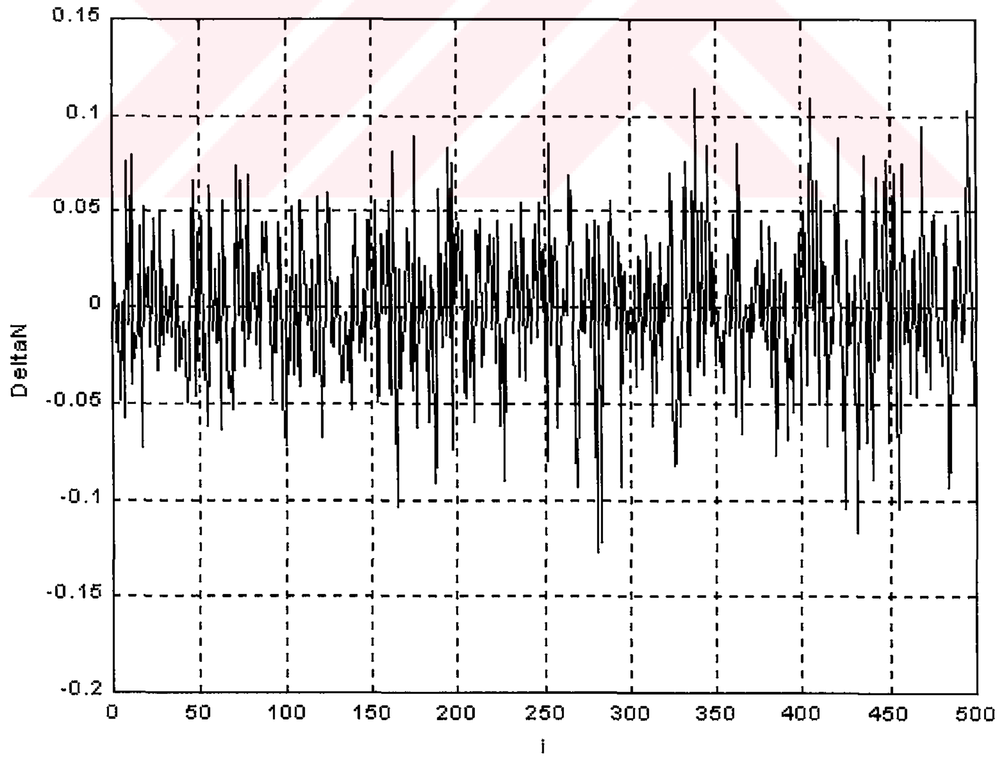

Figure 6.2 Normalized innovation sequence, *DeltaN*. (Optimal Kalman filter)

In Figure 6.1, INS altimeter's drifting error (solid line) character could easily be seen. Meanwhile, the integrated systems error of altitude (dotted line) keeps values around zero, which is a success of the filter design. Figure 6.2 is the graph of normalized *Delta* variation through the simulation.

Figure 6.3 is the combined graph of model error (solid line), estimated error (dotted line), their differences, and error variance of estimation for altitude. Similar graphs for other parameters (vertical speed, vertical acceleration, gravity and radio altitude) are given in Appendix A.

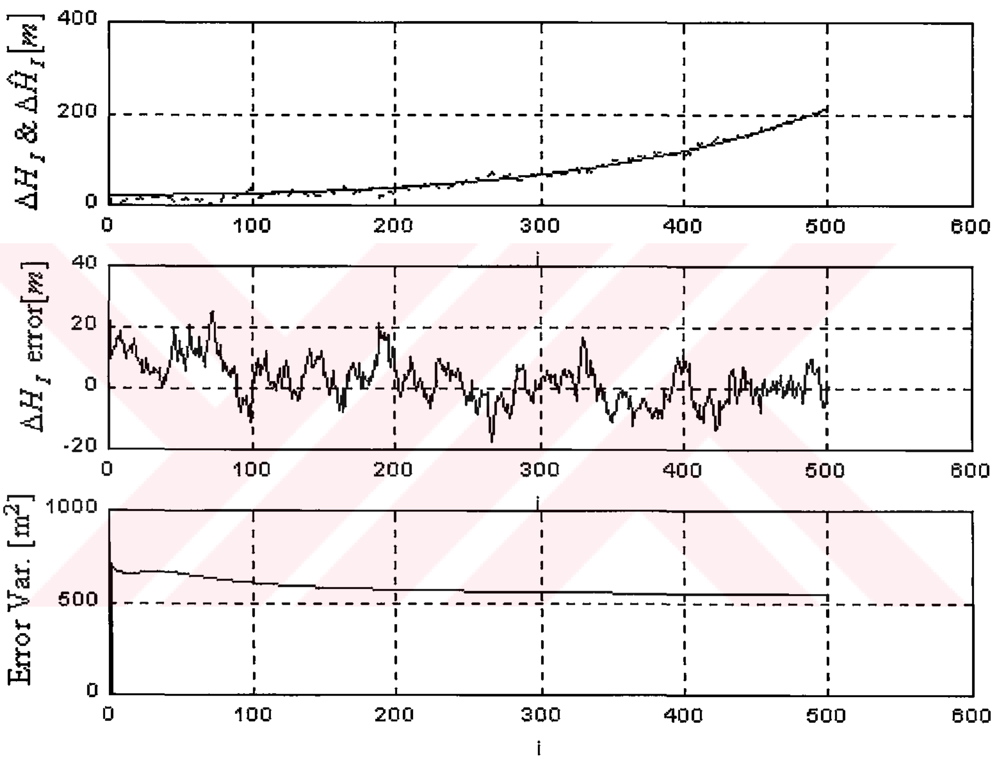

Figure 6.3 Altitude error (INS) (Optimal Kalman filter)

6.5.2 Failure Conditions Simulation

To simulate a possible failure at the measurement channel of the system, abrupt errors with random magnitude were implemented into the algorithm. At the steps of failures, the estimations diverted from the model enormously. In all simulation runs, these peaks were observed higher or lower, but they were anyway unacceptable.

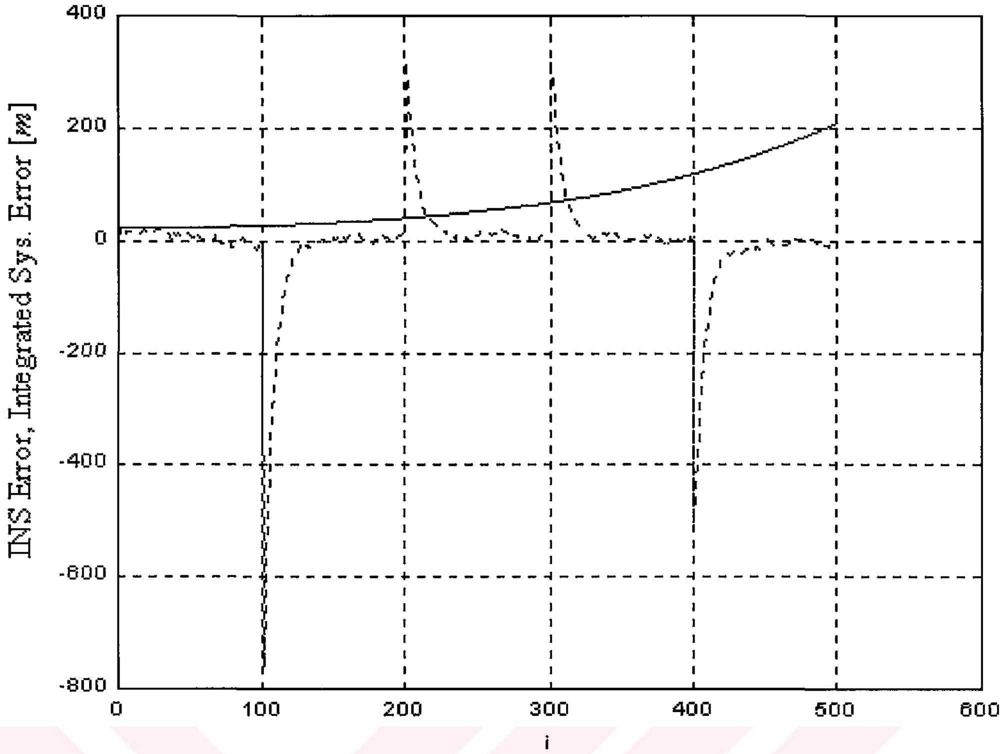

Figure 6.4 INS error versus integrated system error (Failure conditions)

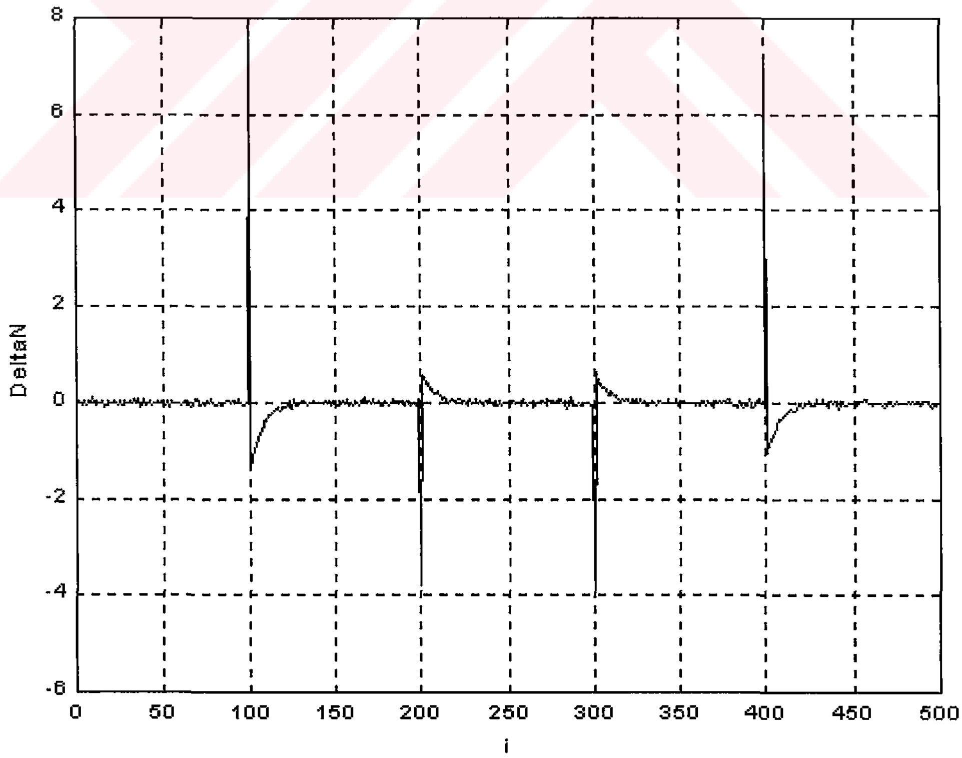

Figure 6.5 Normalized innovation sequence, *DeltaN*. (Failure conditions)

The high peaks of estimated error (dotted line) at the steps, where abrupt error was introduced to the measurement channel, are seen in Figure 6.4. These are at the same time steps, at which *DeltaN* deviation is observed in Figure 6.5.

In Figure 6.6, the combined graph of model (solid line) and estimated (dotted line) errors, their differences, and error variance; the effect of measurement failures at the system is clearly seen. The same figures for other altimeter parameters are given in Appendix B.

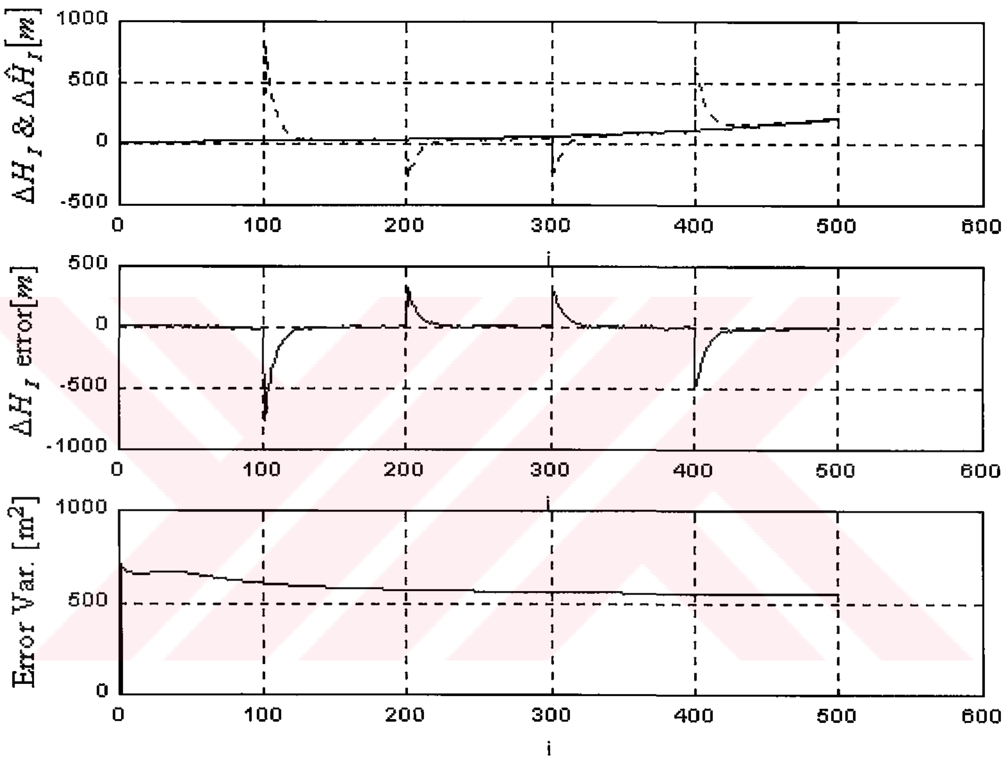

Figure 6.6 Altitude error (INS) (Failure condition)

6.5.3 Robust Algorithm 1 Simulation

The results of the *Robust Algorithm 1* simulation were almost perfect, as the system was successful to get rid of the measurement failures, and it produced acceptable estimations. Dislike the previous simulation 6.5.2, estimations did not divert from the model value, as observed in Figure 6.7. In this figure, again the solid and dotted lines stand for INS and integrated system errors respectively. Figure 6.8 is the graph of *DeltaN* for this case.

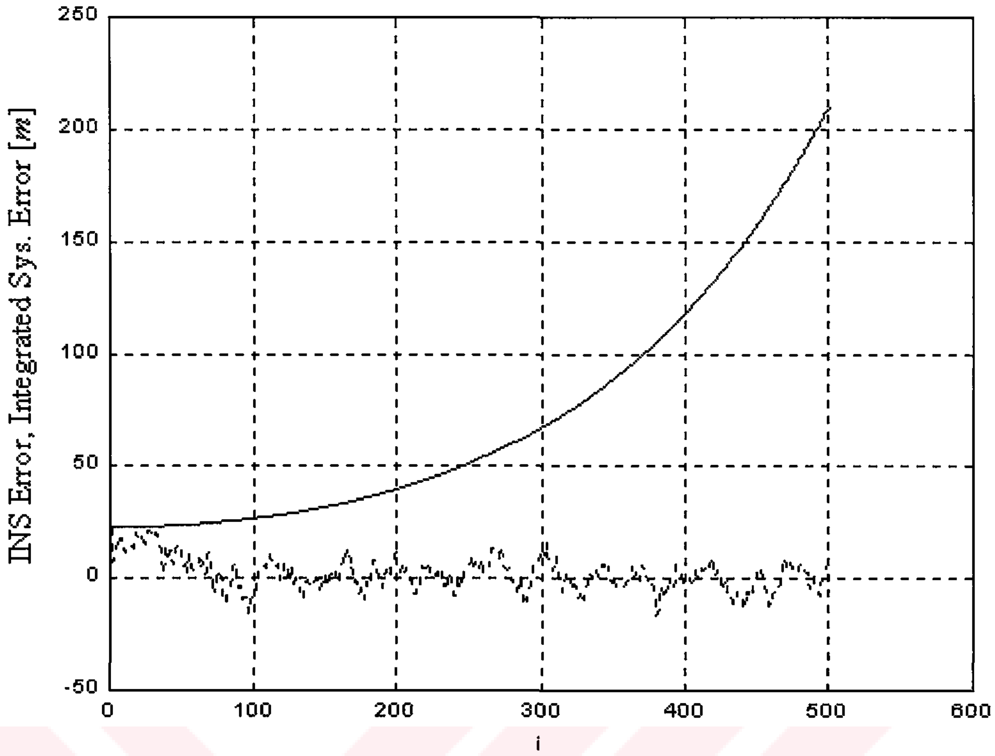

Figure 6.7 INS error versus integrated system error (*Robust Algorithm 1*)

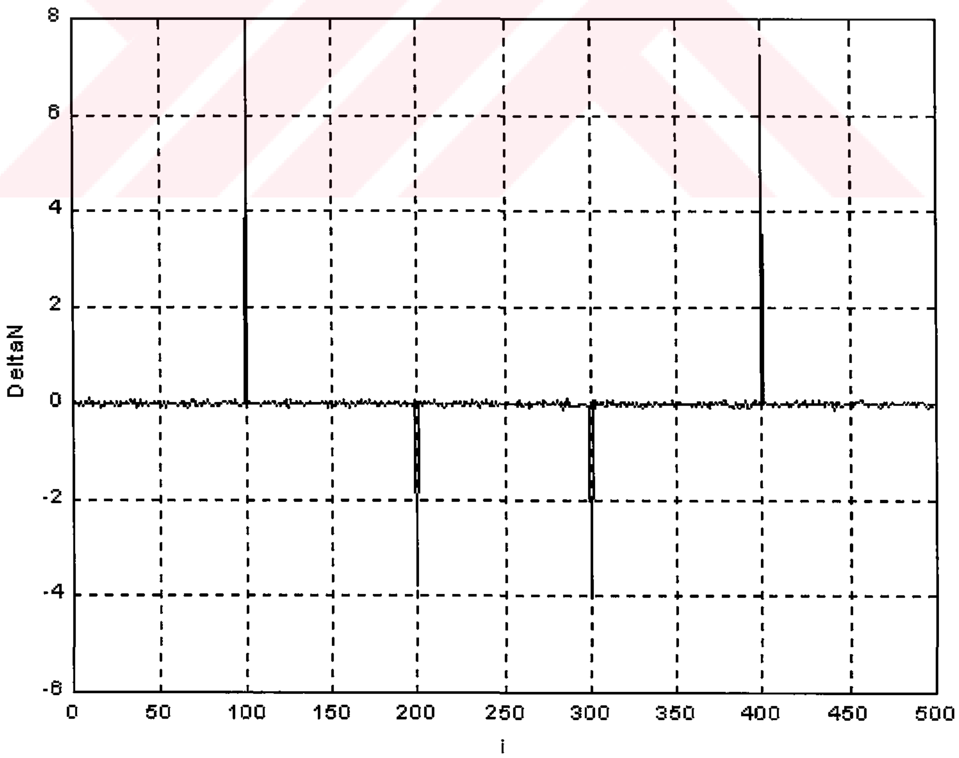

Figure 6.8 Normalized innovation sequence, *DeltaN*. (*Robust Algorithm 1*)

Figure 6.9 is the combined graph of altitude error, model (solid line) and estimated (dotted line), in *Robust Algorithm 1* simulation. The success of this robust algorithm could again be concluded on this graph.

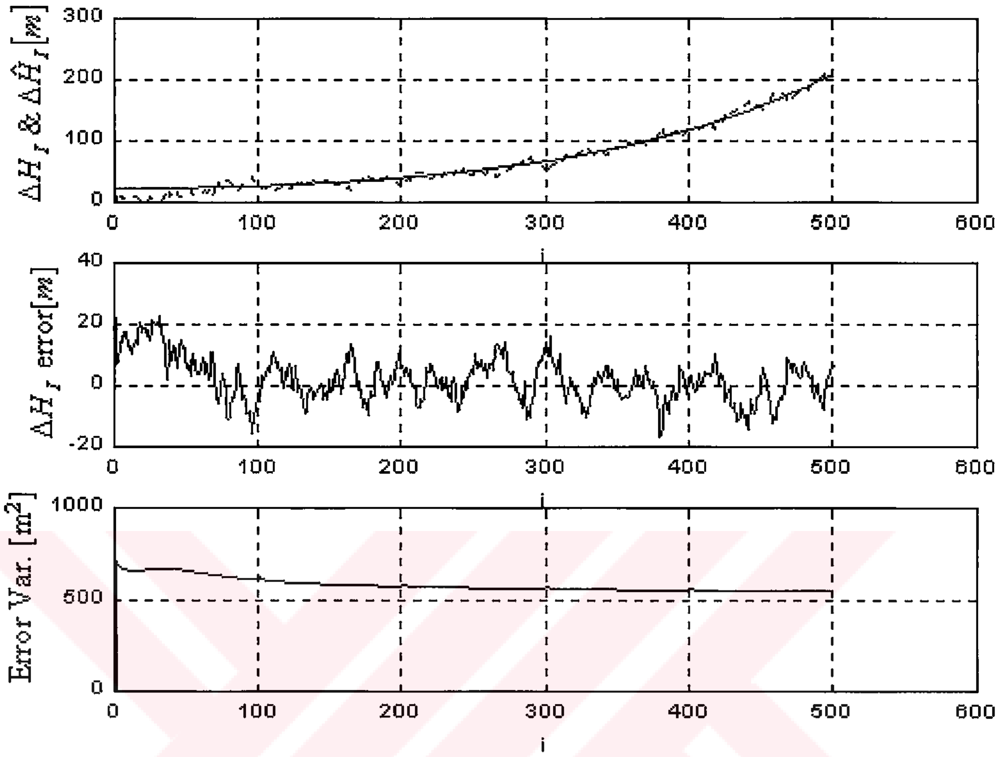

Figure 6.9 Altitude error (INS) (*Robust Algorithm 1*)

The similar graphs for vertical speed, acceleration, gravity and radio altitude are given in Appendix C.

6.5.4 Robust Algorithm 2 Simulation

Evaluating the simulation results, *Robust Algorithm 2* was not as successful as *Robust Algorithm 1*. The *estimation peaks* did not reach to values like those in the failure implemented optimal Kalman filter, but they existed in the measurement failure steps. This was the case for all altimeter parameters.

However, this algorithm should not be totally accepted as unsuccessful, because the results show that the system was able to detect the failures and take action, thus run correctly. Figure 6.10 and 6.11 are the graphs of errors and *DeltaN* respectively.

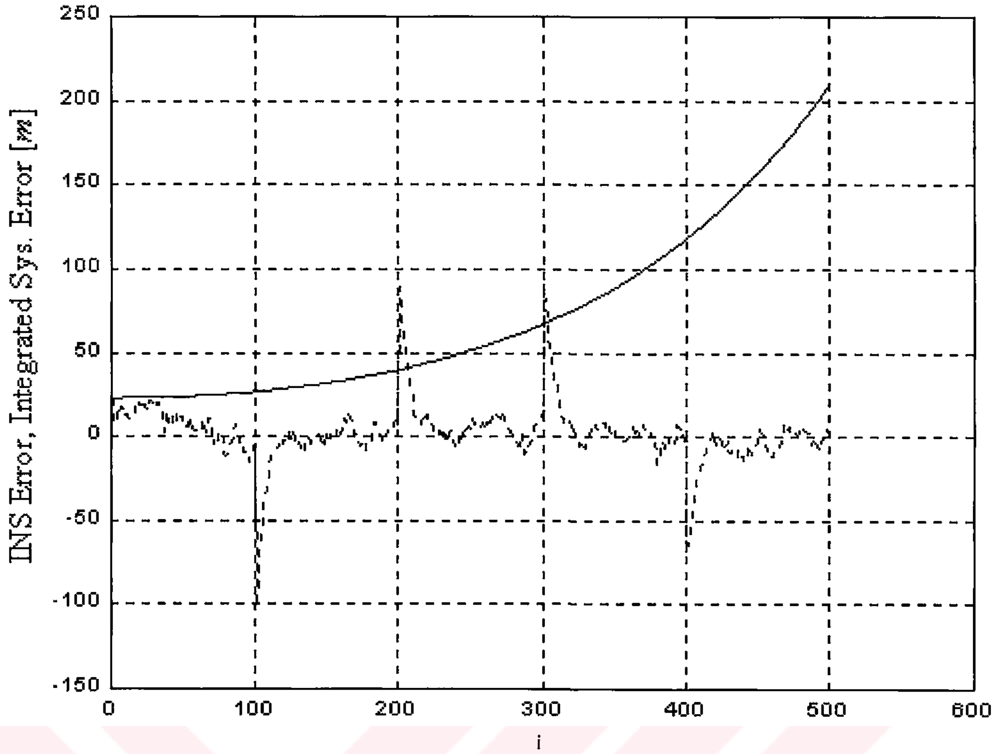

Figure 6.10 INS error versus integrated system error (*Robust Algorithm 2*)

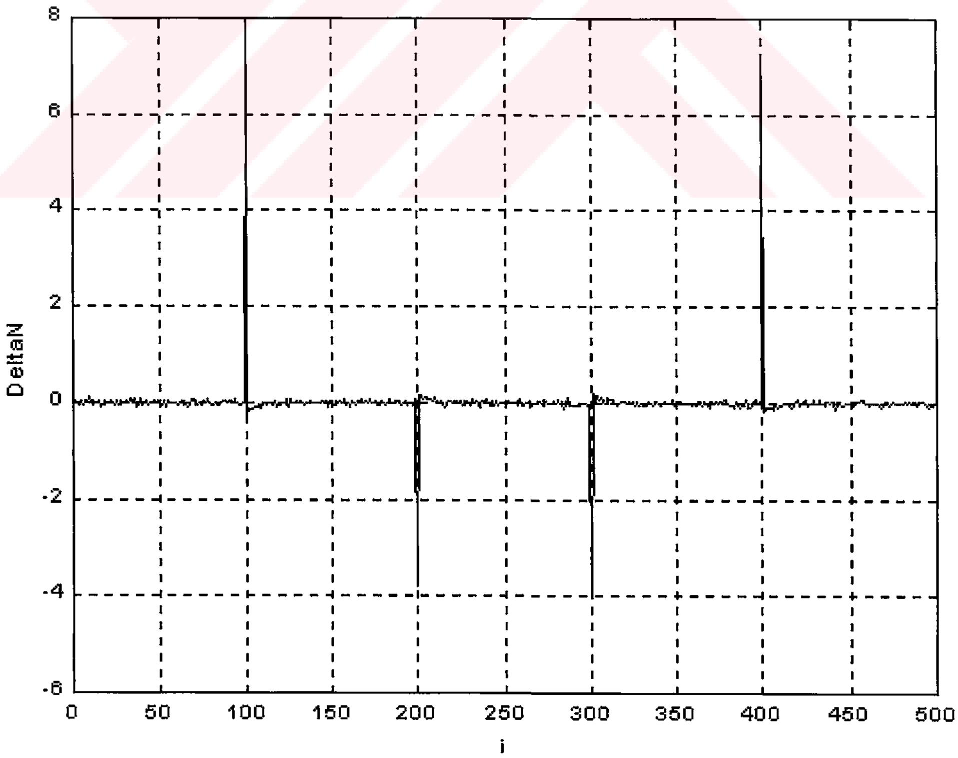

Figure 6.11 Normalized innovation sequence, *DeltaN*. (*Robust Algorithm 2*)

The combined graph for altitude error is given in Figure 6.12, on which the INS model error (solid line), estimated error (dotted line), the difference between model and estimation, and error variance for altitude could be seen.

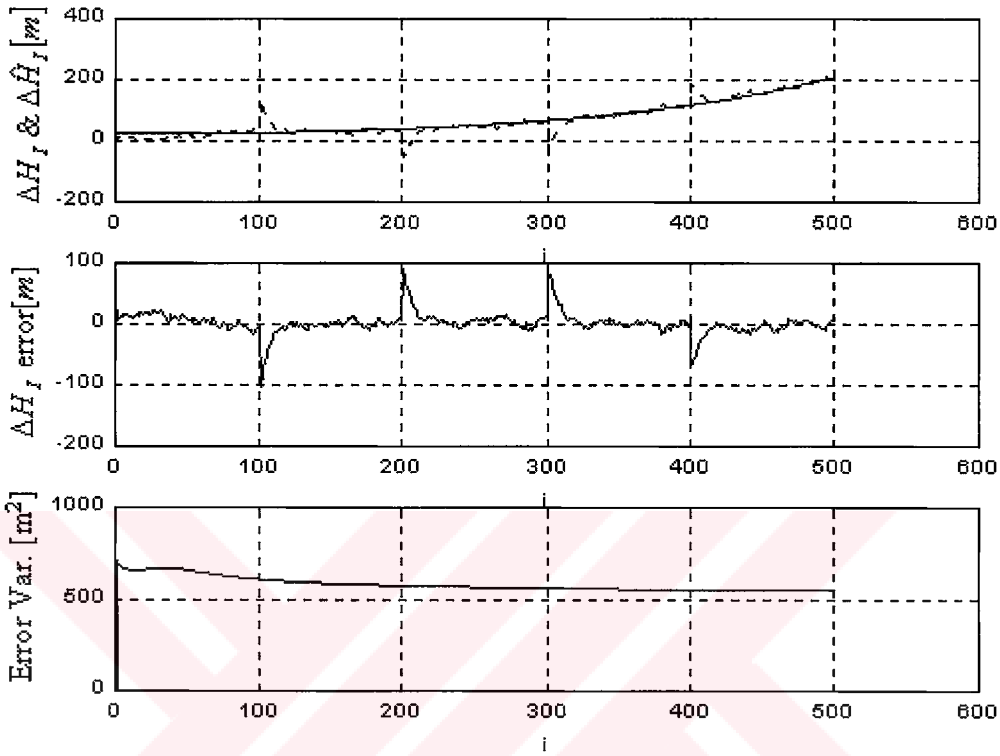

Figure 6.12 Altitude error (INS) (*Robust Algorithm 2*)

Similar graphs for other altimeter parameters are given in Appendix D.

The simulation results, in case of a failure at the measurement channel, are given in Table 6.2. However, it should be noted that, the following data is obtained at three different simulation runs, where the noise character is random.

Appendix E is reserved for additional tables of simulation results.

Table 6.2 Integrated altimeter errors in case of a failure at the measurement channel (Altitude)

Iterations	Optimal Kalman Filter		*Robust Algorithm 1*		*Robust Algorithm 2*	
	Altitude error (m)	*P(1/1)*	Altitude error (m)	*P(1/1)*	Altitude error (m)	*P(1/1)*
50	18.3503	657.4160	18.3503	657.4160	18.3503	657.4160
100	31.5445	607.2174	31.5445	607.2174	31.5445	607.2174
101	789.7662	606,5490	31.9989	622.4219	129.2176	606.5490
150	29.7056	583.9400	33.5450	583.9404	33.0459	583.9400
200	29.4787	571.9199	33.3060	571.9202	32.8085	571.9199
201	-280.5042	571.7351	33.4452	583.2328	-49.1886	571.7351
250	40.3381	564.1401	46.4419	564.1410	45.3371	564.1401
300	48.4811	558.3061	52.8860	558.3065	52.2321	558.3061
301	-255.2256	558.2036	53.0908	567.9666	-22.9978	558.2036
350	79.6121	553.7767	86.6675	553.7784	85.3391	553.7767
400	111.9313	550.4355	115.8765	550.4360	115.2868	550.4355
401	625.2949	550.3806	116.5206	559.3810	188.3200	550.3806
450	164.4886	548.2354	159.2828	548.2373	160.1455	548.2354
500	205.7108	547.0125	202.9625	547.0130	203.5604	547.0125

7. CONCLUSION

When starting this study, the development of the integrated Radio-INS altimeter system, the first goal was successfully adapting the Kalman filter to two different navigation sources, and getting acceptable estimates of the navigation parameters. This goal is achieved, and the Kalman filter algorithm succeeded to estimate not only the altitude information, but also the other vertical channel parameters. The point is that, through the entire simulation, estimated values of error were very close to the accepted model values. The associated simulation outputs are given in section 6.5.1 and appendix A.

After this achievement, the next task was to simulate some possible failures at the measurement channel. Other than the white noise, which is regarded in all of the situations, abrupt errors were implemented into the measurement equations. These *failures* may occur because of any inherent or environmental problem, lack of design, or interference. The simulation, referred as *Failure Conditions*, shows how severe the results of such a case can be (Section 6.5.2 and appendix B).

At the *failure* steps, the Kalman estimations for all parameters deviated in unacceptable magnitudes. A total navigation system in demand of these estimates, or even the pilot monitoring the altimeter display, would face unbearable problems at those instances.

The next issue of the study came up with the necessity to overcome this malfunctioning. To prevent the consequence of a failed measurement channel, the Kalman filter was expanded to have robust character towards measurement channel failures. This was achieved in two different algorithms, and the results were successful as both of the robust filters recognized the failures and took action.

Anyway, the first robust algorithm was more successful to act on the failure conditions. The second algorithm (Section 6.5.4) reduced the divergent estimation outputs, but the *Robust Algorithm 1* was able to totally suppress the estimation errors and gave results even very close to the fail-free mode of operation (Section 6.5.3).

As a conclusion, this study suggests the application of an integrated Radio-INS altimeter, where,

1. The integrated system combines the best features of two different navigation sources, INS and Radio altimeter. The estimated altitude will be 3 times correct that the radio altimeter outputs. While the divergent error characteristic of the INS is restrained, the system has dynamical characteristics as good as the INS.
2. The open loop mechanization of the system tolerates failures at the Kalman filter computations, without causing a total system breakdown.
3. Ground or space based navigation aids are not used, and this brings autonomy to the entire system.
4. The Kalman filter compensates the instant lack of radio altimeter information, as this data is discretely supplied to the system.
5. Abnormal measurements, in cases of measurement channel failures, are detected and corrected by the system, without affecting the good estimation behavior.

REFERENCES

[1] **Kayton, M. and Fried, W. R.,** 1996. Avionics Navigation Systems, 2nd Edition, John Willey & Sons, Inc., New York.

[2] **Biezad, D. J.,** 1999. Integrated Navigation and Guidance Systems, Ed. Przemieniecki J. S., American Institute of Aeronautics and Astronautics, Inc., Reston, Virginia.

[3] **Gray, R. A. and Maybeck, P. S.,** 1995. Integrated GPS/INS/BARO and radar altimeter system for aircraft precision approach landings, *Proceedings of the IEEE 1995 National Aerospace and Electronics Conference, Part 1*, Dayton, KY, USA, May 22-26.

[4] **Deergha, R. K.,** 1997. Integration of GPS and baro-inertial loop aided strapdown INS and radar altimeter, *IETE Journal of Research*, **v 43 n 5**, 383-390.

[5] **Sohne, W., Heinze, O. and Groten, E.,** 1994. Integrated INS/GPS system for high precision navigation applications, *Proceedings of the 1994 IEEE Position Location and Navigation Symposium*, Las Vegas, NV, USA, April 11-15.

[6] **Zelenka, R. E.,** 1994. Design and analysis of a Kalman filter for terrain-referenced positioning and guidance, *Journal of Aircraft,* **v 31 n 2**, 339-344.

[7] **Zelenka, R. E.,** 1993. Flight test development and evaluation of a Kalman filter state estimator for low-altitude flight, *Proceedings of the IEEE Conference on Control Applications, Part 1,* Vancouver, BC, Canada, September 13-16.

[8] **Brandin V. N., et al.,** 1984. Experimental Ballistics of the Space Apparatus, Mashikostroyeniye, Moscow (in Russian).

[9] **Zhukovskiy, A. P. and Rastorguev, V. V.,** 1998. Complex Radio navigation and control systems of aircraft, MAI, Moscow (in Russian).

[10] **AIRBUS Inc.,** 2000. A 310 Aircraft Maintenance Manual Chapter 34, Rev. No: 43.

[11] **Kalman, R. E.,** 1960. A new approach to linear filtering and prediction problems, *Transaction of the ASME-Journal of Basic Engineering*, March, 35-45.

[12] **Welch, G. and Bishop, G.,** 2001. An introduction to the Kalman filter, TR 95 041, UNC-Chapel Hill.

[13] **Chui, C. K. and Chen, G.,** 1987. Kalman Filtering with Real-Time Applications, Eds. Huang T. S. and Schroeder M. R., Springer-Verlag, Heidelberg.

[14] **Hacıyev, C. M.,** 1999. Radyo Navigasyon, İ.T.Ü, Istanbul (in Turkish).

[15] **Hacıyev, C. M.,** 1989. Simplified filtering algorithm in the presence of faults in the measuring channel, *Measurement Techniques*, **v 32 n 6**, 505-507.

[16] **Carlson, N. A.,** 1990. Federated Square Root Filter for Decentralized Kalman Parallel Processes. IEEE tr. on AES, **n 26**, 517-525

[17] **Carlson, N. A. and Berarducci, M.P.,** 1994. Federated Kalman Filter Simulation Results. *Navigation: Journal of Institute of Navigation*, **n 41**, 297-321.

[18] **Levy, L. J.,** 1996. Suboptimality of cascaded and federated Kalman filters. *Navigational Technology for the 3rd Millennium Proceedings of the Annual Meeting - Institute of Navigation*. Inst. of Navigation, Alexandria, VA, USA, 399-407.

[19] **Howard, S., Ko, H. L. and Alexander, W. E.,** 1996. Parallel processing and stability analysis of the Kalman filter. *Proc. of the IEEE 15th Annual International Phoenix Conference on Computers and Communications*, IEEE, Piscataway, NJ, USA, 366-372.

[20] **Paik, B. S. and Oh, O. H.,** 2000. Gain fusion algorithm for decentralized parallel Kalman filters. *IEE Proceedings: Control Theory and Applications*, **v 147 n 1**, 97-103.

[21] **Sage, A. P. and Melse, J. L.,** 1972. Estimation Theory with Application to Communication and Control, McGraw-Hill, New York.

[22] **Wolfe C. and Hart D.,** 1999. Getting started with Matlab, Indiana University.

[23] **The MathWorks,** 1999. Matlab User's Guide, For UNIX Workstations.

[24] **HONEYWELL,** 2001. Component Maintenance Manual, Inertial Reference Unit, **v 1**.

[25] **THOMSON-CSF,** 2001. Component Maintenance Manual, ERT-530 Radio Altimeter Transceiver Unit.

[26] **TRT,** 2001. Component Maintenance Manual, ANT-AHV5-501-2 Radio Altimeter Antenna.

APPENDIXES

APPENDIX A	:	Optimal Kalman Filter Simulation Additional Figures
APPENDIX B	:	Failure Conditions Simulation Additional Figures
APPENDIX C	:	*Robust Algorithm 1* Simulation Additional Figures
APPENDIX D	:	*Robust Algorithm 2* Simulation Additional Figures
APPENDIX E	:	Additional Tables
APPENDIX F	:	Simulation software (Attached to the back cover)

APPENDIX A : Optimal Kalman Filter Simulation Additional Figures

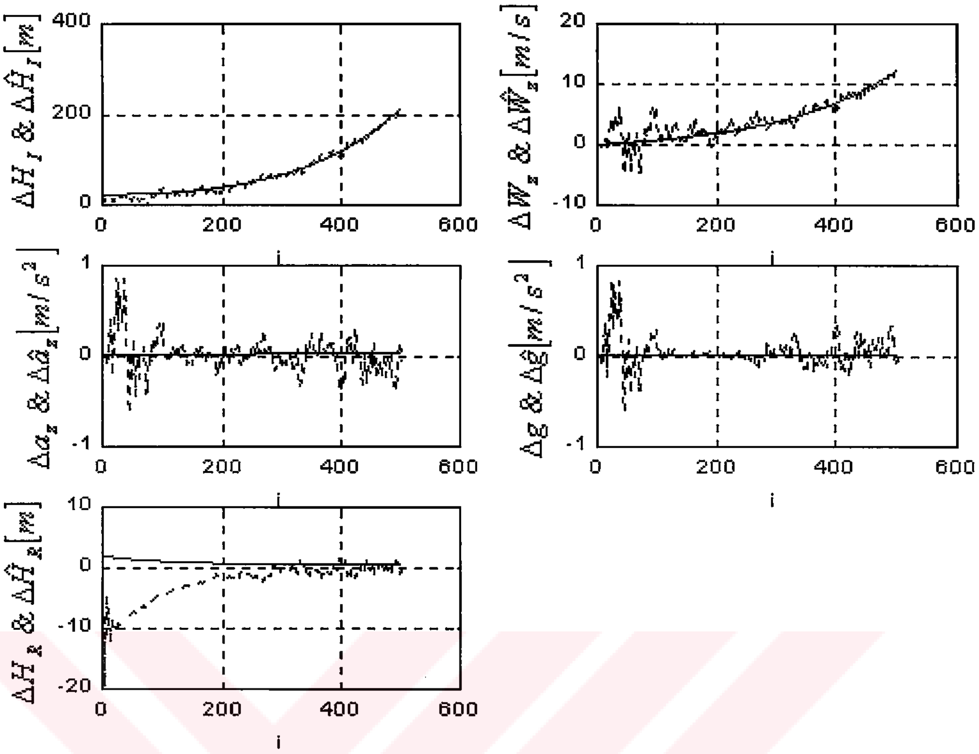

Figure A.1 The estimated (dotted line) and model (solid line) error values.

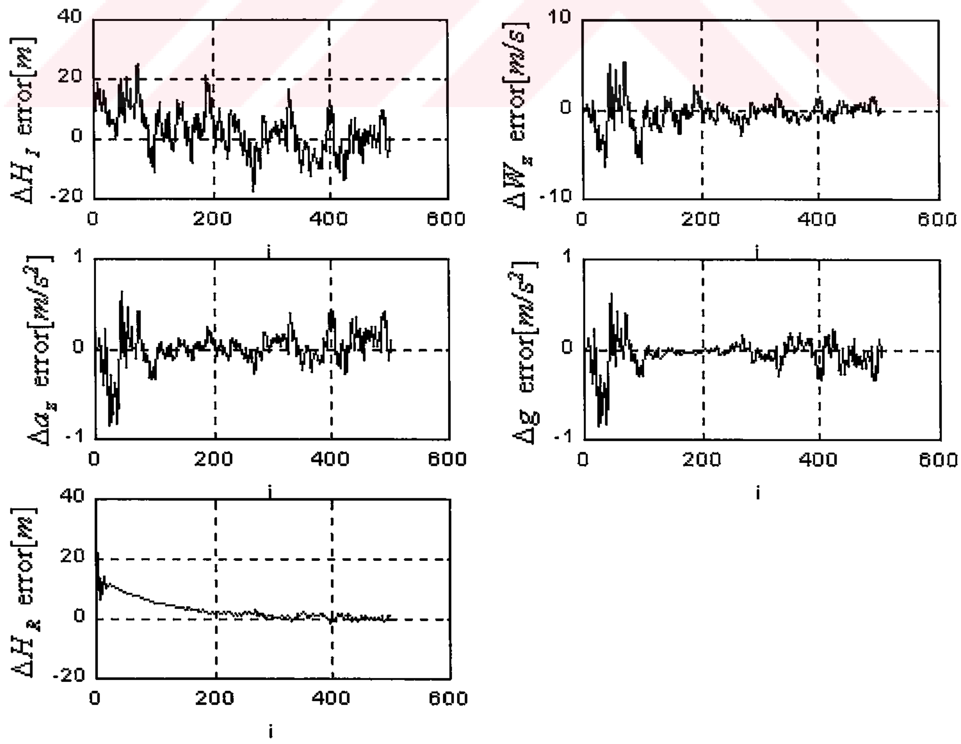

Figure A.2 Difference between estimated and model errors.

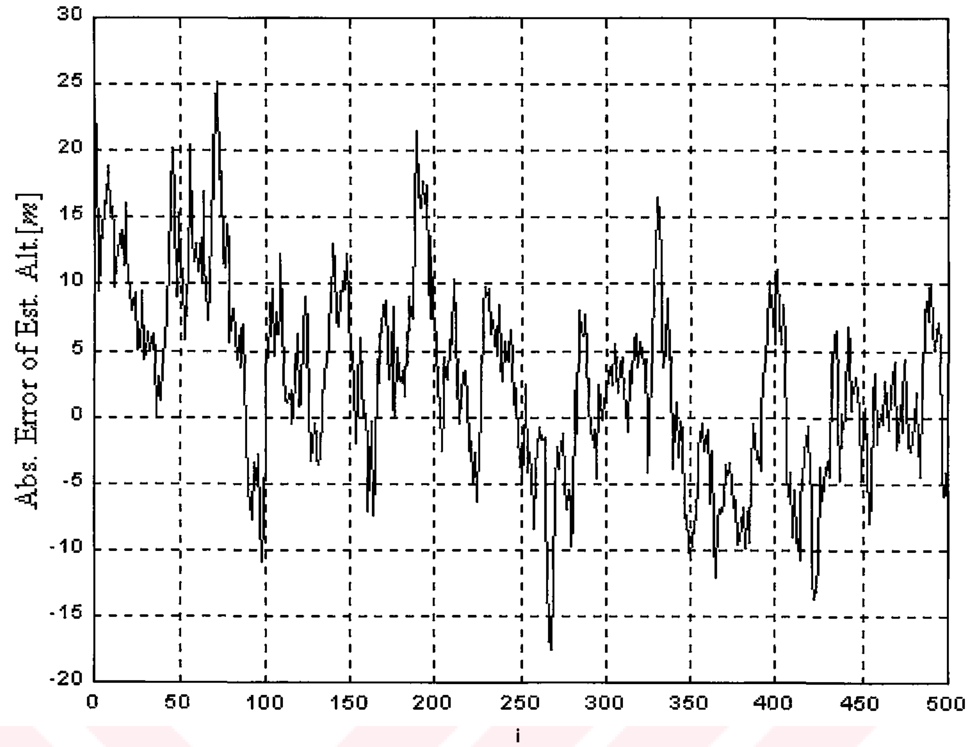

Figure A.3 Absolute error of estimated altitude.

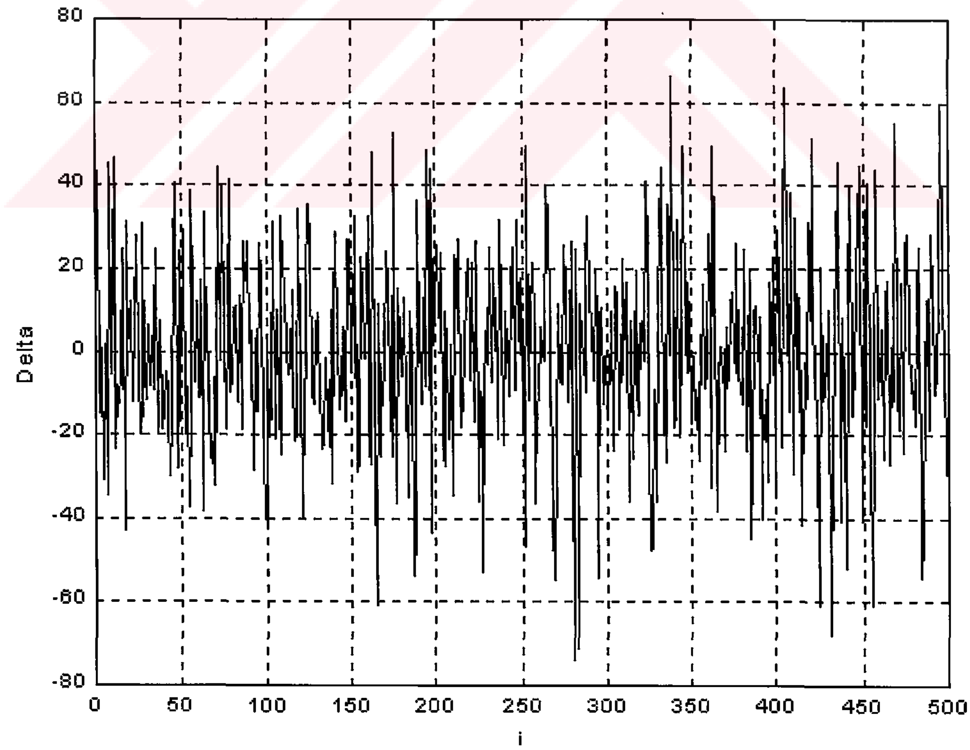

Figure A.4 Innovation sequence, *Delta*.

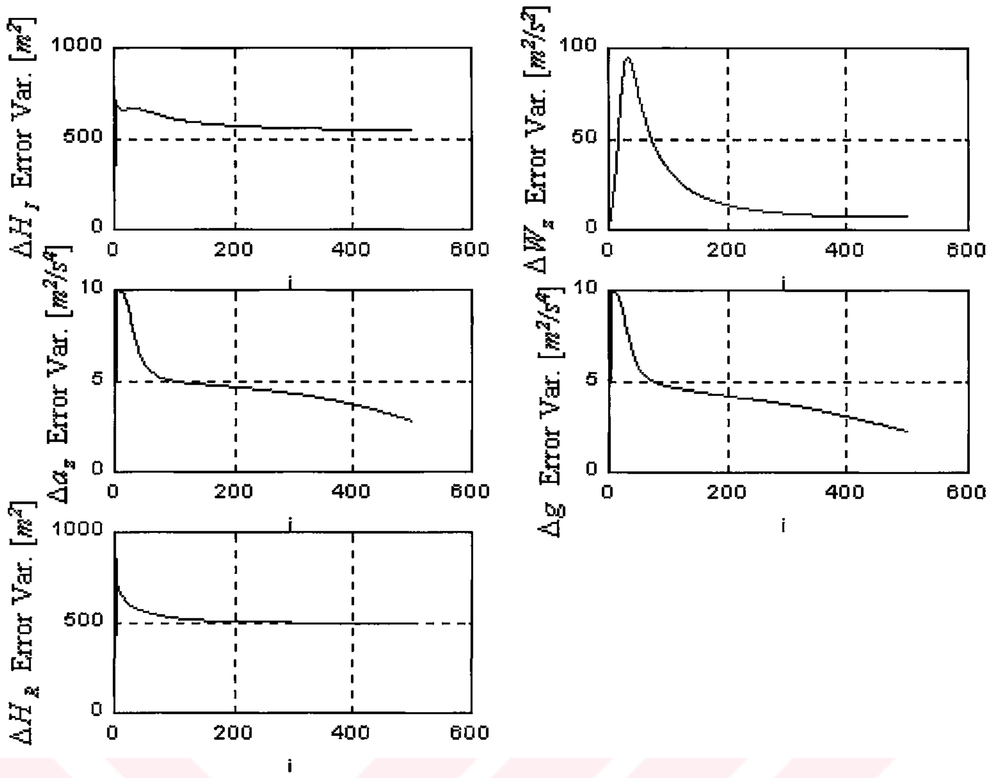

Figure A.5 Error variances for INS altitude, vertical speed, vertical acceleration, gravity and radio altitude respectively.

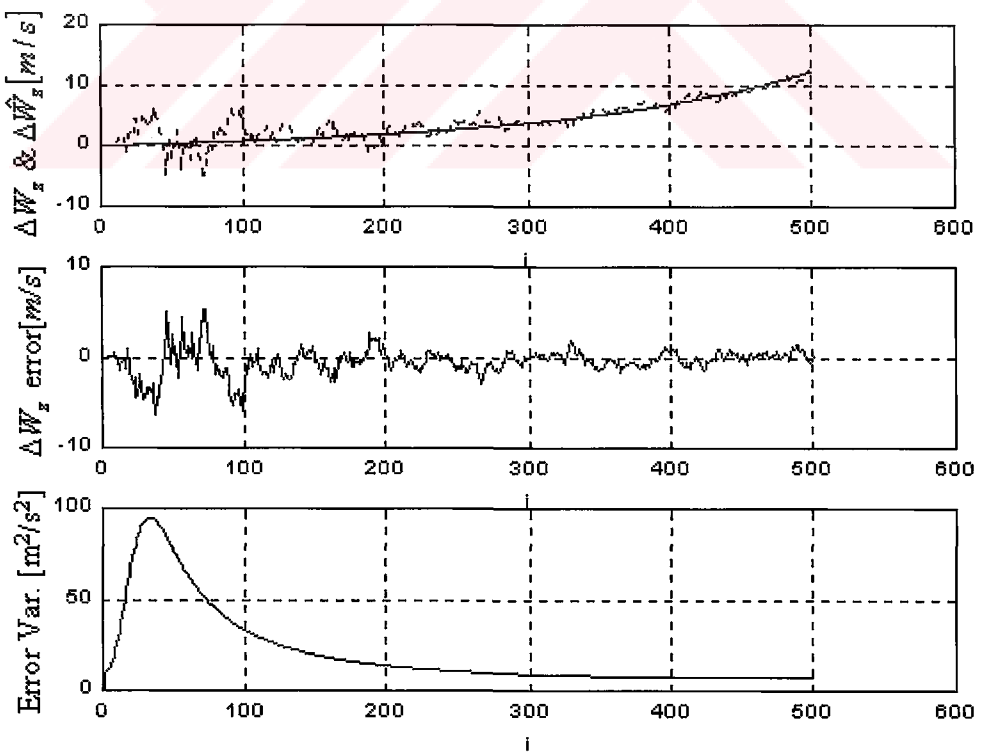

Figure A.6 Combined graph of model (solid line) and estimated (dotted line) errors, their differences, and error variance of vertical speed.

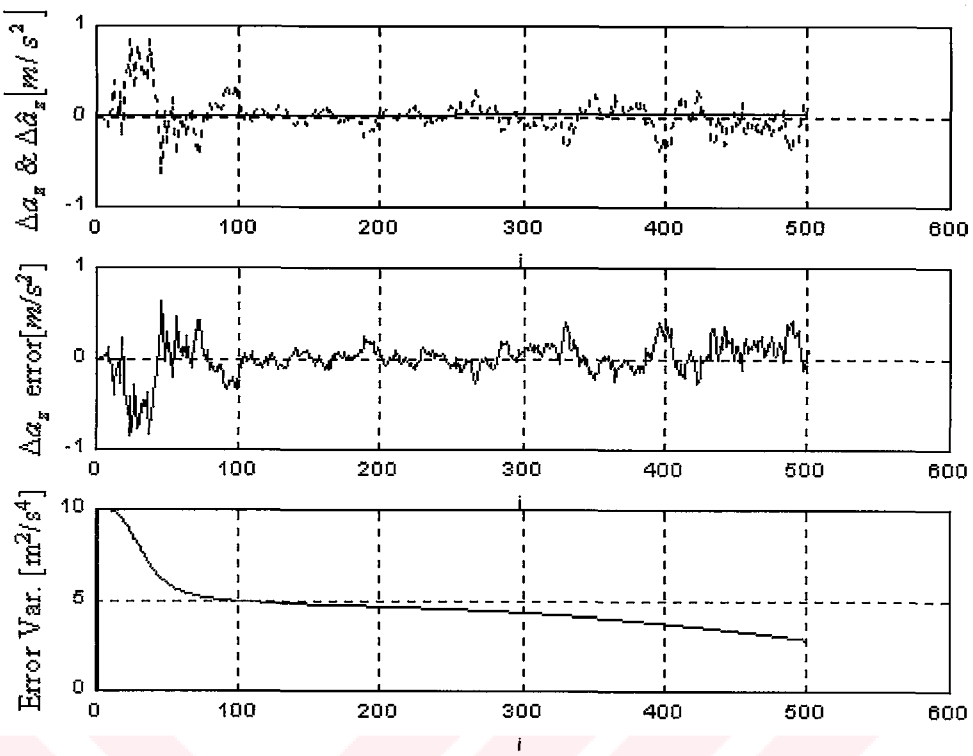

Figure A.7 Combined graph of model (solid line) and estimated (dotted line) errors, their differences, and error variance of vertical acceleration.

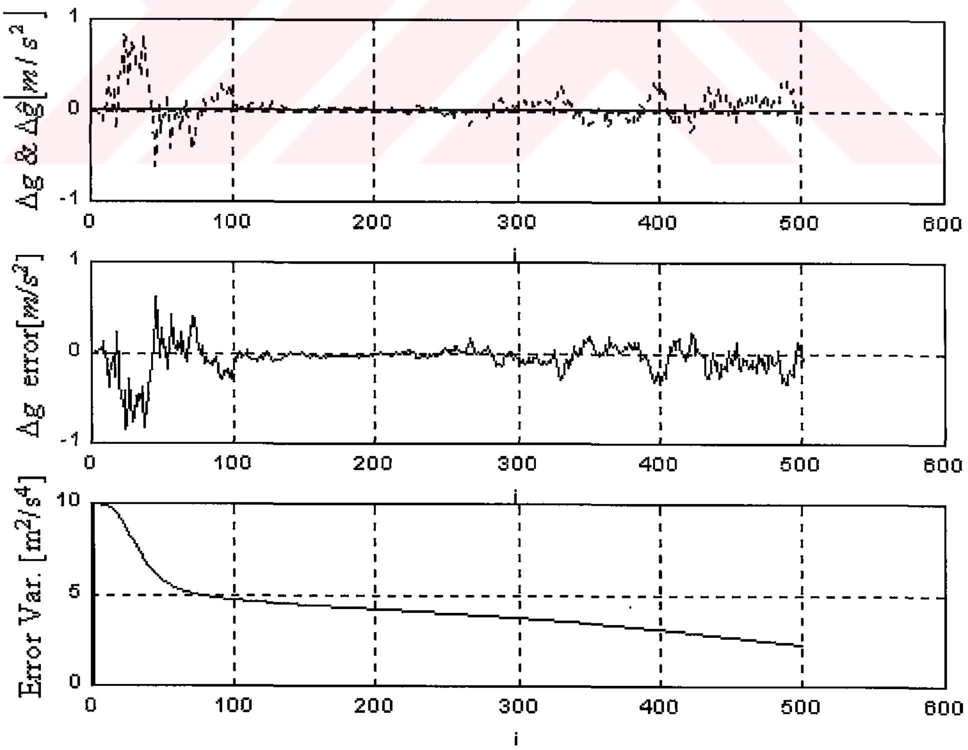

Figure A.8 Combined graph of model (solid line) and estimated (dotted line) errors, their differences, and error variance of gravity.

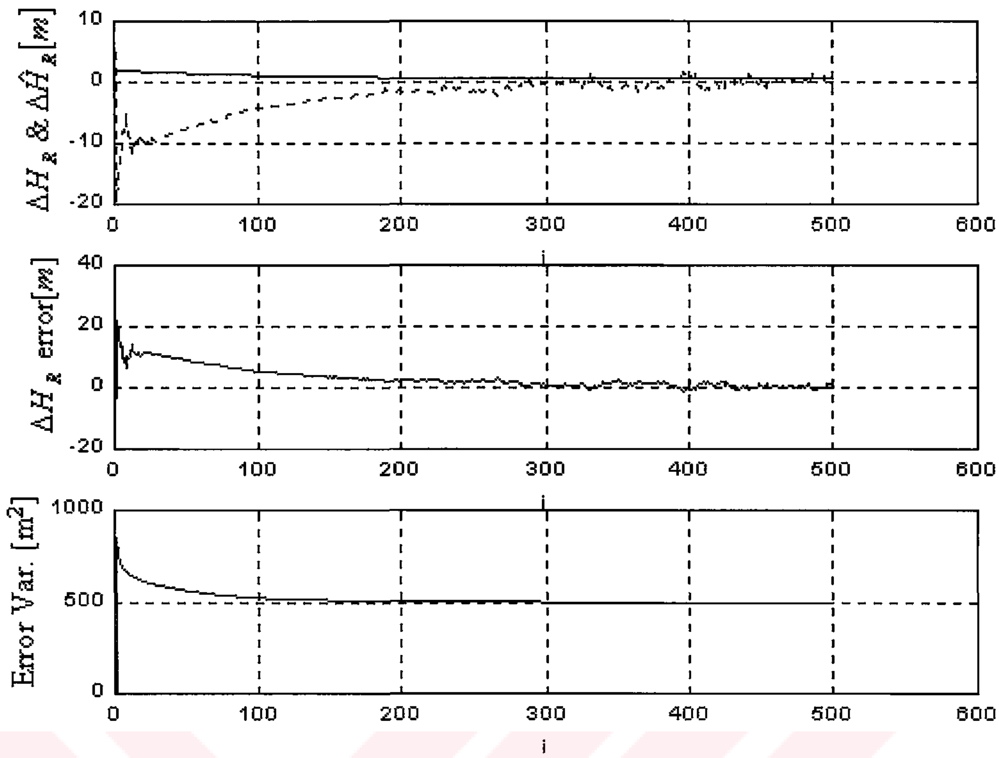

Figure A.9 Combined graph of model (solid line) and estimated (dotted line) errors, their differences, and error variance of radio altitude.

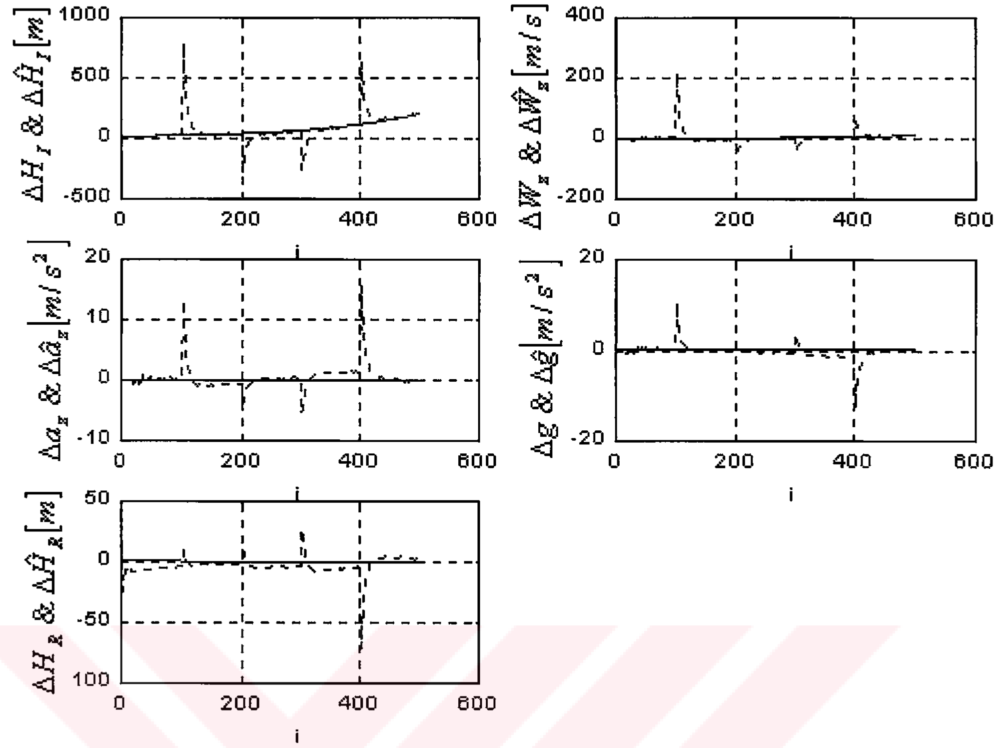

Figure B.1 The estimated (dotted line) and model (solid line) error values.

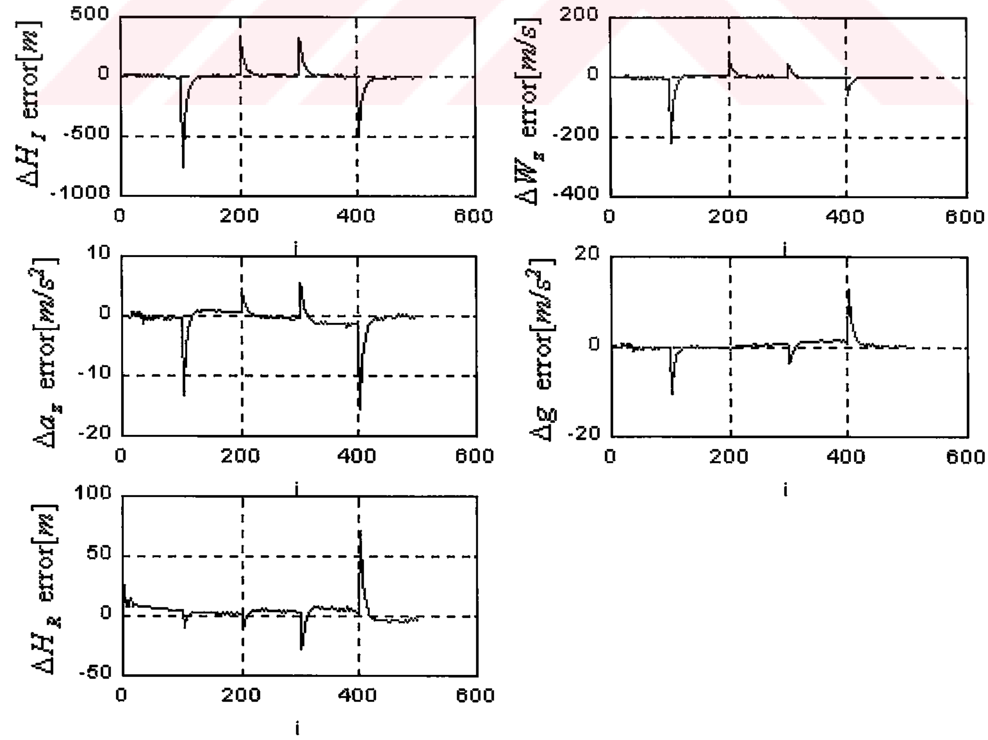

Figure B.2 Difference between estimated and model errors.

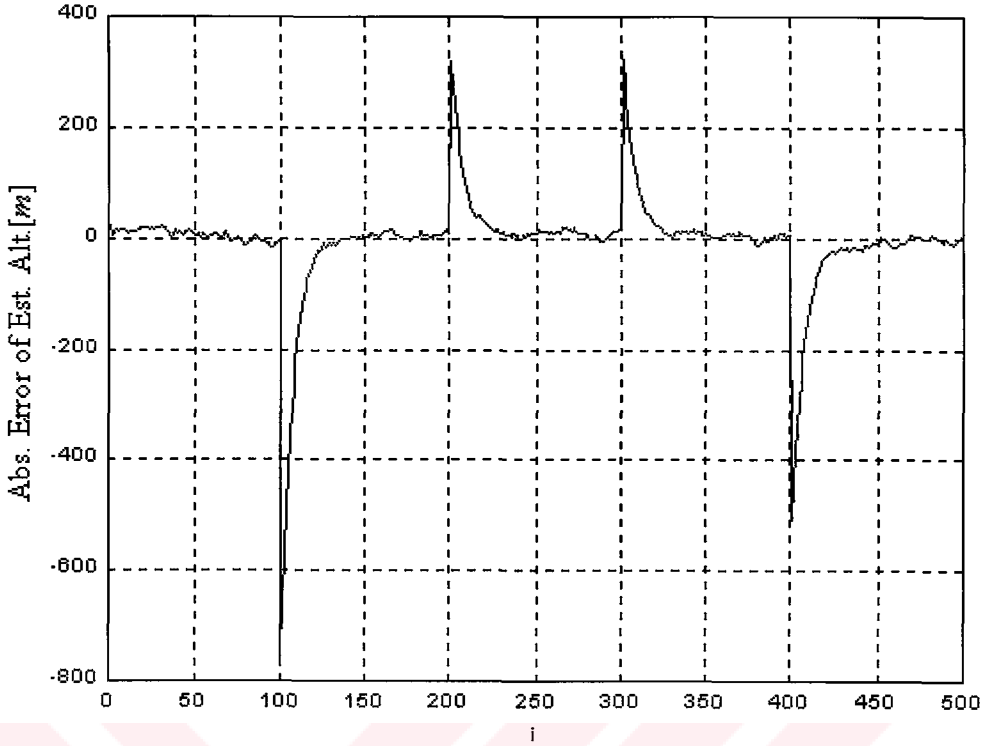

Figure B.3 Absolute error of estimated altitude.

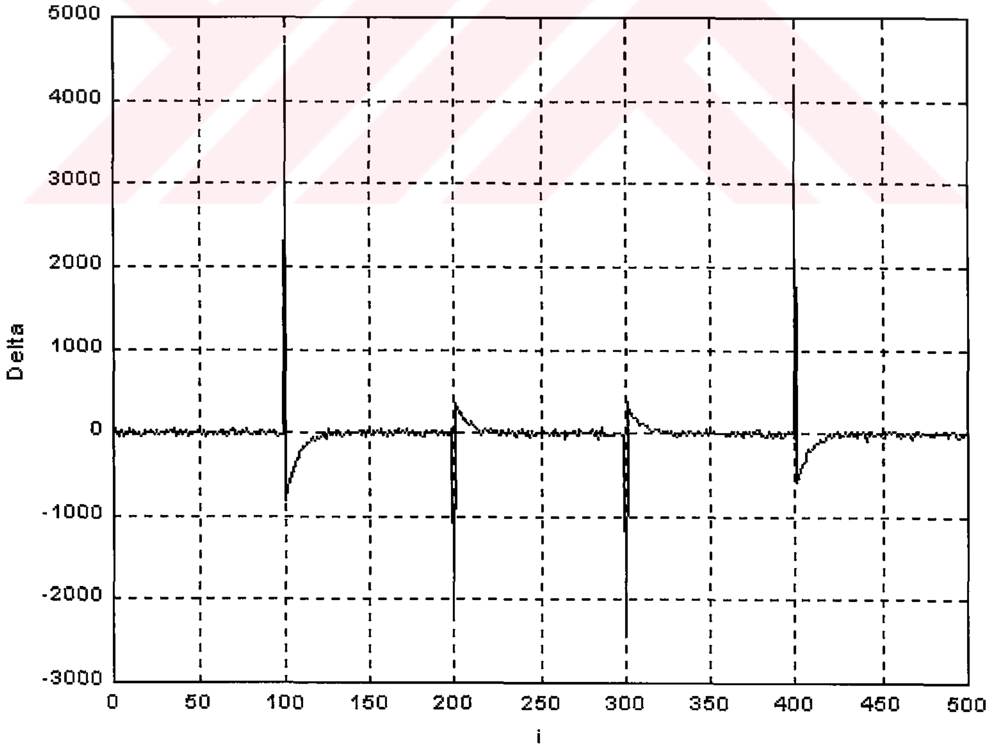

Figure B.4 Innovation sequence, *Delta*.

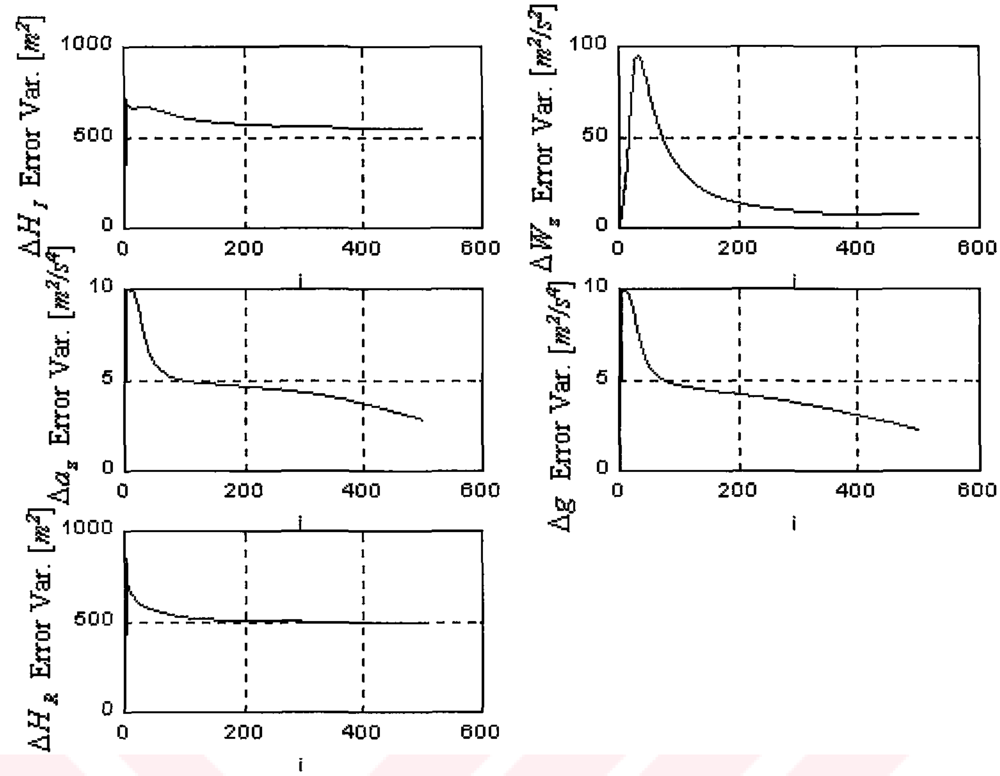

Figure B.5 Error variances for INS altitude, vertical speed, vertical acceleration, gravity and radio altitude respectively.

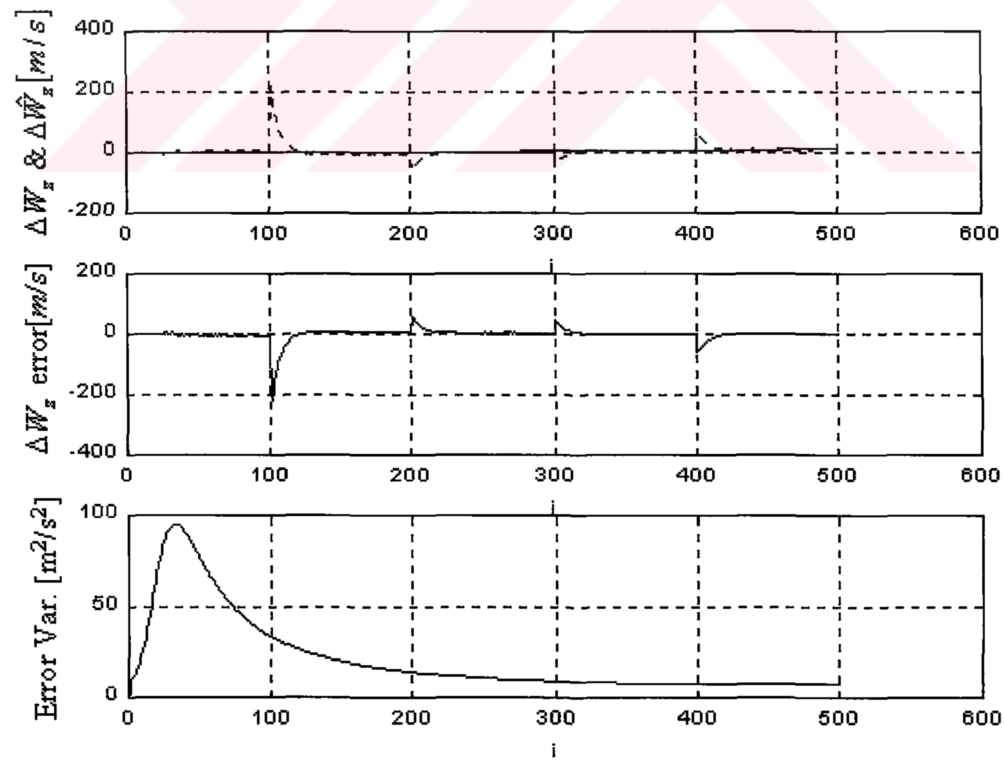

Figure B.6 Combined graph of model (solid line) and estimated (dotted line) errors, their differences, and error variance of vertical speed.

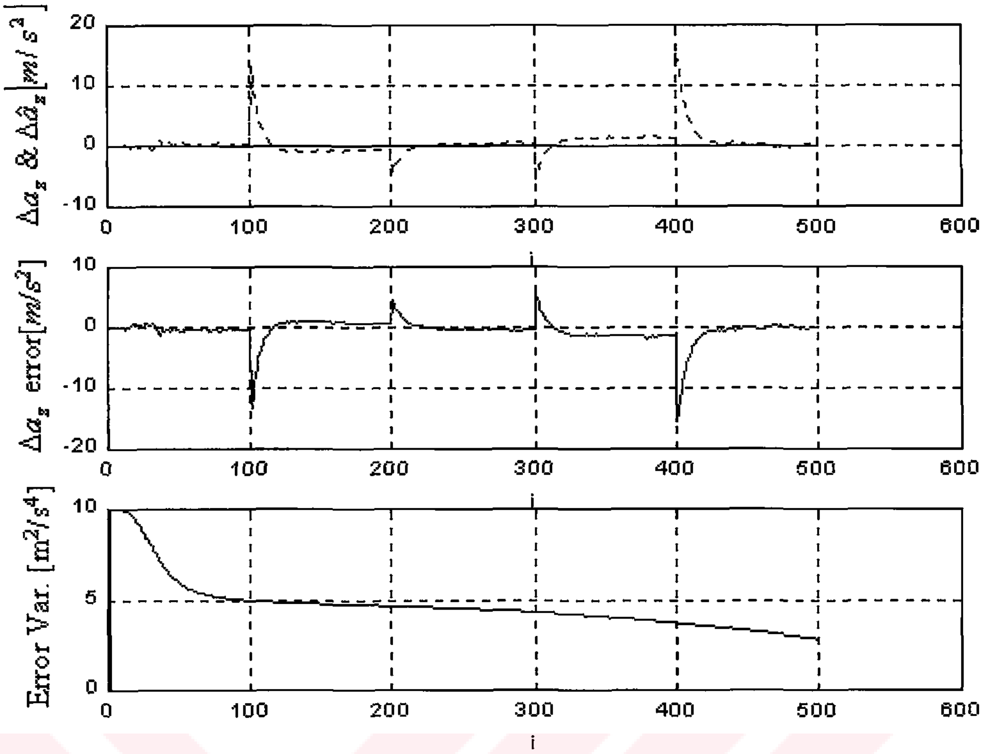

Figure B.7 Combined graph of model (solid line) and estimated (dotted line) errors, their differences, and error variance of vertical acceleration.

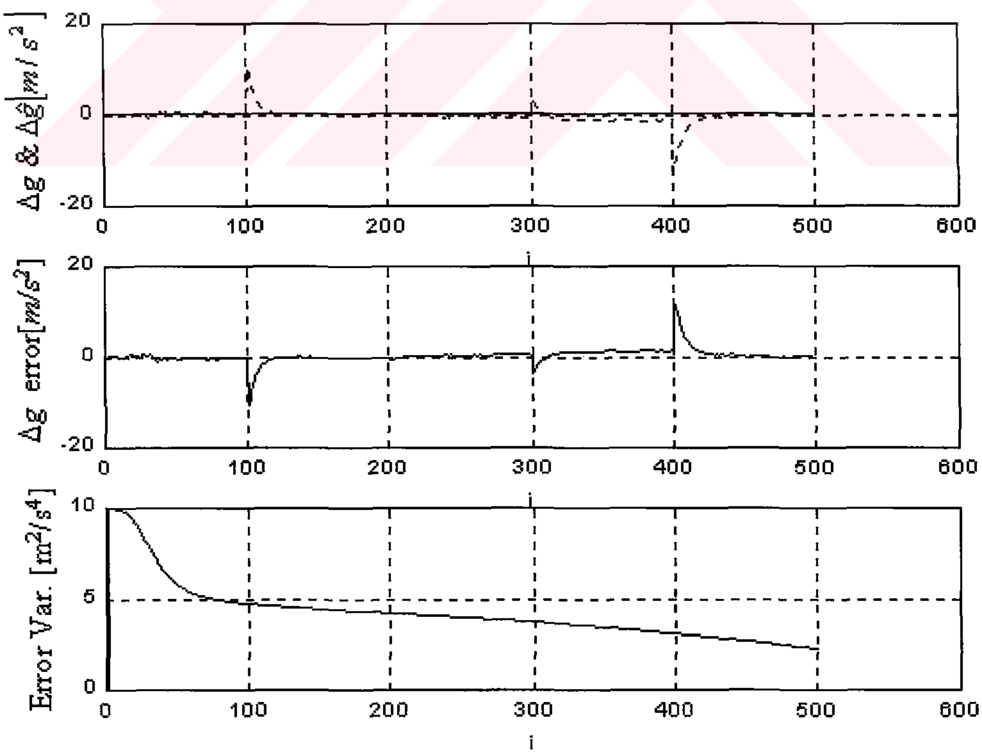

Figure B.8 Combined graph of model (solid line) and estimated (dotted line) errors, their differences, and error variance of gravity.

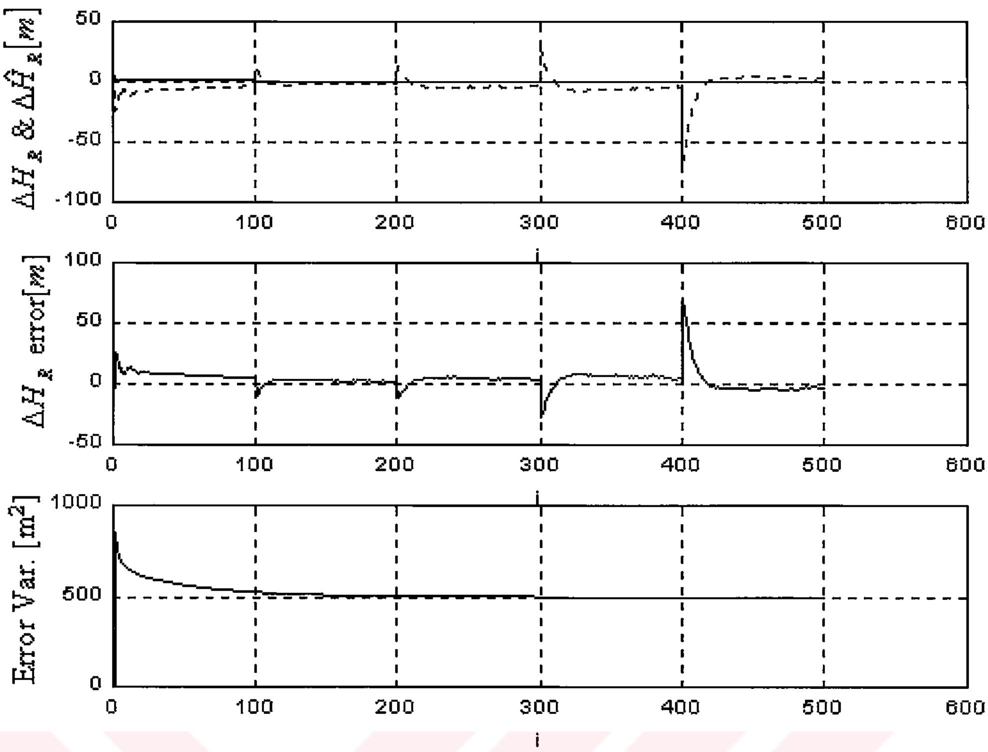

Figure B.9 Combined graph of model (solid line) and estimated (dotted line) errors, their differences, and error variance of radio altitude.

APPENDIX C : *Robust Algorithm 1* Simulation Additional Figures

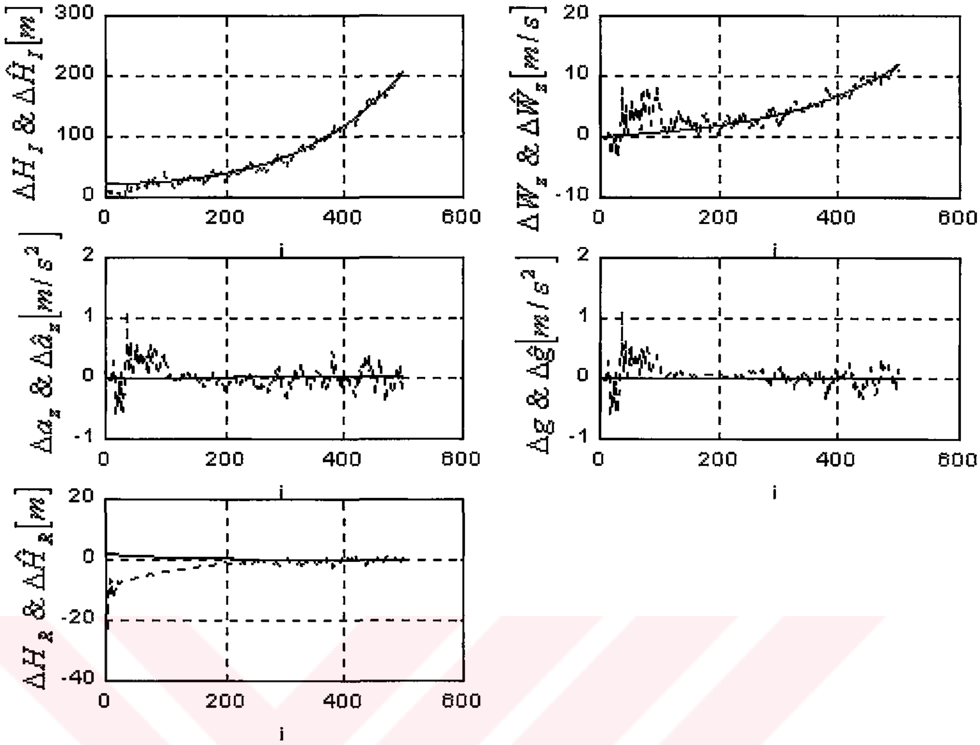

Figure C.1 The estimated (dotted line) and model (solid line) error values.

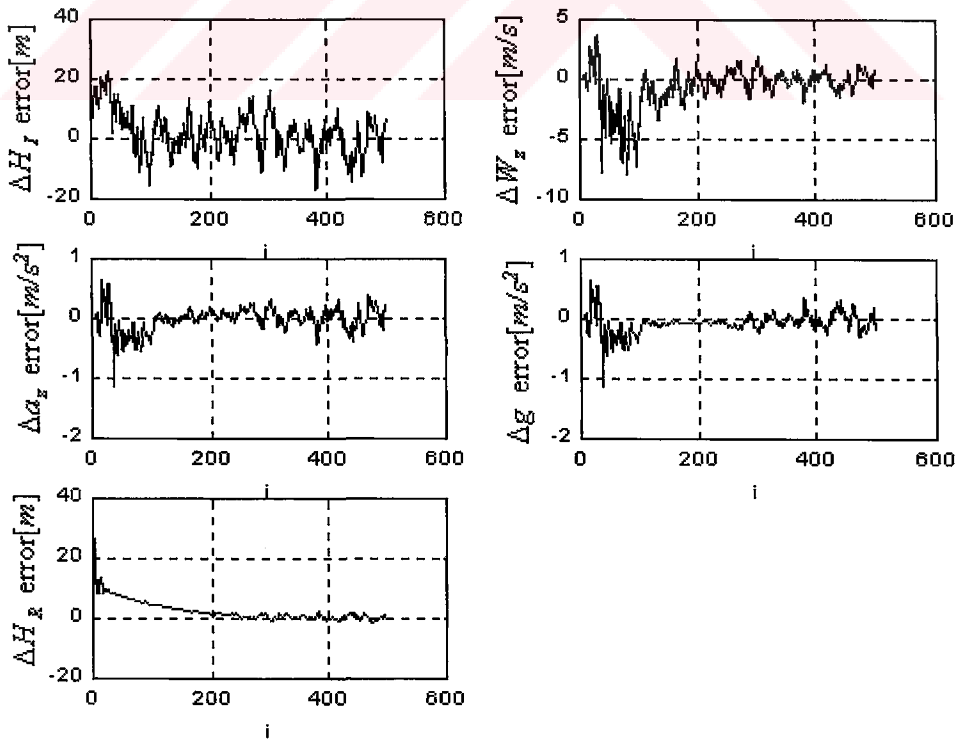

Figure C.2 Difference between estimated and model errors.

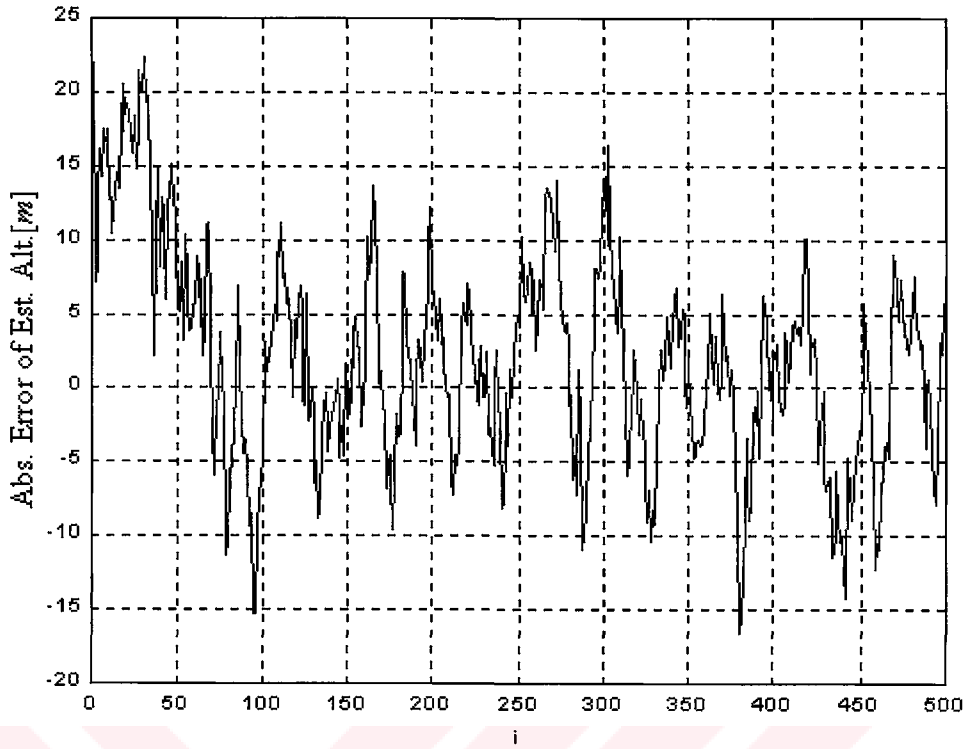

Figure C.3 Absolute error of estimated altitude.

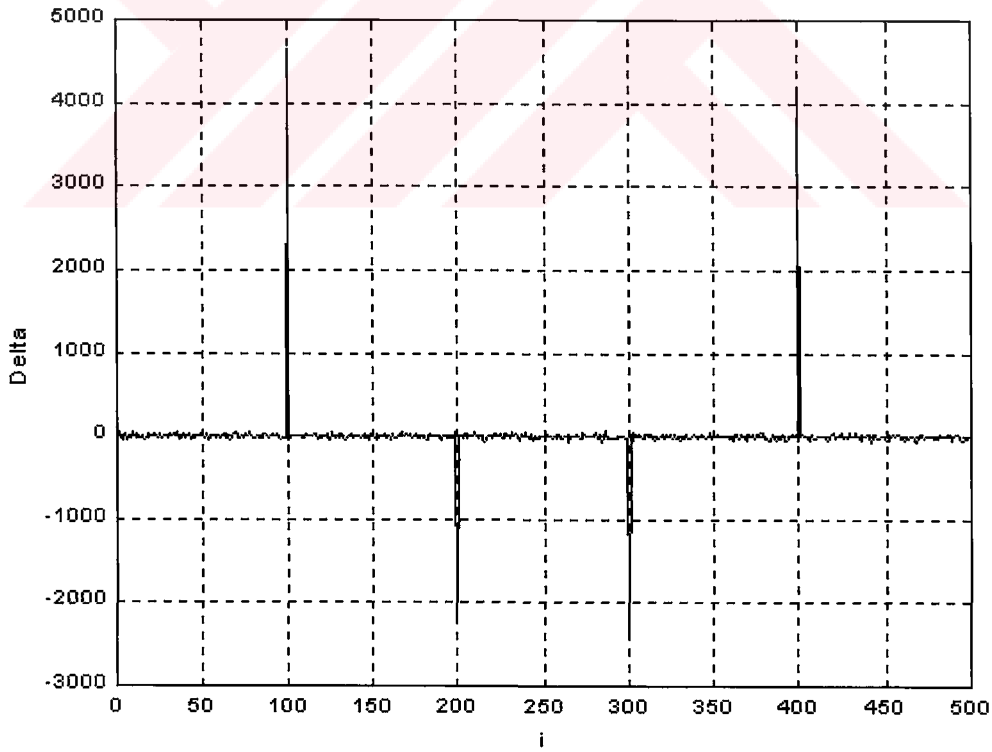

Figure C.4 Innovation sequence, *Delta.*

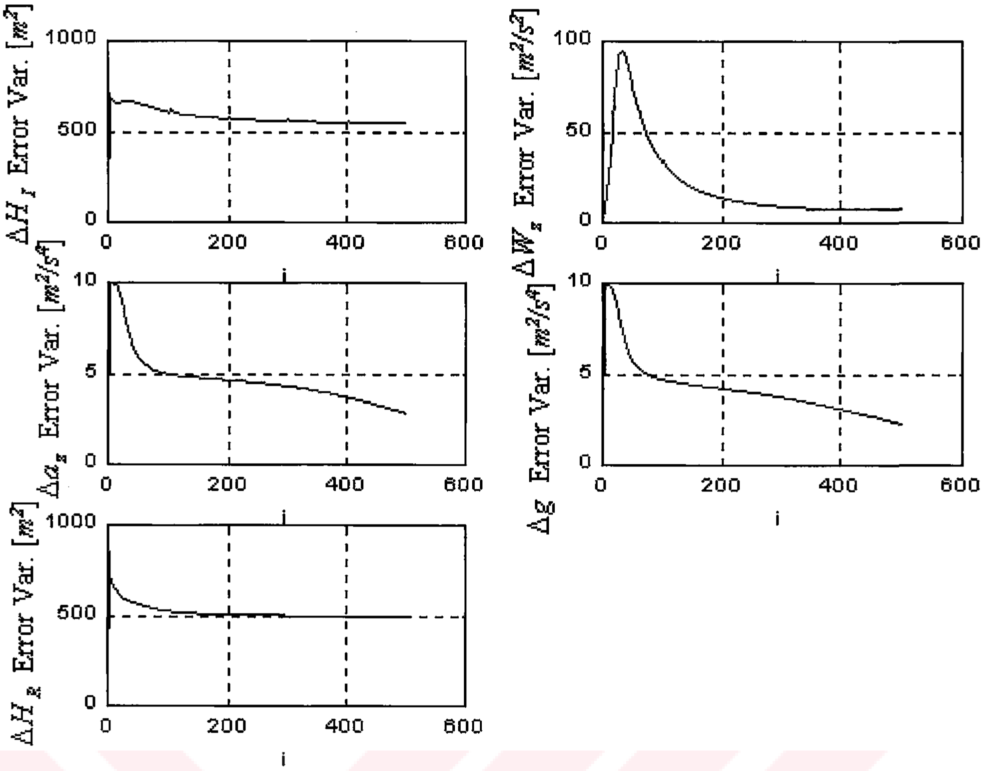

Figure C.5 Error variances for INS altitude, vertical speed, vertical acceleration, gravity and radio altitude respectively.

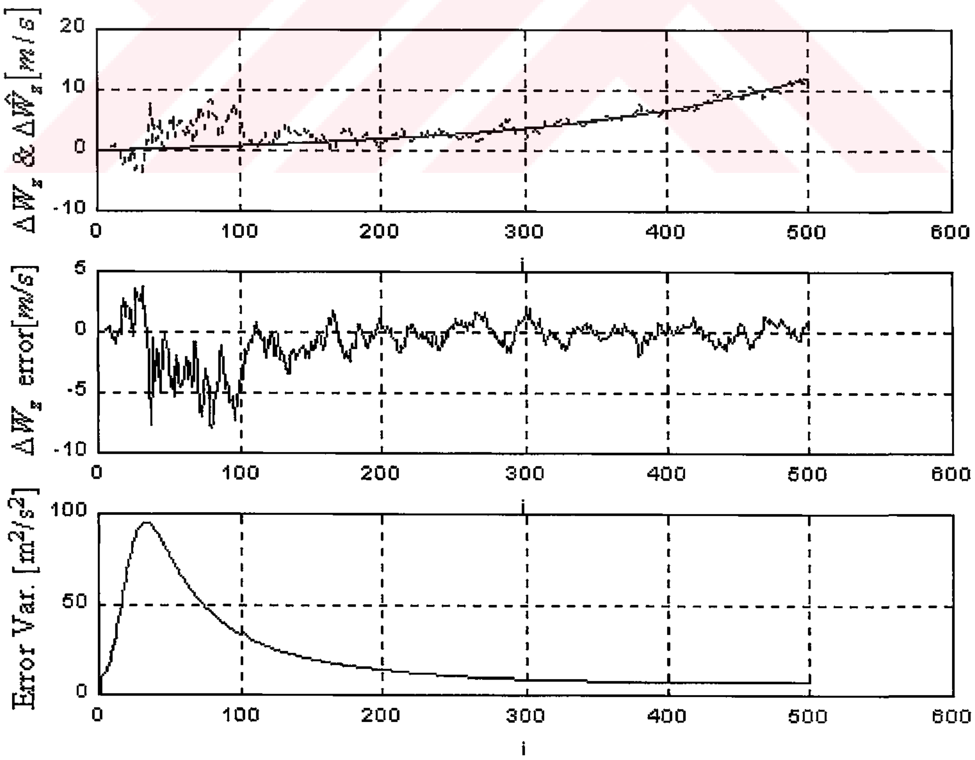

Figure C.6 Combined graph of model (solid line) and estimated (dotted line) errors, their differences, and error variance of vertical speed.

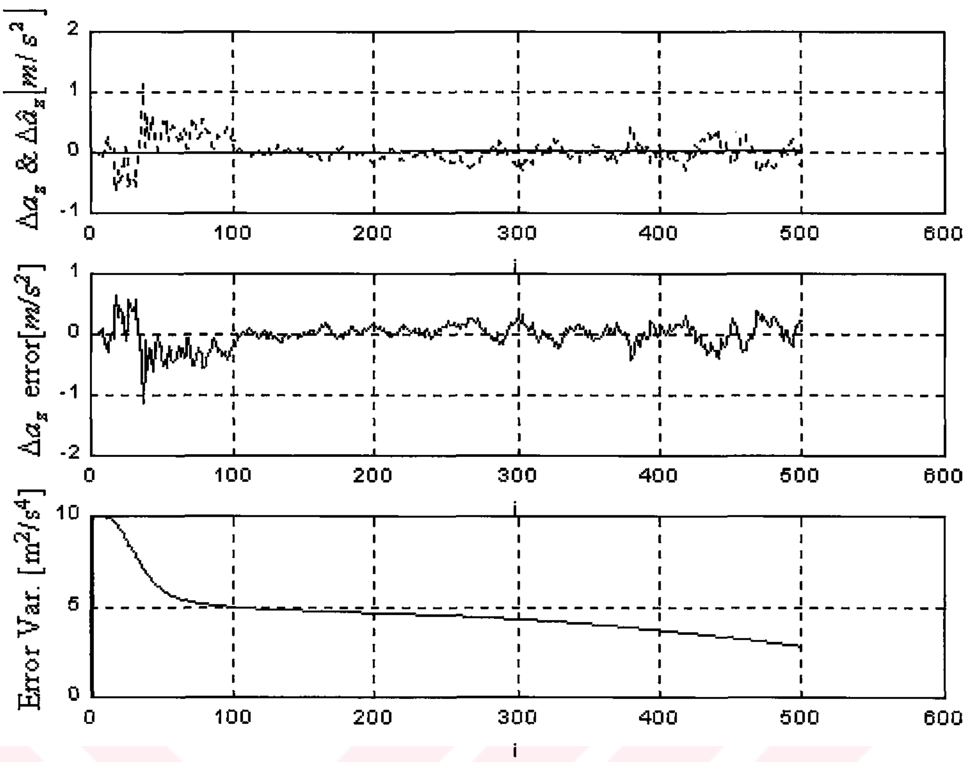

Figure C.7 Combined graph of model (solid line) and estimated (dotted line) errors, their differences, and error variance of vertical acceleration.

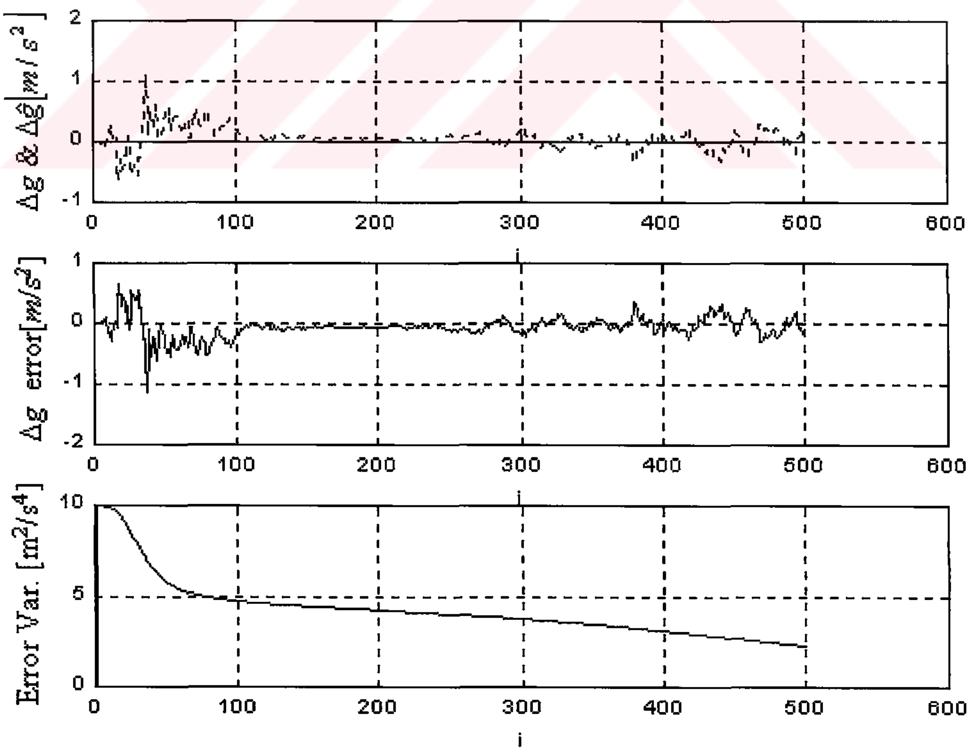

Figure C.8 Combined graph of model (solid line) and estimated (dotted line) errors, their differences, and error variance of gravity.

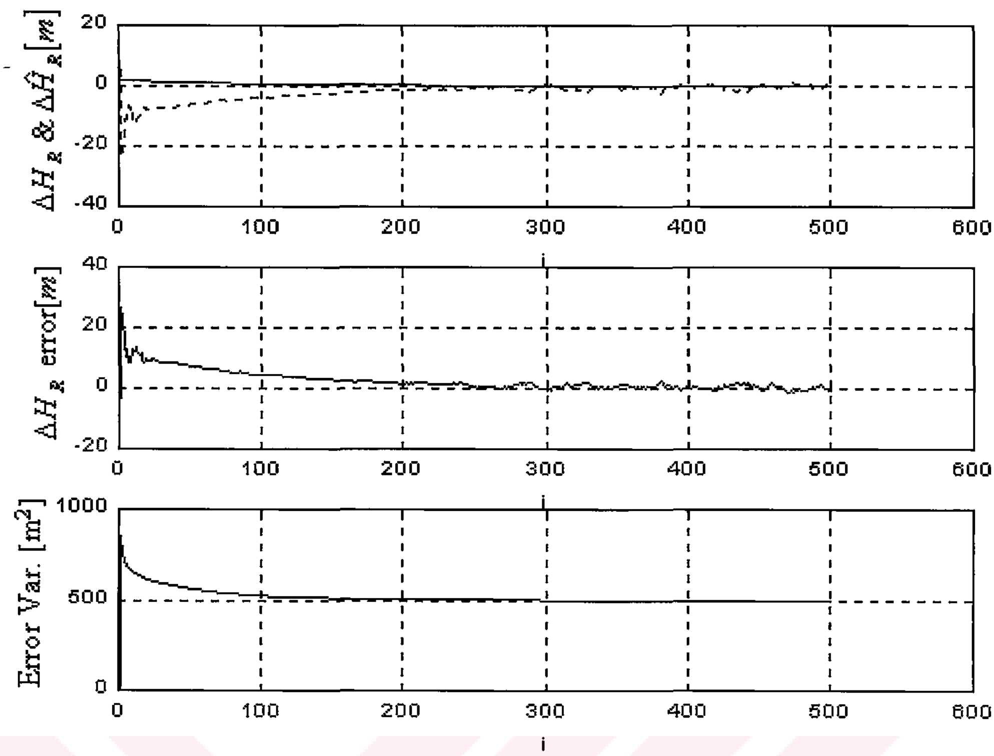

Figure C.9 Combined graph of model (solid line) and estimated (dotted line) errors, their differences, and error variance of radio altitude.

APPENDIX D : *Robust Algorithm 2* Simulation Additional Figures

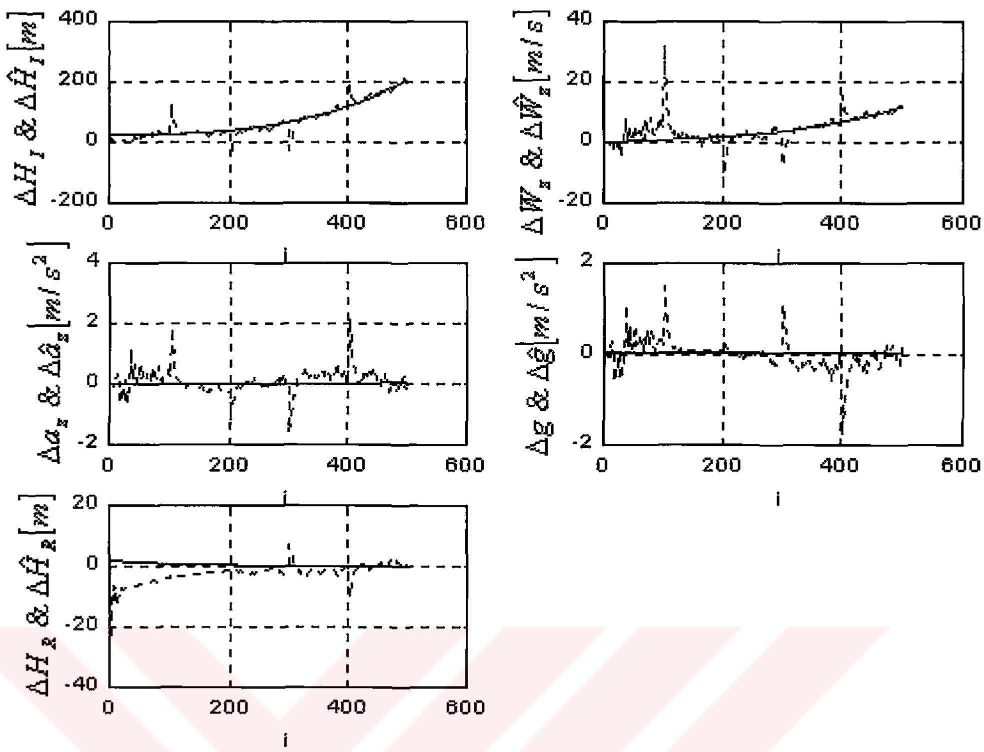

Figure D.1 The estimated (dotted line) and model (solid line) error values.

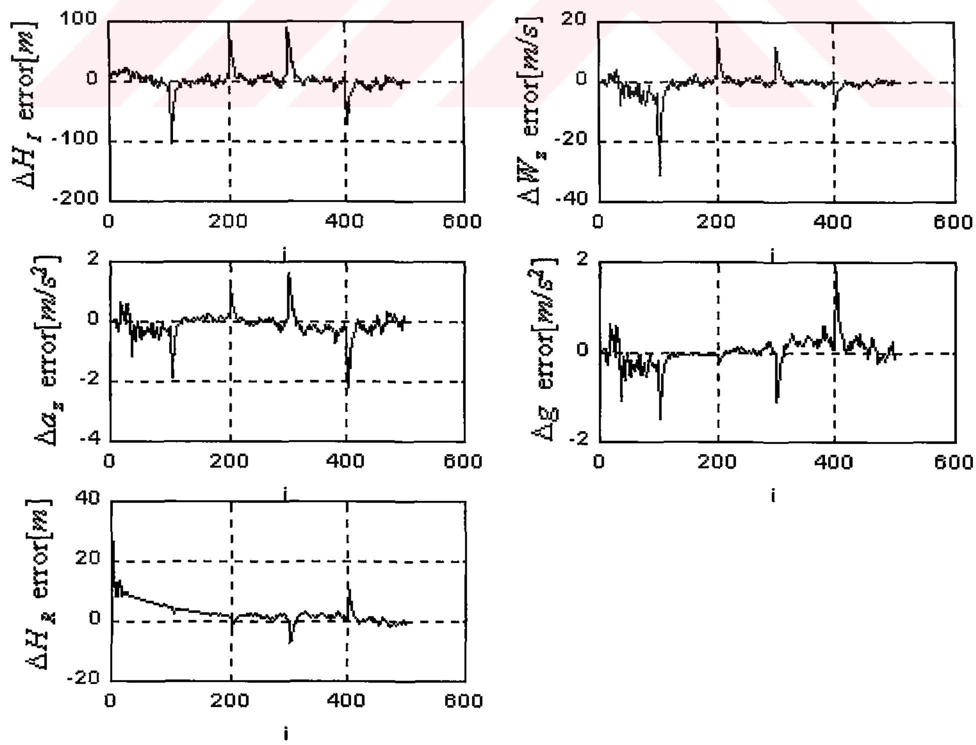

Figure D.2 Difference between estimated and model errors.

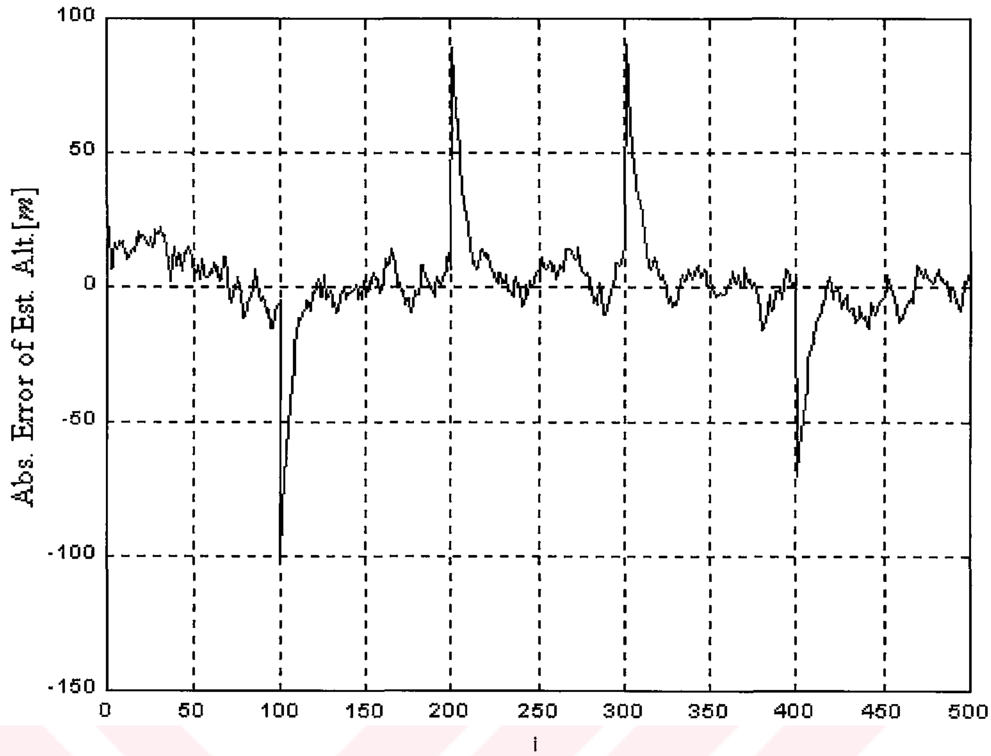

Figure D.3 Absolute error of estimated altitude.

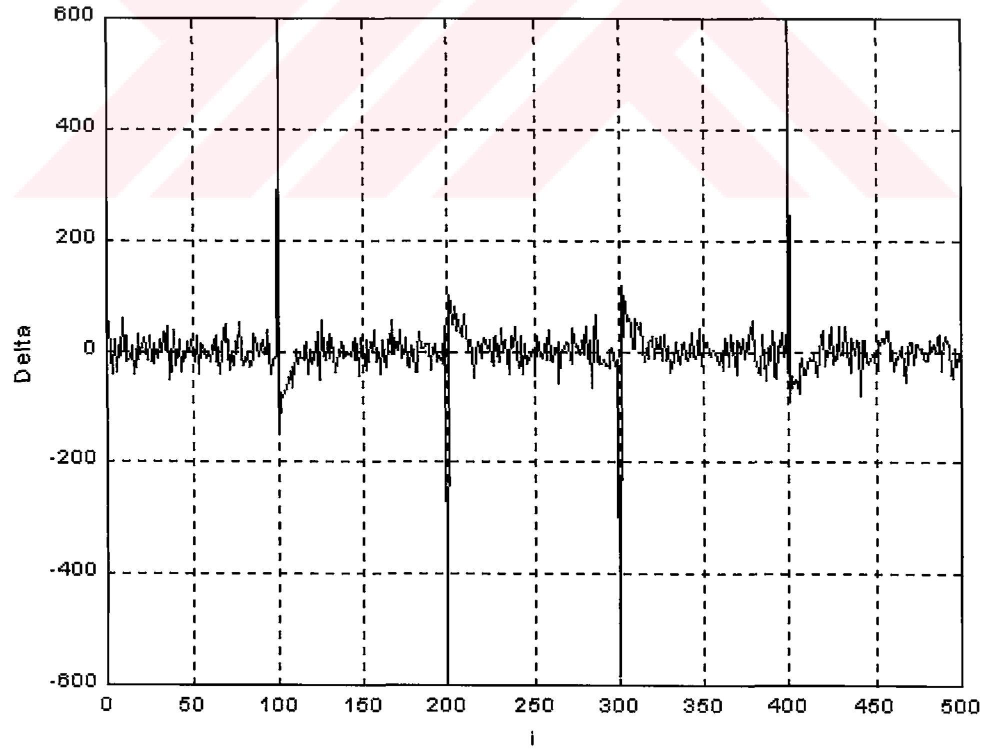

Figure D.4 Innovation sequence, *Delta*.

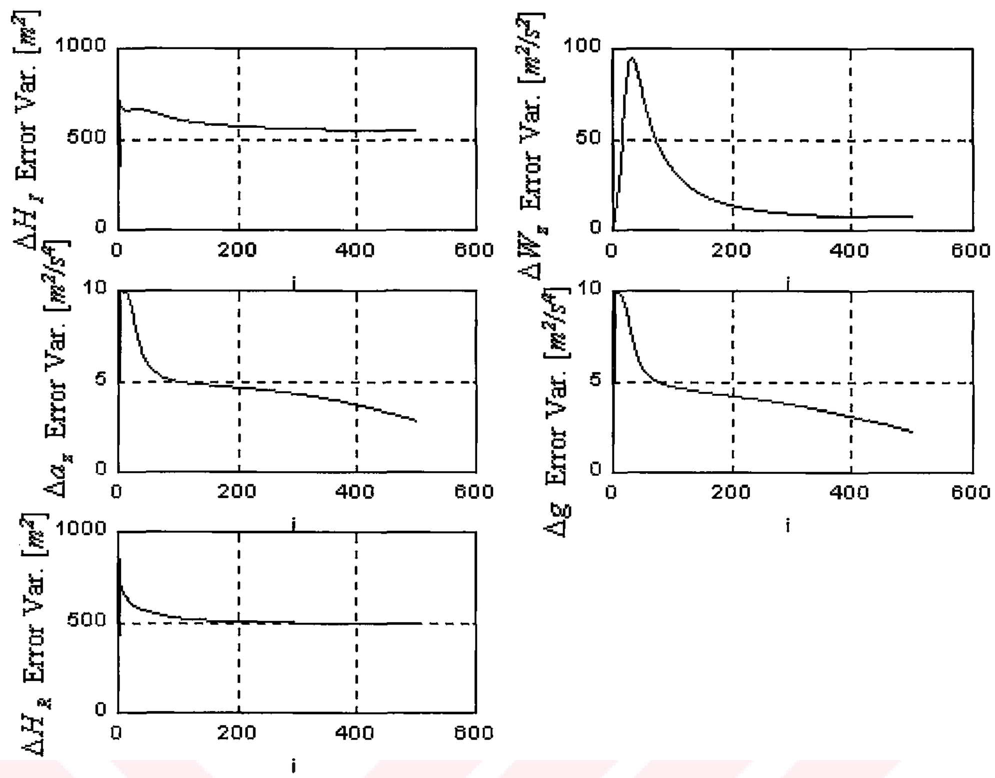

Figure D.5 Error variances for INS altitude, vertical speed, vertical acceleration, gravity and radio altitude respectively.

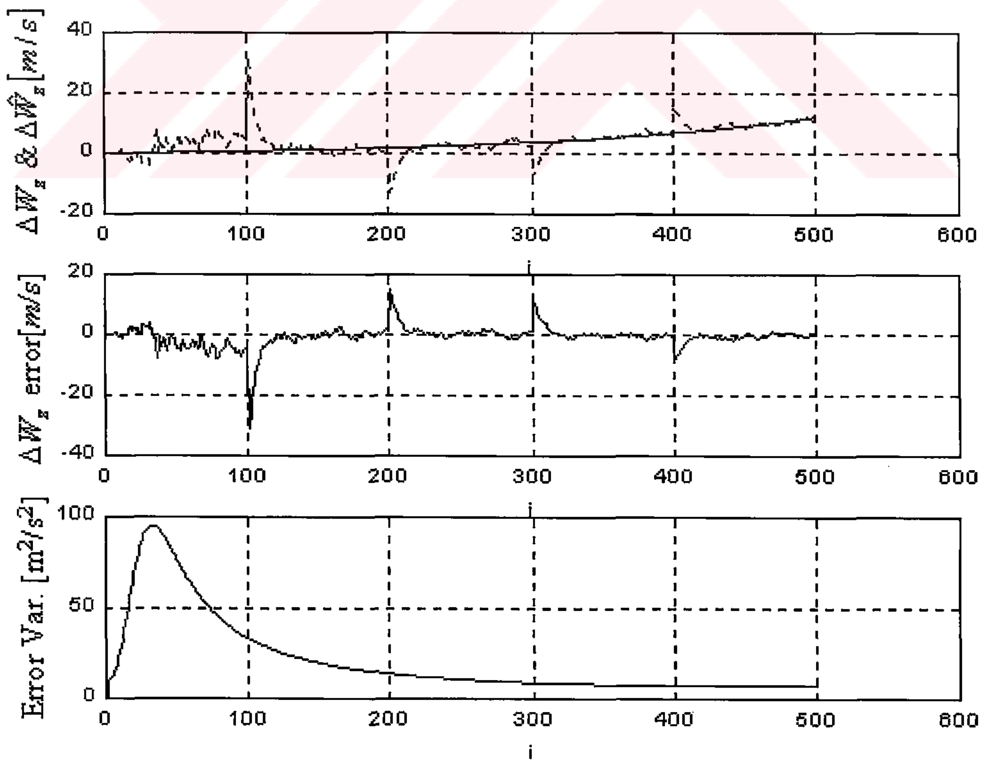

Figure D.6 Combined graph of model (solid line) and estimated (dotted line) errors, their differences, and error variance of vertical speed.

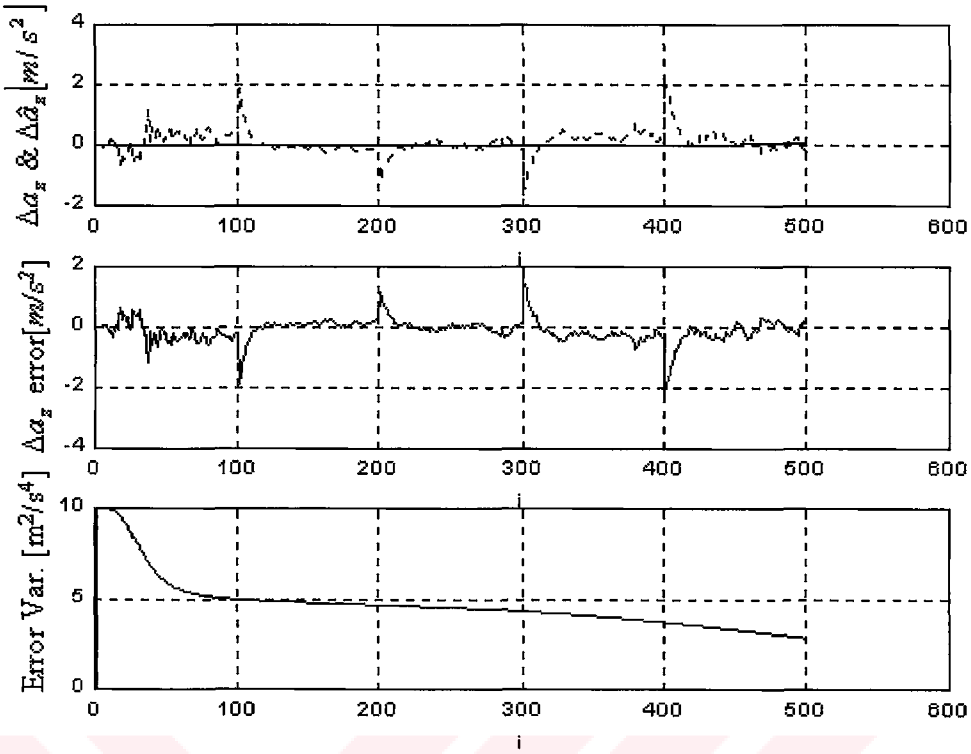

Figure D.7 Combined graph of model (solid line) and estimated (dotted line) errors, their differences, and error variance of vertical acceleration.

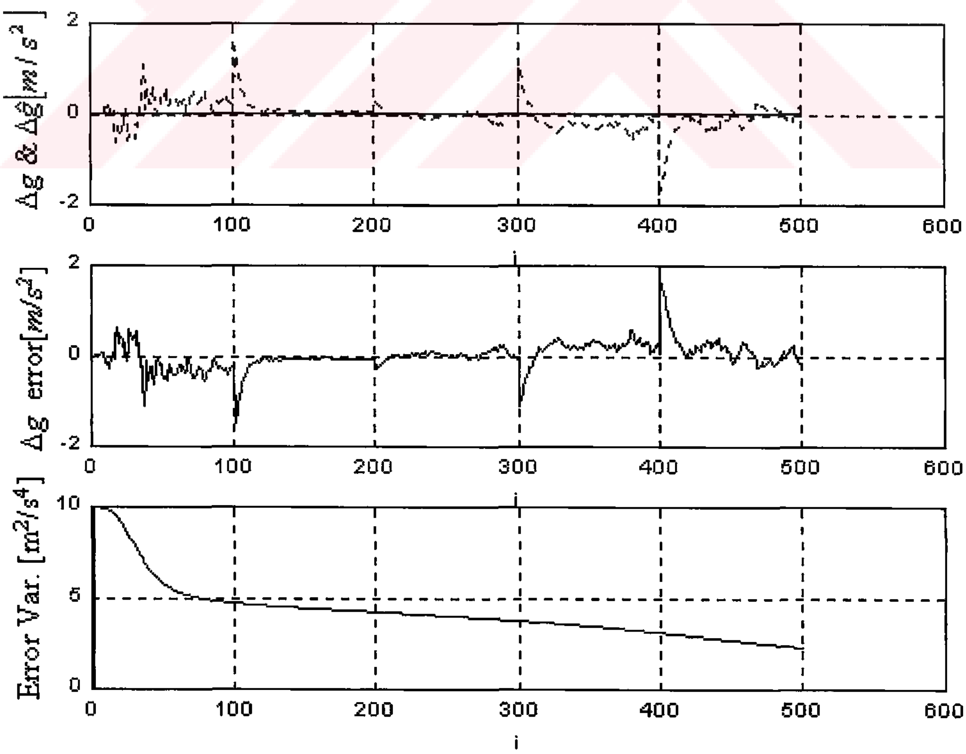

Figure D.8 Combined graph of model (solid line) and estimated (dotted line) errors, their differences, and error variance of gravity.

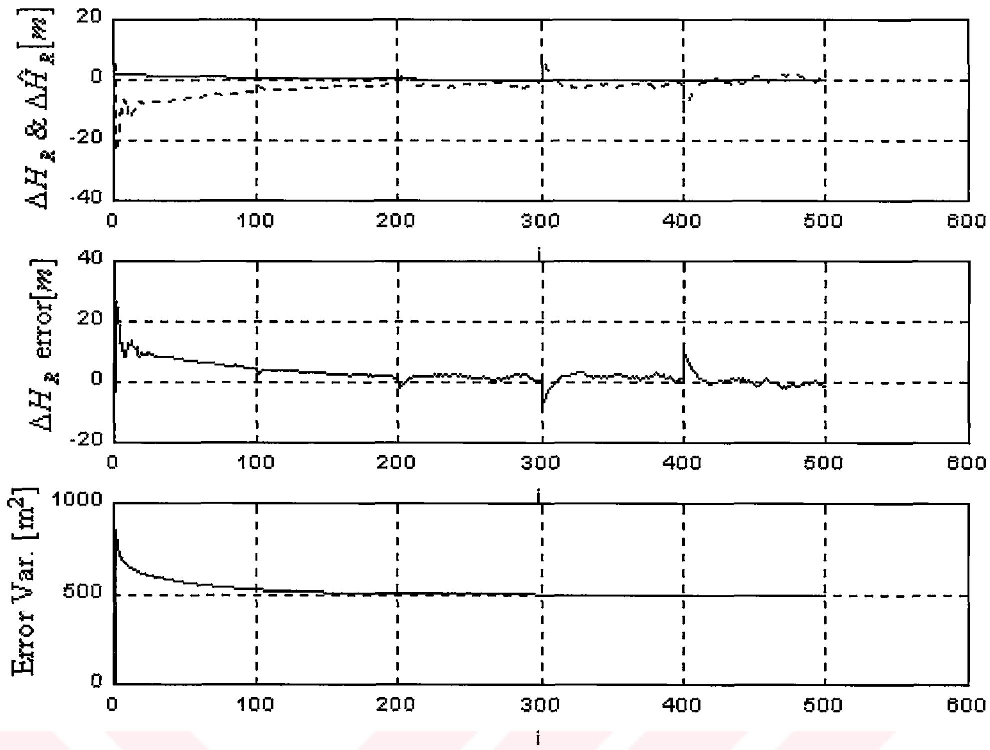

Figure D.9 Combined graph of model (solid line) and estimated (dotted line) errors, their differences, and error variance of radio altitude.

APPENDIX E : Additional Tables

Table E.1 Integrated altimeter errors in case of a failure at the measurement channel (Vertical speed)

Iterations	Optimal Kalman Filter		*Robust Algorithm 1*		*Robust Algorithm 2*	
	Spd. error (*m/s*)	*P(2/2)*	Spd. error (*m/s*)	*P(2/2)*	Spd. error (*m/s*)	*P(2/2)*
50	4.9121	75.4096	4.9121	75.4096	4.9121	75.4096
100	4.5443	33.1113	4.5443	33.1113	4.5443	33.1113
101	218.0502	32.6904	4.5928	33.9499	31.9785	32.6904
150	-5.3016	19.6762	2.7038	19.6778	1.6630	19.6762
200	-3.9290	13.7624	1.3919	13.7631	0.7002	13.7624
201	-54.9144	13.6801	1.3978	13.9921	-12.8041	13.6801
250	-0.3045	10.6578	2.2589	10.6583	2.0936	10.6578
300	0.4617	8.9238	2.0480	8.9241	2.0051	8.9238
301	-38.4529	8.8984	2.0570	9.0590	-7.6493	8.8984
350	4.6395	7.9795	4.8440	7.9798	5.0525	7.9795
400	6.9169	7.5224	6.4410	7.5227	6.7396	7.5224
401	66.7971	7.5168	6.4765	7.6396	15.2235	7.5168
450	8.8654	7.3488	9.1086	7.3490	9.2810	7.3488
500	10.7033	7.3015	11.1012	7.3017	11.2180	7.3015

Table E.2 Integrated altimeter errors in case of a failure at the measurement channel (Vertical acceleration)

Iterations	Optimal Kalman Filter		*Robust Algorithm 1*		*Robust Algorithm 2*	
	Acc. error (m/s^2)	*P(3/3)*	Acc. error (m/s^2)	*P(3/3)*	Acc. error (m/s^2)	*P(3/3)*
50	0.5071	5.9109	0.5071	5.9109	0.5071	5.9109
100	0.1881	4.9741	0.1881	4.9741	0.1881	4.9741
101	13.2931	4.9683	0.1881	4.9731	1.8694	4.9683
150	-0.8268	4.7841	0.0154	4.7841	-0.0940	4.7841
200	-0.5597	4.6515	-0.1082	4.6515	-0.1669	4.6515
201	-4.3666	4.6489	-0.1082	4.6506	-1.1760	4.6489
250	0.2044	4.5053	-0.1218	4.5053	-0.0149	4.5053
300	0.2497	4.3144	-0.2746	4.3144	-0.1528	4.3144
301	-5.5718	4.3099	-0.2746	4.3135	-1.5984	4.3099
350	1.2917	4.0552	-0.0352	4.0552	0.2552	4.0552
400	1.2990	3.7148	-0.0780	3.7148	0.1962	3.7148
401	15.4854	3.7071	-0.0780	3.7141	2.1984	3.7071
450	0.1346	3.2989	0.0275	3.2990	0.0949	3.2989
500	-0.1168	2.8347	-0.2018	2.8347	-0.1650	2.8347

Table E.3 Integrated altimeter errors in case of a failure at the measurement channel (Gravity)

Iterations	Optimal Kalman Filter		*Robust Algorithm 1*		*Robust Algorithm 2*	
	G error (m/s^2)	*P(4/4)*	G error (m/s^2)	*P(4/4)*	G error (m/s^2)	*P(4/4)*
50	0.4891	5.7330	0.4891	5.7330	0.4891	5.7330
100	0.1987	4.7213	0.1987	4.7213	0.1987	4.7213
101	10.3473	4.7138	0.1986	4.7166	1.5006	4.7138
150	0.0219	4.4397	0.0697	4.4397	0.0635	4.4397
200	0.0374	4.2211	0.0639	4.2211	0.0605	4.2211
201	0.8298	4.2168	0.0639	4.2169	0.2705	4.2168
250	-0.3923	3.9993	0.0913	3.9993	-0.0184	3.9993
300	-0.3935	3.7475	0.2001	3.7475	0.0836	3.7475
301	3.6542	3.7420	0.2000	3.7438	1.0887	3.7420
350	-1.2150	3.4475	0.0341	3.4475	-0.2236	3.4475
400	-1.1898	3.0915	0.0726	3.0916	-0.1669	3.0915
401	-12.7457	3.0839	0.0726	3.0885	-1.7979	3.0839
450	-0.1444	2.6879	-0.0129	2.6879	-0.0691	2.6879
500	0.0674	2.2613	0.1779	2.2613	0.1481	2.2613

Table E.4 Integrated altimeter errors in case of a failure at the measurement channel (Radio altitude)

Iterations	Optimal Kalman Filter		*Robust Algorithm 1*		*Robust Algorithm 2*	
	Rad. Alt error (m)	*P(5/5)*	Rad. Alt error (m)	*P(5/5)*	Rad. Alt error (m)	*P(5/5)*
50	-5.9907	561.9924	-5.9907	561.9924	-5.9907	561.9924
100	-3.8353	523.8558	-3.8353	523.8558	-3.8353	523.8558
101	10.0160	523.4258	-3.7969	523.4311	-2.0248	523.4258
150	-2.0424	510.2868	-2.3976	510.2868	-2.3514	510.2868
200	-1.7244	504.9380	-1.1773	504.9380	-1.2484	504.9380
201	12.3433	504.8661	-1.1655	504.8898	2.4885	504.8661
250	-4.4252	502.0578	-0.4667	502.0585	-1.3322	502.0578
300	-2.5956	499.8644	0.5873	499.8646	0.0042	499.8644
301	27.1548	499.8236	0.5814	499.9173	7.3856	499.8236
350	-6.5221	497.9423	-0.3544	497.9437	-1.6413	497.9423
400	-3.8064	496.3110	0.1236	496.3115	-0.5947	496.3110
401	-70.4618	496.2821	0.1224	496.4349	-10.0020	496.2821
450	4.3632	495.0745	-0.1665	495.0761	0.4727	495.0745
500	3.5988	494.2751	0.7966	494.2756	1.2880	494.2751

ABOUT THE AUTHOR

The author, Remzi Saltoğlu, was born in Ankara in 1974. After graduating from T.E.D Ankara College, he entered the School of Aeronautics and Astronautics of İstanbul Technical University. Achieving his undergraduate degree on aeronautical engineering, he began his engineering career at the modernization department of the 1st Air Support and Maintenance Center of the Turkish Air Forces, in Eskişehir, in 1997. At the same year, he entered the Institute of Science and Technology of İ.T.U for his graduate degree on aeronautical engineering. He is continuing his aviation profession, as an Airbus aircraft maintenance engineer, at the engineering department of Turkish Airlines Inc. since 1998.

The author has been contributing to the undergraduate course 'Aircraft Maintenance and Repair' at the School of Aeronautics and Astronautics of İ.T.U as a lecturer for 3 years. He is also voluntarily taking part in the technical courses for aircraft technicians, foreign and native, at the THY training facility.